This is an Accepted Manuscript of an article published by Taylor & Francis in Transportmetrica B: Transport Dynamics on 14 Feb 2022 (Published online), available online: http://www.tandfonline.com/10.1080/21680566.2022.2036651.

Emission-aware adjustable robust flight path planning with respect to fuel and contrail cost

Kam K.H. NG [a,*]

[a] *Department of Aeronautical and Aviation Engineering, The Hong Kong Polytechnic University, Hung Hom, Hong Kong SAR, China*

* *Corresponding author.*

Email Address: kam.kh.ng@polyu.edu.hk (Kam K.H. NG)

Acknowledgment

The research is supported by *Department of Aeronautical and Aviation Engineering, The Hong Kong Polytechnic University, Hong Kong SAR.* Our gratitude is also extended to the Research Committee of the Department of Aeronautical and Aviation Engineering, The Hong Kong Polytechnic University for support of the project (BE3V, UALL). The work described in this paper was supported by grants from Research grants council, the Hong Kong Government (Grant No. PolyU25218321). The authors would like to express their appreciation to the Wyoming weather web, University of Wyoming, Laramie, USA and *FlightTrader24* for their assistance with the data collection and open-source data platform.

Declarations of interest: The authors declare that they have no known competing financial interests or personal relationships that could have appeared to influence the work reported in this paper.

Emission-aware adjustable robust flight path planning with respect to fuel and contrail cost

Abstract

Aviation emission has always been regarded as the major contributor to climate and atmosphere changes. The recent research suggested that flights can be re-routed from sufficiently cold and humid atmospheres to mitigate the level of contrail production in particular regions during the flight planning stage. To address the needs, a weather data-driven flight path planning is proposed in this work. The spatial meteorological condition is generated using historical data and formulated as uncertain factors to develop a robust solution. Airlines can determine their allowance of flight level changes, pre-determined constrained flight levels set and robustness towards the maximum tolerance level of uncertain contrail length of a flight path. The overall cost can be further minimised, with a lowered total contrail length with the least increases in fuel consumption cost. The suggested methods validate the possibility of emission-aware adjustable robust flight path planning and ensure sustainable air transport operations.

Keywords: emission-aware flight path planning; aviation emission control; contrail length; adjustable robust optimisation; decomposition framework

1. Introduction

1.1. Background

The aviation industry is growing at a fast and steady pace, with the number of airline flights around the world increasing by 70% from 2004 to 2019 (IATA 2020). The increasing flights, and subsequently the number of aircrafts in the air, resulted in greater fuel consumption and more engine emissions (Owen, Lee, and Lim 2010; Brueckner and Zhang 2010). Typically, aircraft emissions include carbon dioxide, nitrogen oxides, contrails, and aerosols containing sulphurs and soot. The increase in the number of flights is predicted to cause a rise in the amount greenhouse gases emitted, with the sector estimated to take up around 12% of total CO_2 emission from transportation globally by 2050 (Owen, Lee, and Lim 2010). The predicted increase in air traffic will also result in the rise of contrail formations in the atmosphere, and while the impact of contrails and aviation-induced cirrus clouds on global climate change is not yet fully understood by the scientific community, it is certain that their contribution towards the global radiation budget and climate forcing will increase proportionally. The start of the jet age in the 1950s changed the ways of air travel, with planes flying higher and faster over longer distances. Despite the long history of air travel and the introduction of the jet engine, the effects of them on the global environment were not explored until the 1970s, with concerns over the possible ozone depletion, atmospheric infrared and solar radiation scattering within and above the contrail sheets caused by supersonic aircrafts flying in the stratosphere (Kuhn 1970). Investigations on the effects of subsonic aircrafts emissions in the troposphere only started in late 1990s, with national organisations such as NASA and European Commission DG XII starting the Subsonic Assessment SASS and AERONOX (Friedl 1997; Schumann 1997) project respectively, aiming to better understand the effects of nitrogen oxide emissions on the formation of ozone and contrails. This also marked the first-time aviation atmospheric impact assessment switched from landing and take-off phase to cruising phase where the aircraft spends most of the time in. The shift in research focus is due to the characteristics of the boundary layer between the upper troposphere and lower stratosphere. Air in that location is relatively still and lacks any sufficient means of scrubbing away any unwanted particles and gas such as carbon dioxide. Aircrafts operating in that region will directly emit any materials into the layer, resulting in a build-up of emission particles and gases (Friedl 1997). The location of the emission will also increase their effectiveness in causing chemical and aerosol reaction, such as isobaric cloud formation and ozone generation, which will contribute to climate change.

While an aircraft's turbine engine operates similarly to normal internal combustion engines, with almost identical exhaust emissions, the effects of the emission substances affect the global climate differently when comparing to the greenhouse gases that are emitted at ground level. At higher levels, the effects of contrail and other aircraft emissions on global climate is quantify based on their respective radiative forcing (Lee et al. 2009). The formations of contrail and cirrus clouds are directly linked to the amount of soot particles emitted by the engines, as well as other environmental factors, such as ambient temperature, ice and water saturation, and air pressure. As aircraft enters a sufficiently cold airstream, the hotter and humid exhaust plume will mix with ambient air and form contrails behind the aircraft. As temperature increases, ice saturation ration within the contrail will increase, while larger aerosol radii size will support a lower ice saturation ratio (Koop et al. 2000). Ambient air pressure will affect the isobaric mixing of hot exhaust and cold atmospheric air, and by comparing with the baseline Schmidt-Appleman criterion and ambient water vapour saturation pressure, we will be able to determine if the exhaust plume is sufficient for droplet formation, and thus contrail generation (Bier and Burkhardt 2019). The better developed protocols and system for air flow traffic management can also increase the effectiveness of proposed model. In addition, as previously discussed, contrails and the subsequent cirrus clouds remain the most important

contributing factor towards global climate change. Based on the above reason, we believe that emphases should be placed on contrail and cirrus cloud formation control, while other sustainability measures are still being refined and developed.

The change of the flight path and flight level would raise the fuel consumption and carbon emission. The International Civil Aviation Organisation (2022) studied the resolutions of continuous ICAO policies and practices related to environmental protection and climate change. Sustainable aviation fuels, market-based measures, aircraft technology and operational improvements are the key pillars leading to the long-term CO_2 reduction strategy in the aviation sector. Other than CO_2 emission, Environmental Protection Agnecy (2000) illustrated that contrail cloudiness might contribute to human-induced climate change. Given that water vapour contributes to 50% of greenhouse effect of the globe, the atmosphere traps more heat than other types of greenhouse gases. Persistent contrails can last for several hours if the humidity is high. When there is more water vapour in the atmosphere, the weather turns warmer and more humid, thus created a spiralling cycle. Water vapour has an amplifying effect of greenhouse effect, global warming and to the climate change. In addition, water vapour is an essential element for the formation of aircraft contrails, which the water vapour in atmosphere mixes with the hot water vapour from the exhaust of aircraft engines at low temperature and high altitude (Federal Aviation Administration 2022). Other than greenhouse gases, the greenhouse effect of contrail is found significant. One should note that if the atmospheric temperature and humidity conditions are known beforehand, we can accurately predict and prevent contrail formation (Environmental Protection Agnecy 2000).

The Federal aviation administration's (FAA) and European union aviation safety agency (EASA) have now emphasise more on the public health and environmental protection via promoting contrail prevention strategies. The EUROCONTROL (2021) is currently conducting the contrail prevention trials with the German aerospace centre and investigate the operational feasibility of contrail prevention by ATC instructions. The impact of such prevention strategies are also evaluated. The Federal Aviation Administration (2021) also outlined different initiative to improve aviation sustainability and to leverage the impact of aviation on climate via operational improvements. Yet, no policies have been made with regard to enforce the contrail minimisation and change airlines' business decision. However, operational improvements could be predicted to relief the total contrail production by slightly changing the flight path and flight level in the near future. The trade-off between the induced CO_2 emission and contrail emission is worth to be investigated when the relevant policy is made and applicable to the major air sovereignties. First thing first, it is essential to design an emission-aware adjustable robust flight path planning model with respect to fuel consumption and en-route contrail presence as a foundation to the research problem.

1.2. Problem description

In this paper, we developed an emission-aware adjustable robust flight path planning with respect to fuel consumption and en-route contrail presence. Aviation emission has always been considered as a major contributor to global CO_2 emission and does affect the climate change (Tian et al. 2019; Barrett, Britter, and Waitz 2010). Several aviation programmes, including the airspace technology demonstration 2 and 3 (ATD-2 and ATD-3), the next generation air transportation system (NextGen) (Sheth et al. 2018), attempt to provide an advanced surveillance and communication infrastructure with the ability to share airport and airspace capacities across regions (Ng et al. 2021; Li et al. 2021). The emerging surveillance technology contributed to a 40% reduction in general aviation accidents in the FAA capstone programme, and a 30% noise reduction plus a 34% decrease in fuel consumption in the UPS's demonstration programme. Modern decision support

systems can ensure that the centre and terminal airspace can accommodate the high demand for international travel and achieve better efficient air traffic service (Ng, Keung, et al. 2020). Meanwhile, aviation systems, such as system wide information management (SWIM) (Meserole and Moore 2006; Harkness et al. 2006; Neumayr et al. 2017), provide a collection of real-time data from time-based flow management system, integrated terminal weather system, weather and radar processor, weather message switching centre replacement, to support the flight re-routing approach and adjustment on flight levels for improving airborne delay and aviation safety. It is noteworthy that this information can support the development of eco-friendly flight path planning and contribute to the reduction in aviation emission.

Indeed, during the pandemic, the number of flights has been significantly reduced and the airline fleet has switched to using CAT-C, CAT-D and CAT-E flights (Xue et al. 2021). However, it is expected that the level of air transport operations will resume and return to the pre-coronavirus levels in 2024, as estimated by the international air transport association (IATA). Interestingly, we can observe from the literatures that high-speed rail is substituting civil aviation in the area of domestic travel. (Sun, Wandelt, and Zhang 2021; Liu et al. 2019; Zhang, Wan, and Yang 2019). However, we can expect that flight demand will be substantially increased as air transport retains a major role in long-term aviation economic (Zhang, Zhang, and Huang 2021). The aviation community is attempting to find different eco-friendly approaches, including emissions trading system (Hamaguchi 2021; Girardet and Spinler 2013), incentive and penalty-based aviation emission regulation and control (Liao et al. 2021), alternative fuels (Zhang, Fang, et al. 2020; Goding, Andersson-Franko, and Lagerkvist 2018) and efficient aircraft design (Santos and Delina 2021), to reduce the levels of aviation emission. Alternatively, pricing, taxation, airport charges, congestion cost approaches may somehow reduce and shift the demand from peak to non-peak hours (Brueckner and Zhang 2010; Borbely 2019; Choi 2021; Abeyratne 2019). These approaches either require the involvement, legislation and governance by professional bodies or increase the airline's cost on fleet management (Ng, Lee, Chan, and Lv 2018). The ultimate target would be the zero-carbon flying approach, but we still have a long journey ahead before reaching that goal (Poll 2017). The aviation community is attempting to find a system-wide solution and an inexpensive approach to improve flight path planning and flight trajectory modelling. One can seek to reduce aviation fleet emission in a region with the use of re-routing and flight level adjustments, and we can expect that using data-driven approaches with meteorological data could substantially improve on aviation emission levels, fleet cost, and corporate responsibilities to the environment. Such methods can quantify the impact of additional fuel consumption cost and reduction of contrail cost in the social perspective and promote a sustainable air transport operation.

2. Literature review

Flight path planning and flight trajectory have been well studied in the literature. The common objectives include the fairness criteria, delay and its propagation (Guan et al. 2014), flight path length (Blasi, Barbato, and Mattei 2013), fuel consumption (Malaek, Alaeddini, and Gerren 2011), route charges and extra operation time (Xu et al. 2020) and delay cost for redirected flights (Hu, Chen, and Paolo 2007). It is common to see that 2D flight trajectory optimisation mainly considering distance-based measurement on flight path (García-Heredia, Alonso-Ayuso, and Molina 2019; Guan et al. 2014). The solution methods for solving 2D flight path optimisation problem mainly involve using variables neighbourhood search algorithm (García-Heredia, Alonso-Ayuso, and Molina 2019) or memetic and genetic algorithms (Alam et al. 2009; Malaek, Alaeddini, and Gerren 2011). 3D and 4D flight trajectory optimisation problems are mainly concerned with time-based flow management and trajectory model of flight, with evaluations of the potential conflicts and avoidance strategies

in air traffic flow management (Malaek, Alaeddini, and Gerren 2011; Dougui et al. 2013; Chaimatanan, Delahaye, and Mongeau 2014). The above-mentioned models typically focus on one or few flights trajectories and resolution on intersect waypoints. Flight path planning model is usually referring to a static model with respect to ground and deterministic variables, including the ground delay programme, crossing waypoint location problem and airspace flow programme (AFP). The individual flight information region (FIR) is formed as a flow constrained area (FCA) with the capacity and potential traffic included in the model. In this regard, the airspace and waypoint capacity can be modelled in small-scale (Abdelghany, Abdelghany, and Niznik 2007; Blasi, Barbato, and Mattei 2013). One can link all the subproblems and formulate a full-scale AFP model for en-route traffic control aids purpose. For the details of the modelling methods and optimisation techniques in these areas, readers can refer to Ng, Lee, Chan, and Lv (2018) 's and Chai et al. (2019)'s work.

The current research focuses has shifted from business objectives to environmental objectives. Similar research work can be traced back to Williams, Noland, and Toumi (2002)'s work. Williams, Noland, and Toumi (2002) proposed a model to restrict the allowable cruise altitudes, which is able to minimise the creation of high-altitude contrails. Detwiler and Jackson (2002) explained that aerodynamic contrails are formed by hydrocarbon fuel powered aircraft engines passing through airspace with sufficiently cold and humid atmosphere. Some young or newly formed contrails can spread out due to wind shear and form contrail cirrus (Kärcher 2018; Yin et al. 2018). Once they have formed and became persistence contrails, scientists believe that these contrails will have further impacts on climate change and the Earth's atmosphere (Minnis et al. 2004). Teoh et al. (2020) believe that a minor 1.7% change in flight altitude can reduce 60% of contrail formation. It is worth noting that the price of fuel has dropped recently and airlines now will have more incentives to produce a flight path solution in the senses of social and cooperate responsibility to the environment (Edwards, Dixon-Hardy, and Wadud 2016). Various publications have considered the aviation operative emission and its environmental impacts in flight path planning model (Soler, Zou, and Hansen 2014; van Manen and Grewe 2019). However, the aforementioned publications only considered the contrail presence as a deterministic variable. One should note that the spatial meteorological condition is seasonal factor and changes from time to time. Meanwhile, flight path planning is usually a tactical decision, where the decision must be made before a season. The connection between data-driven model and uncertain factors in the tactical decision-making level is yet to be discussed.

It should be said that uncertainty modelling is not a totally new concept in other areas. Some aviation related problems can be extended with the inclusion of complex constraints from discrete-time network approach (Balakrishnan and Chandran 2010; Ng, Lee, Zhang, et al. 2020), time-space network approach (Kafle and Zou 2016; Bertsimas, Lulli, and Odoni 2011; Yang, Gao, and He 2020), graph theory (Samà, D'Ariano, Corman, et al. 2017; Samà, D'Ariano, D'Ariano, et al. 2017) and rolling horizon method (Samà, D'Ariano, and Pacciarelli 2013; Prakash, Piplani, and Desai 2018), with the integration of these model and their respective uncertainty factors being well-studied in the literature. For instance, for aircraft sequencing and scheduling problem (ASSP) and terminal traffic flow problem (TTFP), the cruise speed and arrival time uncertainty can be modelled to estimate their worst possible outcomes to develop a robust solution. One of the more well-known robust model is to minimise the undesired factors directly, including the total, average or weighted delay time (Ng and Lee 2016b; Ng, Lee, Chan, and Zhang 2018) and makespan (Ng, Lee, and Chan 2017; Ng and Lee 2016a) of a schedule. Other than direct minimisation of undesired factors, we may consider modelling the expected outcomes via stochastic programming (Jacquillat and Odoni 2015b; Jacquillat, Odoni, and Webster 2017; Jacquillat, Odoni, and Webster 2016). For example, the stochastic arrival and departure time can be considered as an expected value and Jacquillat and Odoni

(2015a) proposed the dynamic control of runway configuration setting and stochastic queue conditions for achieving a better turn-a-round time. We may also considered the min-max or min-max regret of the worst-case scenarios to yield a robust solution (Ng, Chen, and Lee 2021; Ng, Lee, Chan, et al. 2020; Ng et al. 2017). Flight time uncertainty can be modelled in 4D trajectory modelling to estimate the most possible arrival time of flights (Takeichi 2018). Franco, Rivas, and Valenzuela (2018) modelled the flight time uncertainty based on wind forecasts, direction and intensity data in flight trajectory modelling. To the best of the author's knowledge, the incorporation of data-driven spatial meteorological factors, contrail length estimation and robust flight path planning are considered in the literatures. However, the potential of using spatial meteorological data to help generate a better estimation of the worst possible outcome for total contrail lengths from a set of alternative paths was not discussed. Airlines can determine a path and corresponding flight attitudes in achieving minimum amount of fuel consumption and total contrail cost with the proposed emission-aware adjustable robust flight path planning model in this work.

2.1. Contribution of the research

The recent research direction mainly considers the emission level of the flight trajectory model for long-haul flights. Their control parameters focus on spatial meteorological condition analysis only and lack the consideration of flight path planning. The contribution of this research includes the following. First, in our proposed model, airlines can determine their desired number of flight level changes and estimate the impact on fuel consumption and contrail cost estimation of a selected flight path in the planning stage. The allowance of flight level changes at each waypoint and the maximum time for flight levels change when cruising along flight path are parameterised as user-specific values. The allowance of flight level changes offers a user-specific parameter for an airline to determine the desired flight levels changes in each round and provide ease of flight operations during operation. Second, we will develop a data-driven emission-aware flight path planning model. Flight paths are usually predetermined three months prior, while the spatial meteorological conditions are subjected to various seasonal factors. It is therefore impossible for real-time flight path planning as airlines cannot make any major changes to a predetermined flight path despite the weather being a near-time factor. Thus, it is important to estimate the spatial meteorological factors through historical data and generate a set of predicted spatial meteorological conditions to support the emission-aware adjustable robust flight path planning model. Third, we model the uncertainty contrail length and propose an adjustable robust optimisation method in emission-aware flight path planning. Users are allowed to adjust their maximum tolerance level to uncertain contrail length of a flight path in the planning stage, in order to yield a profitable and environmentally friendly solution with respect to fuel consumption and contrail cost via scenario analysis. The adjustability of robustness provides flexibility between deterministic and robust scenarios, which means that users can choose a desired solution ranging from zero deterministic variability to a total conservative approach.

2.2. Organisation of the paper

After the introduction of the state-of-the-art flight path planning and flight trajectory modelling from the literature, **Section 3** presents the overall algorithmic framework of our emission-aware adjustable robust flight path planning model. In particular, the interpolation methods and spatial meteorological estimation are presented in **Section 3.1**, while the estimation of contrail length and aircraft performance model via the OpenAP library is introduced in **Section 3.2**. The mathematical modelling of emission-aware adjustable robust flight path planning problem, which is the core part of the research, is illustrated in **Section 3.3**. **Section 4** illustrates two solution approaches: two-stage optimisation framework by Benders decomposition framework and column-and-constraints generation approach. **Section 5** provides the numerical

analysis using real-world flight path instances, including the instances from Hong Kong international airport to Beijing capital international airport (VHHH-ZBAA), from Shanghai Hongqiao international airport to Hong Kong international airport (ZSSS-VHHH), from Chengdu Shuangliu international airport to Hong Kong international airport (ZUUU-VHHH), and from Chengdu Shuangliu international airport to Beijing capital international airport (ZUUU-ZBAA) in China. The selected case study airports mainly cover the regions of the spatial meteorological map for model illustration. Last but not least, **Section 6** provide the conclusion, limitation and future research direction of this work.

3. Emission-aware adjustable robust flight path planning approach

Several assumptions were made before the design of the mathematical modelling for robust flight path planning. First, the actual flight plan can deviate from the solution, as we mainly focus on the design of flight path planning in pre-tactical phase of decision making. The prediction spatial contrail map is generated using historical data, and it is assumed that actual contrail formation will be similar to the predicted model during the planning process. The final pathing is usually submitted to the Civil Aviation Department for approval in the first quarter of the year. Further, abnormal and emergency operations en-route and failure of the auto pilot function are omitted in the analysis. Also, the traffic density en-route is not considered in the proposed model, as one may realise the objective of the model is to deal with emission cost and corporate's environmental responsibility. Aviation emission controls, emissions caps and trading systems developed by various national bodies are not considered in the model. This assumption can be easily realised as they are mainly the cost factors or the changes of feasible en-route in the decision horizon. Last but not least, changes to flight level can only be done at specified waypoints and the aircraft must be maintained at the targeted flight level during the cruising stage. This assumption normalised the non-convexity of flight trajectory modelling in the pre-tactical flight path planning, as the proposed model aims to estimate the cost by changing the flight levels, instead of optimising the flight trajectory profile. Flight trajectory profile optimisation is usually regarded as a tactical decision.

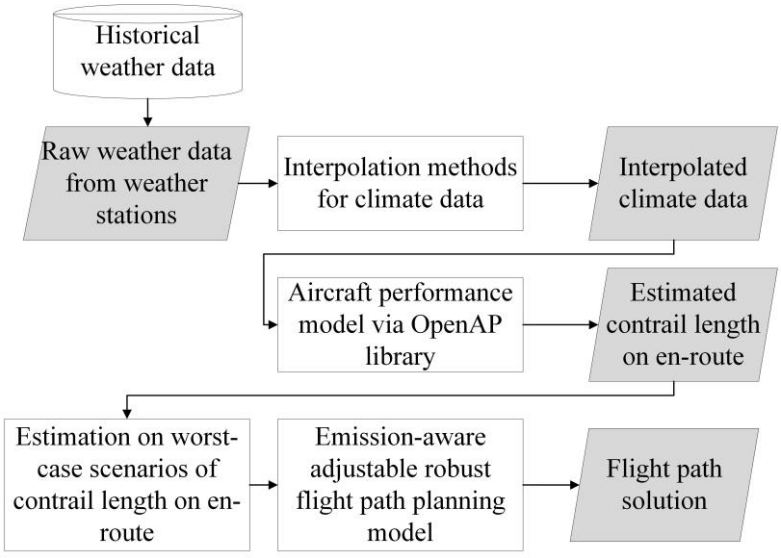

Figure 1. The mission-aware robust flight path planning optimisation framework

The framework of the model is shown in **Figure 1**. We obtained raw weather data from the weather stations and perform interpolation to acquire climate data in the investigated areas. The predicted interpolated climate data and the spatial meteorological map are then built. We can further support the estimation of contrail length en-route by utilising the spatial

meteorological map. The en-route contrail length can then be estimated. The estimated contrail length within particular ranges of dates can be used to formulate the minimum and maximum contrail length en-route at different flight levels. The decision makers can determine their tolerance to the contrail cost index and establish the flight path planning model. The emission-aware adjustable robust flight path planning consists of two decisions: the fuel consumption cost and the contrail length cost. Feasible regions include alternative flight paths that permits civil aviation operation between departing airport to arriving airport, with these paths being commonly adopted for use by airlines. Thus, we can optimise the model and obtain a solution that is in favour of en-route emission costs and high level of corporate environmental responsibility. We will further discuss the details in the coming sections.

3.1. Interpolation methods for climate data and spatial contrail map prediction

In this section, we will illustrate the spatial meteorological estimation, spatial contrail map prediction and contrail length estimation to support the data-driven framework of emission-aware adjustable robust flight path planning problem.

3.1.1. Spatial meteorological estimation

The kriging interpolation method is a well-known methodology for constructing an estimation of meteorological variables in a spatial map with respect to the empirical climate data from weather stations (Rostami et al. 2020; Sluiter 2012). Ordinary Kriging is a linear combination of the measured climate data as mentioned in equation (1). Several studies focused on the comparison of kriging methods, including spherical, exponential, gaussian, cube, logarithmic kriging and co-kriging (Rostami et al. 2020; Kyriakidis 2004; Nas and Berktay 2010; Amirfakhrian and Samavati 2021; Casellas et al. 2020). However, in this study, we are concerned with the cost impact of fuel consumption and contrail length corresponding to the flight path selection. The cost factors of flight path planning should correlate to the changes of interpolation methods. Therefore, we simply use the ordinary kriging method in the numerical study.

$$\hat{\phi}(k_z) = \sum_{h \in H} \lambda_h (k_h) \tag{1}$$

The weather data for the Southeast Asia region was obtained from the Wyoming weather web, University of Wyoming, Laramie, USA[1]. In our study, we are interested in the spatial meteorological estimations in China as we consider domestic flight path planning within the region. 433 weather stations are recognised as Chinese centennial observing station according to the record from the world meteorological organisation[2], while around 75-77 weather reports can be retrieved from the Wyoming weather web every day. The number of weather report depends on the availability of weather stations and may not be available due to station maintenance reasons. The station information, station latitude, longitude and the corresponding meteorological data, including a set of air pressure k_h^{AP}, a set of temperature k_h^{TEMP}, a set of relative humidity to water $k_z^{RH_{water}}$ and their corresponding altitude, are provided in the weather report. We can then calibrate the spatial meteorological estimations of air pressure $\hat{\phi}(k_z^{AP})$, temperature $\hat{\phi}(k_z^{TEMP})$ and relative humidity to water $\hat{\phi}(k_z^{RH_{water}})$ at geographic coordinate z for each flight level $f \in FL$, where $FL = \{300,310,320,330,340,350,360,370,380,390,400,410,430\}$. Selected flight levels are valid for executing instrument

[1] Retrieve from http://weather.uwyo.edu/upperair/seasia.html.
[2] Information from https://public.wmo.int/en/media/news-from-members/433-weather-stations-recognized-chinese-centennial-observing-station

flying rules (IFRs) with reduced vertical separation minima (RVSM) as defined in civil aviation terms"

3.1.2. Spatial contrail map prediction and contrail length estimation

We can obtain the spatial meteorological conditions of air pressure $\hat{\phi}(k_z^{AP})$, temperature $\hat{\phi}(k_z^{TEMP})$ and relative humidity to water $\hat{\phi}(k_z^{RH_{water}})$ at geographic coordinate z for each flight level $f \in FL$ via kriging method. In this section, we illustrate the approach that allows the measurement of the predicted contrail length en-route at each flight level $f \in FL$ and support the proposed emission-aware adjustable robust flight path planning optimisation. The formation of contrail has two conditions: the relative humidity to water $\hat{\phi}(k_z^{RH_{water}})$ needs to satisfy the threshold $\hat{\phi}(r_z^{contr})$, and the relative humidity to ice $\hat{\phi}(k_z^{RH_{ice}})$ should be larger than or equal to 100% (Soler, Zou, and Hansen 2014; van Manen and Grewe 2019; Yin et al. 2018), as illustrated in equation (2). We will briefly introduce the spatial contrail map prediction and we suggest readers to refer to Soler, Zou, and Hansen (2014)'s work for the details on contrail estimation.

$$\hat{\phi}(k_z^{contr}) = \begin{cases} 1, & \left(\hat{\phi}(r_z^{contr}) \leq \hat{\phi}(k_z^{RH_{water}}) \leq 100\%\right) \cap \left(\hat{\phi}(k_z^{RH_{ice}}) \geq 100\%\right), \forall z \in Z \\ 0, & otherwise \end{cases} \quad (2)$$

One may note that the threshold $\hat{\phi}(r_z^{contr})$, temperature threshold t_z^{contr} and the relative humidity to ice $\hat{\phi}(k_z^{RH_{ice}})$ cannot be directly measured. We can utilise the spatial meteorological estimations and predict the possibility of contrail formation in particular areas. The contrail estimation function $\hat{\phi}(k_z^{contr})$ in equation (2) provides the binary value of contrail formation at geographic coordinate z. If a flight is passing through the geographic coordinate z and $\hat{\phi}(k_z^{contr})$ equals to one, the chance of contrail formation is high. No contrail will be produced, otherwise. Thus, we can estimate the total contrail length of a flight path considering the function $\hat{\phi}(k_z^{contr})$. The estimation of $\hat{\phi}(r_z^{contr})$ and $\hat{\phi}(k_z^{RH_{ice}})$ are presented in **Appendix A**.

The estimation of contrail length

The estimation of contrail map is in spatial form. In the proposed model, we emphasise the impact of contrail and flight may produce contrail at geographic coordinate z for each flight level $f \in FL$.

We measure the contrail length $CL_{ij}^{f_i f_j}$ en-route at each flight level $f \in FL$ between waypoints i and j. The two waypoints are associated with two geographic coordinates z_i and z_j. Please note that the estimation of contrail at geographic coordinate z is in a grid-based form, and the area is a polygon area of the grid as grid-based contrail size. The size of the grid map is highly sensitive to the computational power and memory of the unit when calculating the contrail map. We maximised the number of grids as a rules-of-thumb in our computational setting. Thus, we summarise all the valid polygon areas between the geographic coordinates z_i and z_j for each flight level $f \in FL$, which is the grid lying on the Euclidean distance from z_i to z_j, to estimate the contrail length $CL_{ij}^{f_i f_j}, \forall (i,j) \in E, \forall f_i \in FL_i, \forall f_j \in FL_j, f_i \neq f_j$ in the decision horizon. The estimated contrail length will further support the flight path planning in **Section 2.3**.

3.2. Aircraft performance model via OpenAP library

The proposed model attempts to evaluate the contrail length at cruising stage, with spatial contrail prediction via data-driven approach. Instead of considering the flight profile via flight mechanics, we developed a quick estimation method to

obtain contrail length en-route. An open-source aircraft performance (OpenAP) model is a practical model used for flight path and trajectory estimation (Sun, Hoekstra, and Ellerbroek 2020), while WRAP is a data-driven kinematic performance database for supporting the OpenAP (Sun, Ellerbroek, and Hoekstra 2019). Compared to the license-based Base of Aircraft Data (BADA) developed by the Eurocontrol (Poles 2009), the OpenAP model was empirically proven that it yields a sufficient computational efficiency for air transport studies (Sun, Hoekstra, and Ellerbroek 2020; Sun 2019). Furthermore, in our proposed method, we considered pre-tactical flight path planning instead of tactical or last-minute flight path planning. A reliable and efficient contrail length estimation method is sufficient to support the design of the path planning problem. The description of the OpenAP library is presented in **Appendix B**.

3.3. Mathematical modelling for robust flight path planning

The mathematical modelling of the emission-aware adjustable robust flight path planning is proposed via a directed graph $G = (V, E)$ with a set of waypoints V and a set of predetermined routes E in the decision horizon. The set of flight level is denoted as FL, while the constrained flight levels is the subset of flight levels $\overline{FL_i} \subseteq FL_i$. The highest flight level available is restricted due to the constraints of flight mechanics described in the previous section and preference of the airlines. Each waypoint in the en-route operations is indexed by $i, j, p \in V$ and the route is denoted as $(i, j), (j, p) \in E, i \neq j \neq p$. The set of flight levels available en-route is denoted as FL_i and the set of constrained flight levels $\overline{FL_i}$ is the subset of FL_i. The flight level separation in air traffic services is classified in two categories. The even flight levels include $\{300,320,340,360,380,400\}$, while the odd flight levels include $\{310,330,350,370,390,410,430\}$ in the RVSM configuration using IFR. A flight path is described as $(\alpha, i_1, i_2, \dots, \omega)$, where α represents the initial waypoint at cruising phase after climbing and ω represents the last waypoint at cruising phase before descending. The proposed model is designed as a joint decision of routes selection y_{ij} and flight levels determination $r_i^{f_i}$. The details and explanation of sets, parameters and decision variables are presented in **Table 1**. One may note that the deterministic flight path planning problem can be formulated based on the structure of the shortest path problem. The robust shortest path problem is NP-hard in nature (Chassein, Dokka, and Goerigk 2019; Wang et al. 2020; Ketkov, Prokopyev, and Burashnikov 2021). We are interested in the impact of uncertain parameters in the robust version of the emission-aware flight path planning problem and as such the problem is also regarded as NP-hard.

Table 1

Notations and decision variables of the nominal model.

Emission-aware adjustable robust flight path planning	
Sets with indices	Explanation
V	A set of waypoints in the decision horizon (indexed by i, j, p)
E	A set of routes in the decision horizon
G	A directed graph consisting of a nonempty vector set of waypoints V and an edge set of en-route E
FL_i	A set of flight levels $FL_i \in FL$ on waypoint i
$\overline{FL_i}$	A set of constrained flight levels $\overline{FL_i} \subseteq FL_i$ on waypoint i in responding to flight mechanic constraints
$\widetilde{FL_i}$	A valid set of constrained flight levels $\widetilde{FL_i} \subseteq \overline{FL_i}$ excluding the unchanged flight level from precedent waypoint
Parameters	Explanation
i, j, p	Waypoint in en-route operations $i, j, p \in V$
$(i, j), (j, p)$	Route $(i, j), (j, p) \in E, i \neq j \neq p$
α	The initial waypoint at cruising phase after climbing $\alpha \in V$
ω	The last waypoint at cruising phase before descending $\omega \in V$
f_i	At waypoint i, the valid flight level $f_i \in FL_i$

Δ	A User-specific parameter of maximum number of flight levels changes
D_{ij}	The estimated kilometre from waypoints i to j
$CL_{ij}^{f_i f_j}$	The estimated contrail length from waypoint i at f_i to waypoint j at f_j
C^{fuel}	The estimated fuel cost index (in kilometre) in planning stage
$C^{contrail}$	The estimated contrail cost index (in kilometre) in planning stage
S_i	The accumulated contrail length at waypoint i
M	Large artificial variable

Decision variables	Explanation
y_{ij}	1, if flight is assigned en-route from waypoints i to j for cruising operations; 0, otherwise.
v_{ij}	1, if flight change the flight levels on en-route from waypoints i to j; 0, otherwise.
$r_i^{f_i}$	1, if flight is assigned to reach flight level f_i at waypoints i for flight lifting, cruising or descending operations; 0, otherwise.

We consider a complete en-route flight path as starting from a predefined initial waypoint α at the start of the cruising phase to a predefined last waypoint ω at the end of the cruising phase. Only cruising phase is modelled as the take-off and landing phases are not the key areas of concern with minimising fuel consumption and contrail length via re-routing and changing of flight level manoeuvres. Two decision variables y_{ij} and $r_i^{f_i}$ are introduced to determine the flight path planning. The decision variable y_{ij} is the route selection. If route $(i,j) \in E$ is selected, $y_{ij} = 1.0$, otherwise. The flight level selection is determined by $r_i^{f_i}$. If flight level f_i is selected to execute the cruising operations, $r_i^{f_i} = 1.0$, otherwise. En-route flight level decision is a joint decision of y_{ij}, $r_i^{f_i}$ and $r_j^{f_j}$. Given that $r_i^{f_i}$ and $r_j^{f_j}$ equal to 1, flight is expected to continue cruising at the same flight level if $f_i = f_j$. If $f_i \neq f_j$, flight will change flight levels at waypoint i and remain at flight level f_j until it reaches waypoint j.

3.3.1. Mathematical modelling of emission-aware adjustable robust flight path planning master problem

The following explains the objective function and constraints of emission-aware adjustable robust flight path planning problem. Objective function (3) is designed as a two-stage optimisation problem. The first part of the objective function aims to minimise the estimated cost of fuel consumption when executing flight path $\sum_{(i,j)\in E} C^{fuel} D_{ij} y_{ij}$. C^{fuel} is the estimated fuel cost index (in kilometre) during the planning stage, while D_{ij} is the estimated kilometre from waypoints i to j. The second part of the objective function $C^{contrail} S_\omega$ is denoted as the estimated contrail cost index (in kilometre) during the planning stage without the presence of uncertain factors, while the third part of the objective function present an estimated contrail length function $Q(y,r)$. The uncertain model of estimated contrail length function $Q(y,r)$ will be discussed in later part.

The master problem of the emission-aware adjustable robust flight path planning model is presented as follows: Constraint (4) restricts that a flight must leave from the initial waypoint α to only one waypoint i, $\forall(\alpha,i) \in E$, while constraint (5) restricts that a flight must enter to last waypoint ω for the approach phase from adjacent waypoint i, $\forall(i,\omega) \in E$. Constraint (6) illustrates the path selection and ensure the connectivity for any pair of $(i,j) \in E$ and $(j,p) \in E$ in order to formulate a path. If a route is selected by the decision variable y_{ij}, there must be one flight level selected for $r_i^{f_i}$ and $r_j^{f_j}$ by Constraint (7). Constraint (8) provide more limitations on the constrained flight levels at waypoint j with respect to the flight mechanics and airline preferences. To facilitate stable cruising, available flight levels are limited by a predefined set of constrained flight levels $\overline{FL_j}$. Constraints (9) and (10) enforced that the selected flight levels at each waypoint cannot exceed one. The decision variable v_{ij} in Constraints (11) indicates any changes of flight levels from

waypoints i to j. The predefined set of constrained flight levels $\widetilde{FL}_j$ excludes the unchanged cruising flight level from precedent waypoint. We can then limit the maximum number of flight levels change in a path with a user-specific parameter Δ by Constraint (12). Constraints (13), (14) and (15) calculate the contrail length S_ω without the presence of the uncertainty set. Constraints (16), (17) and (18) illustrate that y_{ij} and $r_i^{f_i}$ are binary variables. The model is presented in two-stage decomposition framework structure and we can perform modelling relaxation by Benders decomposition or Column-and-constraint generation (C&CG) approaches. We enjoy the benefits of higher convergence performance (Bodur and Luedtke 2017; de Sá, Morabito, and de Camargo 2018; Ng, Lee, Chan, et al. 2020; BnnoBRs 1962).

Robust FPP master problem

$$\min_{y,r} \sum_{(i,j)\in E} C^{fuel} D_{ij} y_{ij} + C^{contrail} S_\omega + Q(y,r) \tag{3}$$

$$s.t.$$

$$\sum_{\{i:(\alpha,i)\in E\}} y_{\alpha i} = 1 \tag{4}$$

$$\sum_{\{i:(i,\omega)\in E\}} y_{i\omega} = 1 \tag{5}$$

$$\sum_{\{i:(i,j)\in E\}} y_{ij} - \sum_{\{p:(j,p)\in E\}} y_{jp} = 0, \forall j \in V/\{\alpha,\omega\} \tag{6}$$

$$\sum_{f_i\in FL_i} r_i^{f_i} + \sum_{f_j\in FL_j} r_j^{f_j} \geq 2y_{ij}, \forall (i,j) \in E \tag{7}$$

$$\sum_{f_j\in \widetilde{FL}_j} r_j^{f_j} \geq r_i^{f_i} + y_{ij} - 1, \forall (i,j) \in E, \forall f_i \in FL_i \tag{8}$$

$$\sum_{f_i\in FL_i} r_i^{f_i} \leq \sum_{(i,j)\in E, j\neq i} y_{ij}, \forall j \in V/\{\omega\} \tag{9}$$

$$\sum_{f_i\in FL_i} r_i^{f_i} \leq 1, \forall i \in V \tag{10}$$

$$v_{ij} \geq y_{ij} + r_i^{f_i} + \sum_{f_j\in \widetilde{FL}_j} r_j^{f_j} - 2, \forall (i,j) \in E, \forall f_i \in FL_i \tag{11}$$

$$\sum_{i\in I} \sum_{j\in I, i\neq j} v_{ij} \leq \Delta \tag{12}$$

$$S_\alpha = 0 \tag{13}$$

$$S_j - S_i \geq \overline{CL}_{ij}^{f_i f_j} - M(1-y_{ij}) - M\left(2 - r_i^{f_i} - r_j^{f_j}\right), \forall (i,j) \in E, \forall f_i \in FL_i, \forall f_j \in FL_j \tag{14}$$

$$S_i \geq 0, \forall i \in V \tag{15}$$

$$y_{ij} \in \{0,1\}, \forall (i,j) \in E \tag{16}$$

$$v_{ij} \in \{0,1\}, \forall (i,j) \in E \tag{17}$$

$$r_i^{f_i} \in \{0,1\}, \forall i \in V, \forall f_i \in FL_i \tag{18}$$

3.3.2. Uncertain contrail length estimates

In this section, we will present the description of the uncertainty set Δ in contrail length estimation. The contrail formation is subjected to the meteorological conditions including air pressure $\hat{\phi}(k_z^{AP})$, temperature $\hat{\phi}(k_z^{TEMP})$ and relative humidity

to water $\hat{\phi}\left(k_z^{RH_{water}}\right)$ at geographic coordinate z for each flight level $f \in FL$. These values may vary from date to date and are affected by seasonal effects. The estimation of contrail formation is always a post-hoc analysis, which means that we can only realise the actual impact when weather data is collected. However, flight paths are pre-determined, and the planning is completed at the beginning of the quarter for each year. Airlines can therefore only estimate other possible alternate routes and their impacts towards contrail formations and aviation emission. In this regard, we may consider the robust optimisation approach and measure the contrail length estimation in its worst-case scenarios.

The budgeted uncertainty set of contrail length is estimated by $\mathbb{U}$ in equation (19). The uncertain contrail length $\widetilde{CL}_{ij}^{f_i f_j}$ falls into an interval of $[\overline{CL}_{ij}^{f_i f_j}, \widehat{CL}_{ij}^{f_i f_j}]$, which imply the minimum and maximum contrail length for route (i,j) from flight levels f_i to f_j. The term $\overline{CL}_{ij}^{f_i f_j}$ refers to the nominal contrail length, while the term $\widehat{CL}_{ij}^{f_i f_j}$ is the maximum contrail length. The realised deviation from nominal contrail length is controlled by $\delta_{ij}^{f_i f_j}$ such that the realised contrail length is $\delta_{ij}^{f_i f_j}\widehat{CL}_{ij}^{f_i f_j}$. The binary decision variable $\delta_{ij}^{f_i f_j}$ helps determine the realised contrail length in the worst-case scenarios. The budget parameter Γ control the level of robustness of the solution $\sum_{(i,j)\in[E]}\sum_{f_i\in FL_i}\sum_{f_j\in FL_j}\delta_{ij}^{f_i f_j}$. When $\Gamma = 0$, the problem is deterministic, whereas $\Gamma = [E]$ represents an interval uncertainty set. Solving the problem with $\Gamma = [E]$ provides a robust solution but is also regarded as an overly-conservative approach. By reducing the value Γ, we can adjust the level of robustness via budgeted uncertainty. We define $[E]$ as the number of waypoints for a given optimal solution $(\hat{y}, \hat{r})$. One may notice that the control parameter includes three summation signs $\sum_{(i,j)\in[E]}\sum_{f_i\in FL_i}\sum_{f_j\in FL_j}\delta_{ij}^{f_i f_j}$, but only the first summation term was counted. This is due to only one flight level being selected on each waypoint i, and thus, $\Gamma = [E]$ is sufficient in defining the interval uncertainty set in the proposed model.

$$\mathbb{U} = \left\{ \widetilde{CL}_{ij}^{f_i f_j}, \forall (i,j) \in E, \forall f_i \in FL_i, \forall f_j \in FL_j : \widetilde{CL}_{ij}^{f_i f_j} = \overline{CL}_{ij}^{f_i f_j} + \delta_{ij}^{f_i f_j}\widehat{CL}_{ij}^{f_i f_j}, 0 \le \delta_{ij}^{f_i f_j} \le 1, \sum_{(i,j)\in[E]}\sum_{f_i\in FL_i}\sum_{f_j\in FL_j}\delta_{ij}^{f_i f_j} \le \Gamma \right\} \tag{19}$$

3.3.3. Mathematical modelling of the emission-aware adjustable robust flight path planning subproblem

The estimated contrail length function $Q(y,r)$ is presented as follows: The objective function (20) aims to minimise the maximum contrail length S_ω with respect to the uncertainty set Δ. Constraint (21) illustrates that the initial value of the accumulate contrail length equals to zero. Constraint (22) calculates the accumulated contrail length S_j at waypoint j with the sum of precedent contrail length S_i and the realised contrail length $\overline{CL}_{ij}^{f_i f_j} + \delta_{ij}\widehat{CL}_{ij}^{f_i f_j}$, if a flight selected route y_{ij} and cruised from flight level $f_i \in FL_i | r_i^{f_i} = 1$ to flight level $f_j \in FL_j | r_j^{f_j} = 1$. It is intuitive that the accumulated contrail length is a positive real number as explained in equation (23).

<u>The primal form of robust FPP subproblem</u>

$$Q(y,r) = \min_{y,r}\max_{\delta\in\mathbb{U}} C^{contrail} S_\omega \tag{20}$$

$$s.t.$$

$$S_\alpha = 0 \tag{21}$$

$$S_j - S_i \geq \overline{CL}_{ij}^{f_i f_j} + \delta_{ij}\widehat{CL}_{ij}^{f_i f_j} - M(1 - y_{ij}) - M\left(2 - r_i^{f_i} - r_j^{f_j}\right), \forall (i,j) \in E, \forall f_i \in FL_i, \forall f_j \in FL_j \tag{22}$$

$$S_i \geq 0, \forall i \in V \tag{23}$$

4. Solution methods

The multi-stage robust optimisation problem attempts to resolve the intractability of robust optimisation via a robust counterpart. The second-stage optimisation problem is the deterministic equivalent of the inner optimisation problem, e.g., the maximisation problem in min-max and min-max regret optimisation problem. Solving multi-stage robust optimisation problem could be complex as stage optimisation problem can be a NP-hard problem. The computational effort needed is usually increased dramatically with the rising number of scenarios and model complexity. Based on Beck and Ben-Tal (2009)'s study, the robust counterparts of an uncertain convex problem can be reformulated from min-max to min-min problem. Benders decomposition and column-and-constraints generation are two well-known methods in solving two-stage robust optimisation problem.

In the Benders decomposition structure, duality of the inner optimisation problem could be applied to formulate the robust counterparts as cutting plane (Beck and Ben-Tal 2009). The first-stage optimisation problem can be reformulated as a relaxed integer programming. Solving the relaxed integer programming is fast as no continuous variables are involved. In order to generate the optimality cut plane and feasible cutting plane, the min-max form of the second-stage optimisation problem can be reformulated via duality, after which the set of Benders optimality cutting plane and the set of Benders feasibility cut are added in the relaxed integer programming, allowing for convergence to the global optimality iteratively (Geoffrion 1972).

In the column-and-constraints generation approach, we derived the equivalent formulation from the recourse decision variables by enumerating all the possible uncertain scenarios obtained in the second-stage optimisation problem. The partial enumeration approach is done by adding non-trivial scenarios gradually. One can expect that the lower bound can be gradually increased by generating corresponding recourse decision variables in the first-stage optimisation problem (Zeng and Zhao 2013).

4.1. Two-stage optimisation framework with Benders decomposition approach

The objective function (20) is presented in a min-max form and solving the subproblem directly could be complex and time consuming. Meanwhile, the estimated contrail length function $Q(y,r)$ measures the contrail length of a path. In this connection, one could solve the master problem, obtain the fixed en-route and flight levels optimal solution $(\hat{y},\hat{r})$, and measure the contrail length with the given $\hat{y},\hat{r}$ in the subproblem. The computational burden can be significantly reduced by partitioning the non-linear problem into a linear master problem and subproblem. We attempted to covert the min-max optimisation problem into a max-max optimisation problem via duality by introducing the dual variables u and $d_{ij}^{f_i f_j}$. Furthermore, the uncertain contrail length $\widetilde{CL}_{ij}^{f_i f_j}$ can be reformulated as the realised contrail length $\overline{CL}_{ij}^{f_i f_j} + \delta_{ij}^{f_i f_j}\widehat{CL}_{ij}^{f_i f_j}$ in the optimisation problem. The parameter $\delta_{ij}^{f_i f_j}$ is control by the budget parameter Γ as illustrated in Constraints (29) and (30). The dual variables $d_{ij}^{f_i f_j}$ is a binary variable and the matrix $d_{ij}^{f_i f_j}$ is a unimodular matrix (Bruni et al. 2017,

2018; Montemanni and Gambardella 2005; Ford and Fulkerson 2015; Ng, Chen, and Lee 2021), where the determinant of every square of the submatrices equal to 0, 1 or -1 (Ghouila-Houri 1962; de Werra 1981).

The dual form of robust flight path planning subproblem is shown as follows:

$$Q(\hat{y},\hat{r}) = \max_{y,r,\delta} \sum_{(i,j)\in E|\hat{y}_{ij}=1} \sum_{f_i\in FL_i|\hat{r}_i^{f_i}=1} \sum_{f_j\in FL_j|\hat{r}_j^{f_j}=1} \left(\overline{CL}_{ij}^{f_i f_j} + \delta_{ij}^{f_i f_j} \widehat{CL}_{ij}^{f_i f_j} - M\left(1-\hat{y}_{ij}\right) - M\left(2-\hat{r}_i^{f_i}-\hat{r}_j^{f_j}\right)\right) d_{ij}^{f_i f_j} \tag{24}$$

$s.t.$

$$\sum_{(\alpha,i)\in E|\hat{y}_{\alpha i}=1} \sum_{f_i\in FL_i|\hat{r}_i^{f_i}=1} d_{ij}^{f_\alpha f_i} = 1 \tag{25}$$

$$\sum_{(i,\omega)\in E|\hat{y}_{i\omega}=1} \sum_{f_i\in FL_i|\hat{r}_i^{f_i}=1} d_{i\omega}^{f_i f_\omega} = 1 \tag{26}$$

$$\sum_{(i,j)\in E|\hat{y}_{ij}=1} \sum_{f_i\in FL_i|\hat{r}_i^{f_i}=1} \sum_{f_j\in FL_j|\hat{r}_j^{f_j}=1} d_{ij}^{f_i f_j} - \sum_{(j,p)\in E|\hat{y}_{jp}=1} \sum_{f_j\in FL_j|\hat{r}_j^{f_j}=1} \sum_{f_p\in FL_p|\hat{r}_p^{f_p}=1} d_{jp}^{f_j f_p} = 0, \forall j \in V/\{\alpha,\omega\} \tag{27}$$

$$d_{ij}^{f_i f_j} \in \{0,1\}, \forall (i,j)\in E|\hat{y}_{ij}=1, \forall f_i \in FL_i|\hat{r}_i^{f_i}=1, \forall f_j \in FL_j|\hat{r}_j^{f_j}=1, f_i \neq f_j \tag{28}$$

$$0 \leq \delta_{ij}^{f_i f_j} \leq \hat{y}_{ij}, \forall (i,j)\in E|\hat{y}_{ij}=1, \forall f_i \in FL_i|\hat{r}_i^{f_i}=1, \forall f_j \in FL_j|\hat{r}_j^{f_j}=1 \tag{29}$$

$$\sum_{(i,j)\in E|\hat{y}_{ij}=1} \sum_{f_i\in FL_i|\hat{r}_i^{f_i}=1} \sum_{f_j\in FL_j|\hat{r}_j^{f_j}=1} \delta_{ij}^{f_i f_j} \leq \Gamma \tag{30}$$

The term $\widehat{CL}_{ij}^{f_i f_j} \delta_{ij}^{f_i f_j} d_{ij}^{f_i f_j}$ in the objective function is a disjoint bilinear programme over a polyhedron. Therefore, we can replace the disjoint term by an auxiliary variable $w_{ij}^{f_i f_j}$ as illustrated in Constraints (32), (33) and (34). The dual linear form of the robust FFP subproblem is presented as follows:

The dual form of robust FPP subproblem

$$Q(\hat{y},\hat{r}) = \max_{\delta,w} \sum_{(i,j)\in E|\hat{y}_{ij}=1} \sum_{f_i\in FL_i|\hat{r}_i^{f_i}=1} \sum_{f_j\in FL_j|\hat{r}_j^{f_j}=1} \left(\overline{CL}_{ij}^{f_i f_j} - M\left(1-\hat{y}_{ij}\right) - M\left(2-\hat{r}_i^{f_i}-\hat{r}_j^{f_j}\right)\right) d_{ij}^{f_i f_j} + \sum_{(i,j)\in E|\hat{y}_{ij}=1} \sum_{f_i\in FL_i|\hat{r}_i^{f_i}=1} \sum_{f_j\in FL_j|\hat{r}_j^{f_j}=1} w_{ij}^{f_i f_j} \widehat{CL}_{ij}^{f_i f_j} \tag{31}$$

$s.t.$ Constraints (30) – (35)

$$w_{ij}^{f_i f_j} \leq \delta_{ij}^{f_i f_j}, \forall (i,j)\in E|\hat{y}_{ij}=1, \forall f_i \in FL_i|\hat{r}_i^{f_i}=1, \forall f_j \in FL_j|\hat{r}_j^{f_j}=1 \tag{32}$$

$$w_{ij}^{f_i f_j} \leq d_{ij}^{f_i f_j}, \forall (i,j)\in E|\hat{y}_{ij}=1, \forall f_i \in FL_i|\hat{r}_i^{f_i}=1, \forall f_j \in FL_j|\hat{r}_j^{f_j}=1 \tag{33}$$

$$w_{ij}^{f_i f_j} \geq 0, \forall (i,j)\in E|\hat{y}_{ij}=1, \forall f_i \in FL_i|\hat{r}_i^{f_i}=1, \forall f_j \in FL_j|\hat{r}_j^{f_j}=1 \tag{34}$$

In order to associate the optimal solution solved by the subproblem, a Benders dual cutting plane is introduced. Solving the dual form of the robust flight path planning subproblem, we could yield the optimal dual solution and utilise the dual

information $d_{ij}^{f_i f_j \zeta}$ to generate a cutting plane. We can acquire a set of Benders optimality cut Z at each iteration ζ. When adding back the Benders optimality cut to the master problem, we can converge the two-stage decomposition framework with the presence of auxiliary variable Q in the objective function (35) and constraint (37). The termination of the iterative procedure occurs when lower bound value is equal to upper bound value, and thus, global optimum is reached. Since the contrail length has unlimited scratch of schedule in the range of $[0, \infty]$ and the design of the master problem guarantees that the solution $(\hat{y}, \hat{r})$ is always feasible in the subproblem $Q(\hat{y}, \hat{r})$, infeasibility and unbounded scenarios can be omitted.

The relaxed emission-aware adjustable robust flight path planning master problem is presented as follows:

The relaxed robust FPP master problem in Benders decomposition approach

$$\min_{y,r} \sum_{(i,j)\in E} C^{fuel} D_{ij} y_{ij} + Q \tag{35}$$

$$s.t.$$

Constraints (9) – (23)

$$Q \geq C^{contrail} S_{\omega} \tag{36}$$

$$Q \geq \sum_{(i,j)\in E} \sum_{f_i \in FL_i} \sum_{f_j \in FL_j} d_{ij}^{f_i f_j \zeta} \left(\overline{CL}_{ij}^{f_i f_j} - M(1 - y_{ij}) - M\left(2 - r_i^{f_i} - r_j^{f_j}\right) \right) + \sum_{(i,j)\in E} \sum_{f_i \in FL_i} \sum_{f_j \in FL_j} w_{ij}^{f_i f_j \zeta} \widehat{CL}_{ij}^{f_i f_j}, \forall \zeta \in \mathrm{Z} \tag{37}$$

4.2. Two-stage optimisation framework with column-and-constraint generation approach

C&CG method has proven to be efficient in solving two-stage optimisation approach, since the algorithm enforced the corresponding worst-case scenarios as specific constraints into the master problem (Zeng and Zhao 2013; Cheng et al. 2018; An and Zeng 2015). First, the model solves the dual form of robust FPP subproblem to determine the optimal condition as mentioned in previous section. We can yield the realised contrail length $CL_{ij}^{f_i f_j \zeta}$ under budgeted uncertainty at iteration ζ with a given solution $(\hat{y}, \hat{r})$ from the master problem. Then, the corresponding variables and constraints under this specific scenario will be generated and added back to the master problem. The realised accumulated contrail length S_i^{ζ} and realised total contrail length S_{ω}^{ζ} are associated with the decision variables y_{ij} and $r_i^{f_i}$ in the master problem. The realised contrail length $CL_{ij}^{f_i f_j \zeta}$ equals to the $\overline{CL}_{ij}^{f_i f_j} + w_{ij}^{f_i f_j \zeta} \widehat{CL}_{ij}^{f_i f_j}$, where the dual solution $w_{ij}^{f_i f_j \zeta}$ can be obtained at iteration ζ. For each optimal scenario in the subproblem, we can generate a set of constraints at iteration ζ, and thus, we will have an accumulated set of constraints Z. Additional constraints (39) to (42) are added into the master problem and the relaxed robust FFP master problem is presented as follows:

The relaxed robust FPP master problem in column-and-constraint generation approach

$$\min_{y,r} \sum_{(i,j)\in E} C^{fuel} D_{ij} y_{ij} + Q \tag{38}$$

$$s.t.$$

Constraints (9) – (23)

$$Q \geq C^{contrail} S_{\omega} \tag{39}$$

$$Q \geq C^{contrail} S_{\omega}^{\zeta}, \forall \zeta \in Z \quad (40)$$

$$S_j^{\zeta} - S_i^{\zeta} \geq CL_{ij}^{f_i f_j \zeta} - M(1 - y_{ij}) - M\left(2 - r_i^{f_i} - r_j^{f_j}\right), \forall (i,j) \in E, \forall f_i \in FL_i, \forall f_j \in FL_j, \forall \zeta \in Z \quad (41)$$

$$S_i^{\zeta} \geq 0, \forall i \in V, \forall \zeta \in Z \quad (42)$$

5. Numerical study

5.1. Description of case study

We obtained the spatial meteorological data from the Wyoming weather web, University of Wyoming, Laramie, US, starting from 1st Jan 2019 to 30th Jan 2019. The weather stations in China collect the local weather data at 00Z and 12Z each day. We believe that the weather should be of the same pattern during a particular period. We divided the test instances in into weekly and A/PM basic. Thus, we have ten group of instances (A/PM and five weeks from 1st Jan 2019 to 30th Jan 2019). The number of weather reports obtained ranges from 75 to 77 for each instance depending on the availability of the weather stations. The locations of the weather stations are presented in **Figure 2** and the station ID and coordinates of the weather stations are provided in **Appendix C**. According to the interpolation method presented in **Section 3.1**. We can generate the spatial meteorological estimation at each flight level $FL = \{300,310,320,330,340,350,360,370,380,390,400,410,430\}$ as illustrated in **Figure 4**. In **Figure 4**, we illustrate the air pressure, relative humidity to water and temperature at different flight levels. These meteorological data are collected from areological balloon. Based on the estimated value of the meteorological data as illustrated in **Appendix A**., we can estimate the possibility of contrail formation, if a flight is passing through the airspace at a flight level. One can further develop an emission-ware flight route planning to minimise the total contrail length and total fuel consumption and determine an optimal flight path for execution. **Figure 3** illustrated the relationship between the contrail length and the flight path. The grey areas refer to the region that contrail will be produced if a flight is cruising at that flight level, while the white areas refer to the region that no contrail will be produced at cruising. This factor is associated with the total contrail length and the total fuel consumption of a flight path. In this regard, we can evaluate the total cost from a set of alternative flight paths.

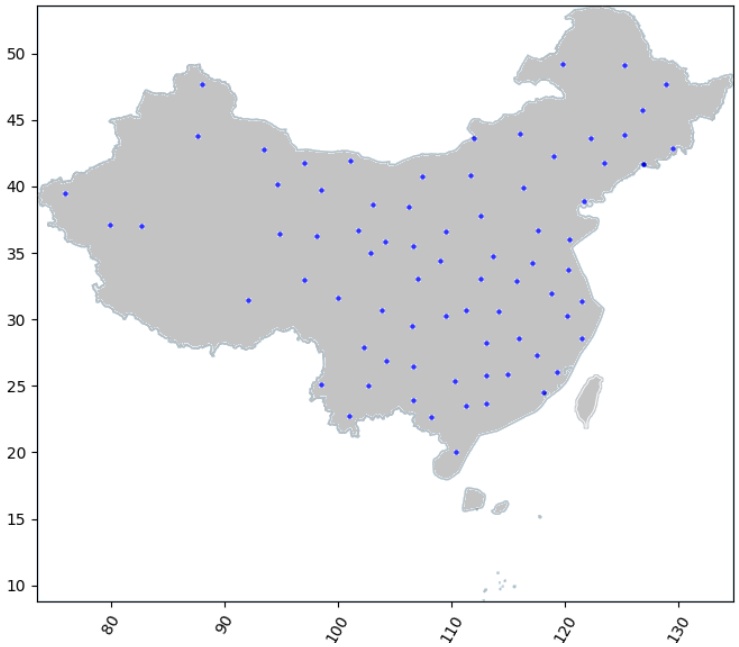

Figure 2. The location of weather stations provided the Wyoming weather web, University of Wyoming, Laramie, USA

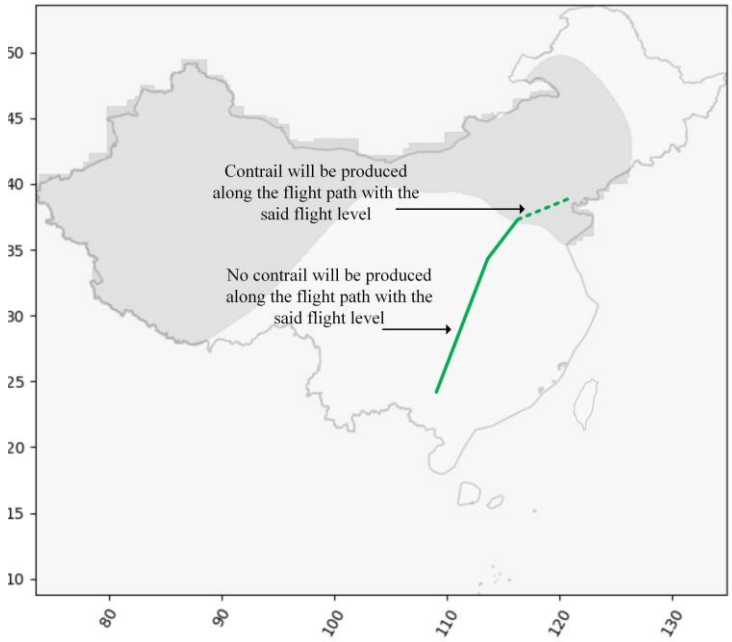

Figure 3. The conceptual idea of contrail length and flight path

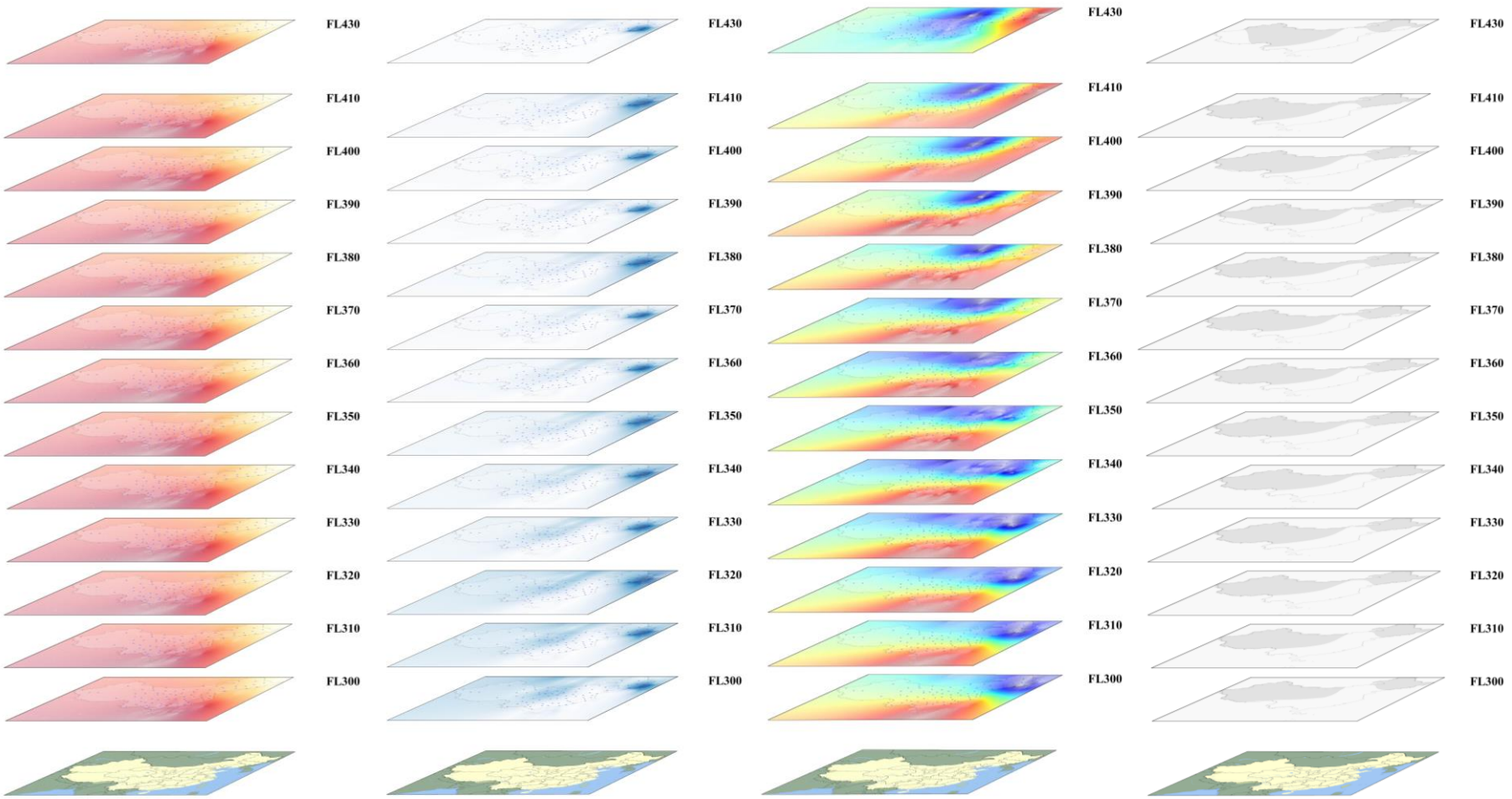

Figure 4. Illustration of spatial map at different flight levels (1st from the left: air pressure, 2nd from the left: relative humidity, 2nd from the right: temperature, 1st from the right: contrail)

Figure 5. The areas of interests and the corresponding waypoints of the test instances

The complete flight path planning instances; as shown in **Figure 5**, includes the following instances; from the Hong Kong international airport to the Beijing capital international airport (VHHH-ZBAA) in **Figure 6**; from the Shanghai Hongqiao international airport to the Hong Kong international airport (ZSSS-VHHH) in **Figure 7**, from the Chengdu Shuangliu international airport to the Hong Kong international airport (ZUUU-VHHH) in **Figure 8** and the Chengdu Shuangliu international airport to the Beijing capital international airport (ZUUU-ZBAA) in **Figure 9**. As each airline will adopt a different flight path and since these types of information are not made available to the general public, we will select the most common routes based on several flight simulations as presented in Appendix B.

Figure 6. Alternative paths from VHHH to ZBAA

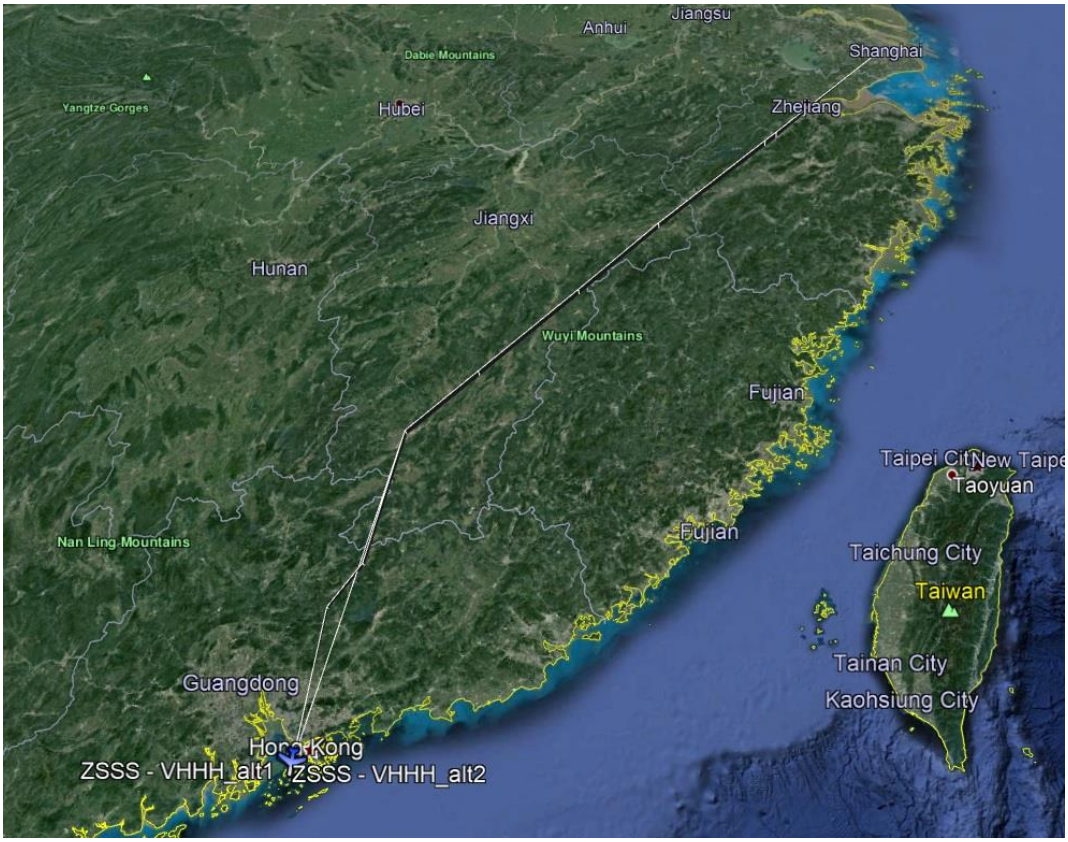

Figure 7. Alternative paths from ZSSS to VHHH

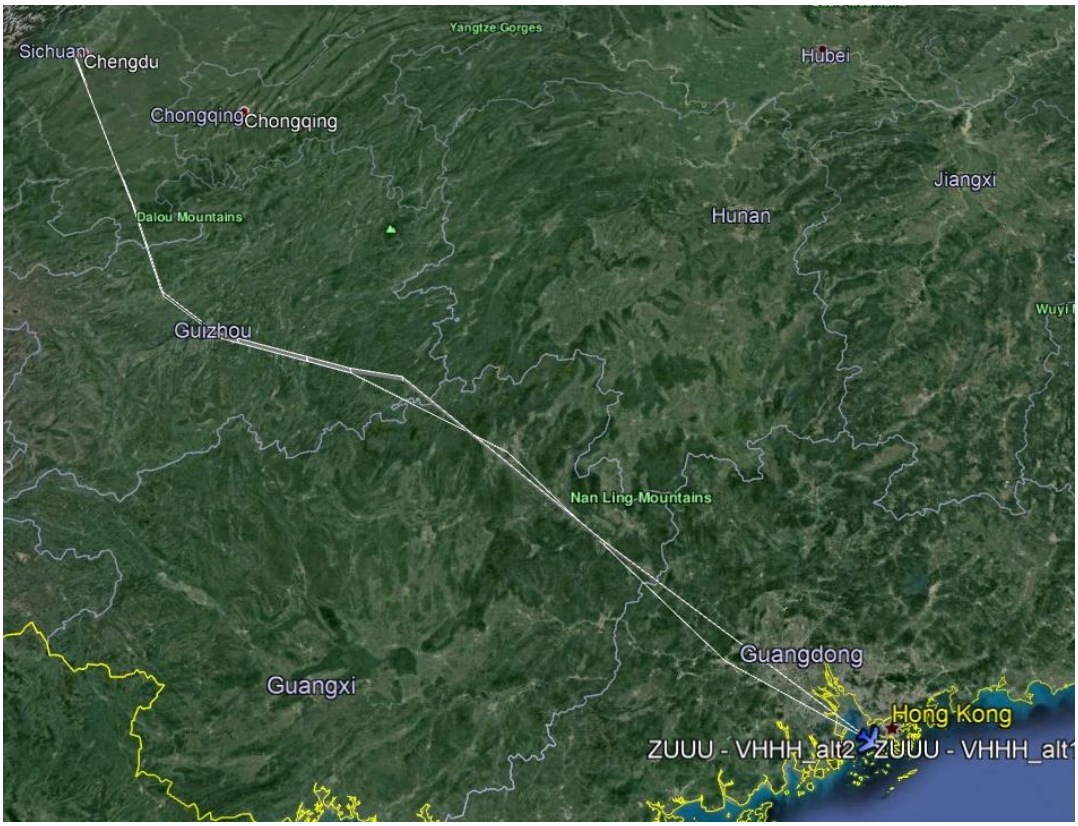

Figure 8. Alternative paths from ZUUU to VHHH

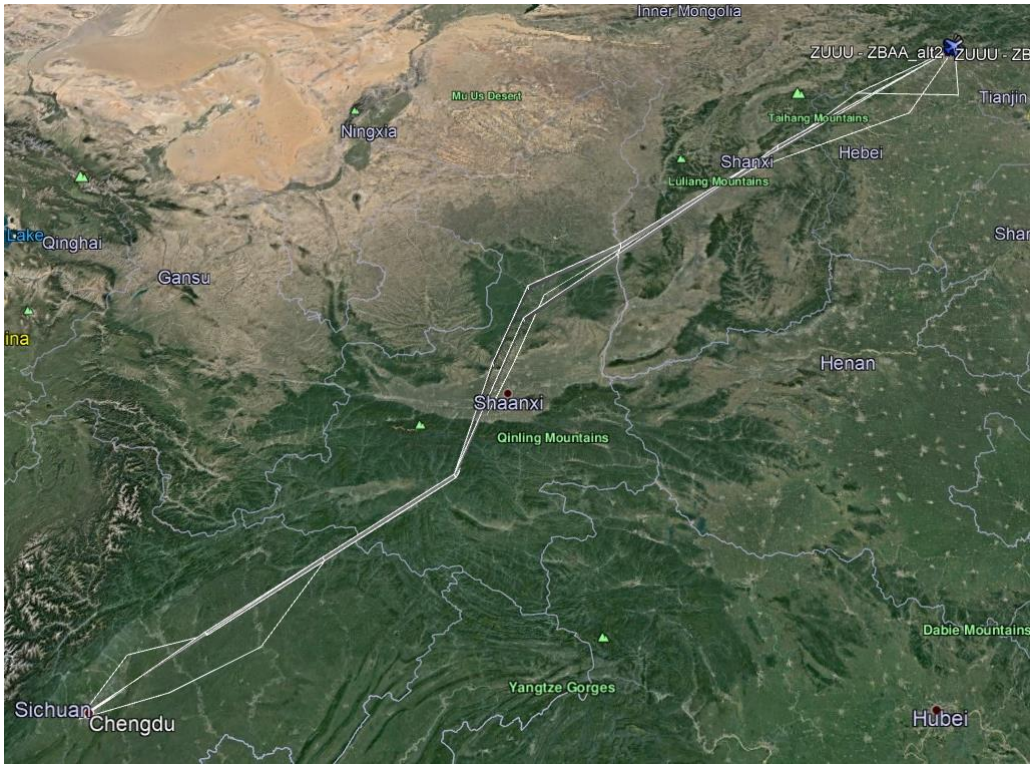

Figure 9. Alternative paths from ZUUU to ZBAA

The computation was performed with a desktop unit with the configuration of *Intel Core i9-10900KF @ 3.70GHz, 3696 MHz, 10 Cores CPU* and *128.0GB RAM* under *Windows 10 Enterprise 64-bit* operating system. The algorithm was coded using *Python 3.8.7* with *Microsoft Visual Studio Code* and *IBM ILOG CPLEX optimisation Studio 20.1.0*.

In the numerical analysis, the model has the following initial setting. First, the set of constrained flight levels $\overline{FL_j} \subseteq FL_j$ on waypoint j is set to be at most one flight levels deviated from f_i. In other word, the constrained flight levels set is set to be plus and minus one flight level. For example, if the flight leaves waypoint i at $FL330$, the set of constrained flight levels on route (i,j) would be $\overline{FL_j} = [310,330,350]$; If flight leave waypoint i at $FL310$, the set of constrained flight levels on route (i,j) would be $\overline{FL_j} = [310, 330]$; and so on. This setting was adopted as in our preliminary study, the exact algorithms cannot solve the problem within one day when constraints flight levels set is plus and minus two. This number can be increased if a more efficient algorithm is adopted. Second, the user-defined maximum number of flight level changes allowed en-route Δ, explained in constraint (17), is set to be $\Delta = [0,2]$. It should be stated that a model with $\Delta = 1$ will yield the same solution as a model with $\Delta = 0$, as the aircraft will be unable to reach the predetermined waypoint marking the ending of the cruising stage. Third, the budgeted uncertainty in constraint (35) is set to be $\Gamma = [0.0, 0.2, 0.4, 0.5, 0.6, 0.8, 1.0]$. The variable $\Gamma = 0.0$ implies a deterministic solution, while robust solution could be obtained by $\Gamma = 1.0$. Forth, we estimate the cost index of fuel C^{fuel} as \$37.715, from the figures of aviation fuel prices of \$USD 3.97 per gallon at the time of writing, and averaging a flight normally consuming 9.5 gallons per kilometre at Mach 0.77. The cost index of contrail $C^{contrail}$ may vary due to the expected value of global temperature change potential, we, therefore, considered \$282.0295 as reference value (25 years of time horizon of the contrail) in our model (Tian et al. 2019). One should note that the coefficient can be adjusted in accordance with the application scenarios. The computation time limit is set to be 1 hour.

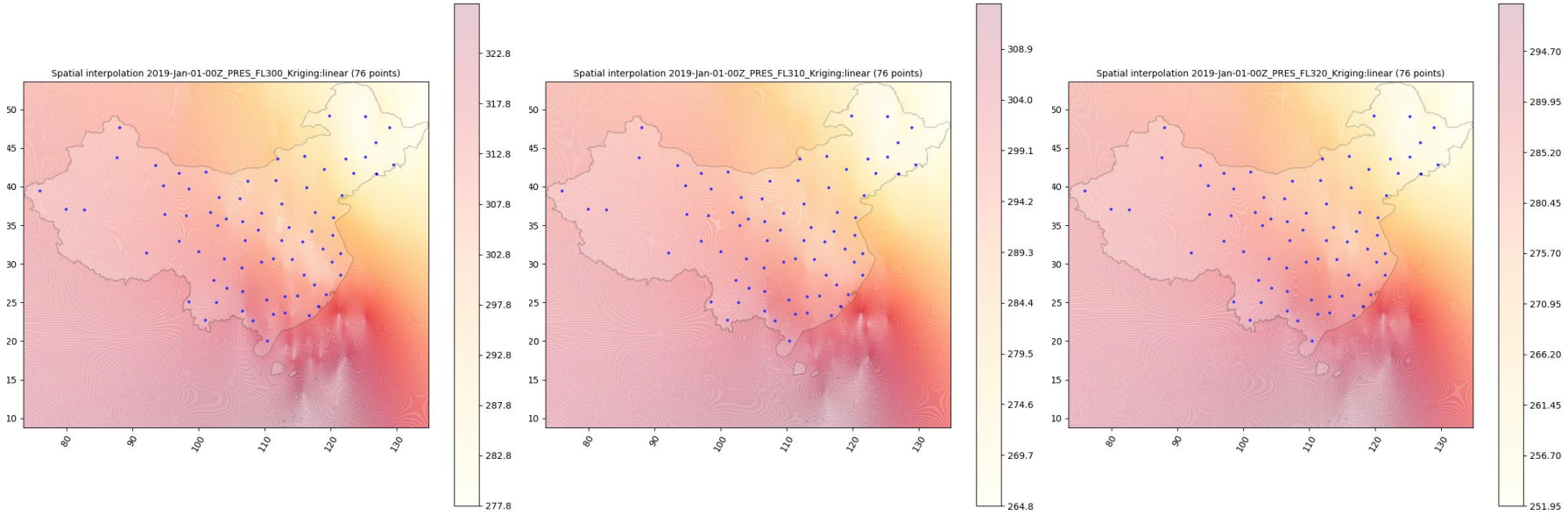
Spatial interpolation 2019-Jan-01-00Z_PRES_FL300_Kriging:linear (76 points)
Spatial interpolation 2019-Jan-01-00Z_PRES_FL310_Kriging:linear (76 points)
Spatial interpolation 2019-Jan-01-00Z_PRES_FL320_Kriging:linear (76 points)

1

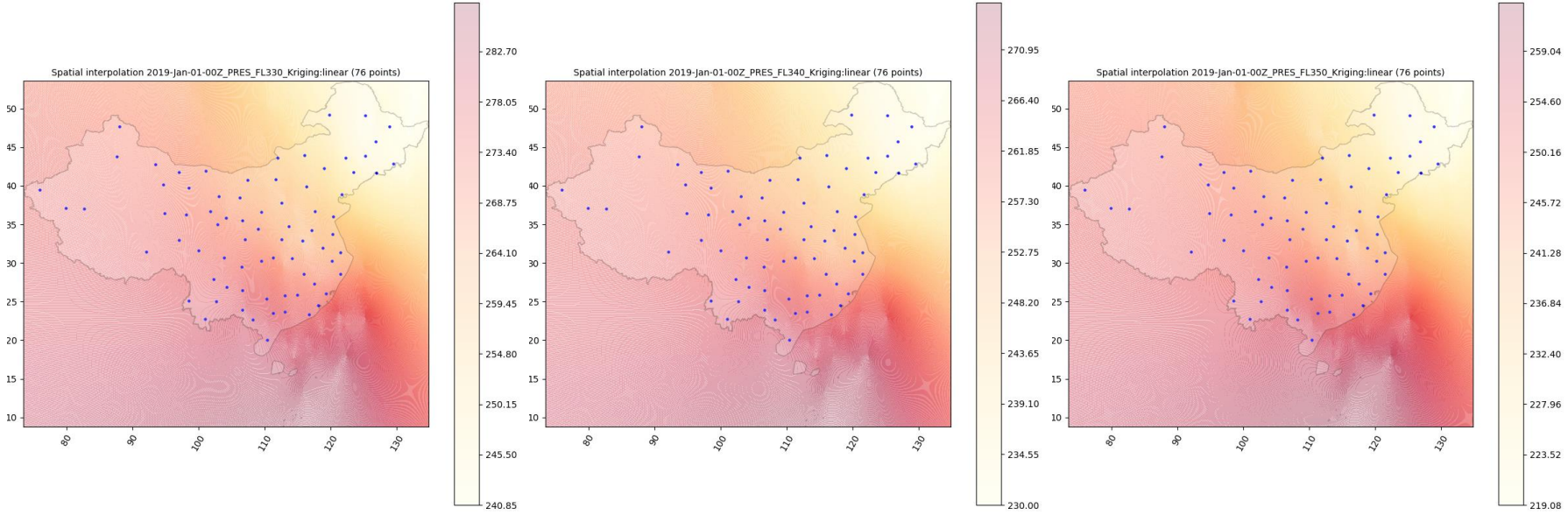
Spatial interpolation 2019-Jan-01-00Z_PRES_FL330_Kriging:linear (76 points)
Spatial interpolation 2019-Jan-01-00Z_PRES_FL340_Kriging:linear (76 points)
Spatial interpolation 2019-Jan-01-00Z_PRES_FL350_Kriging:linear (76 points)

2

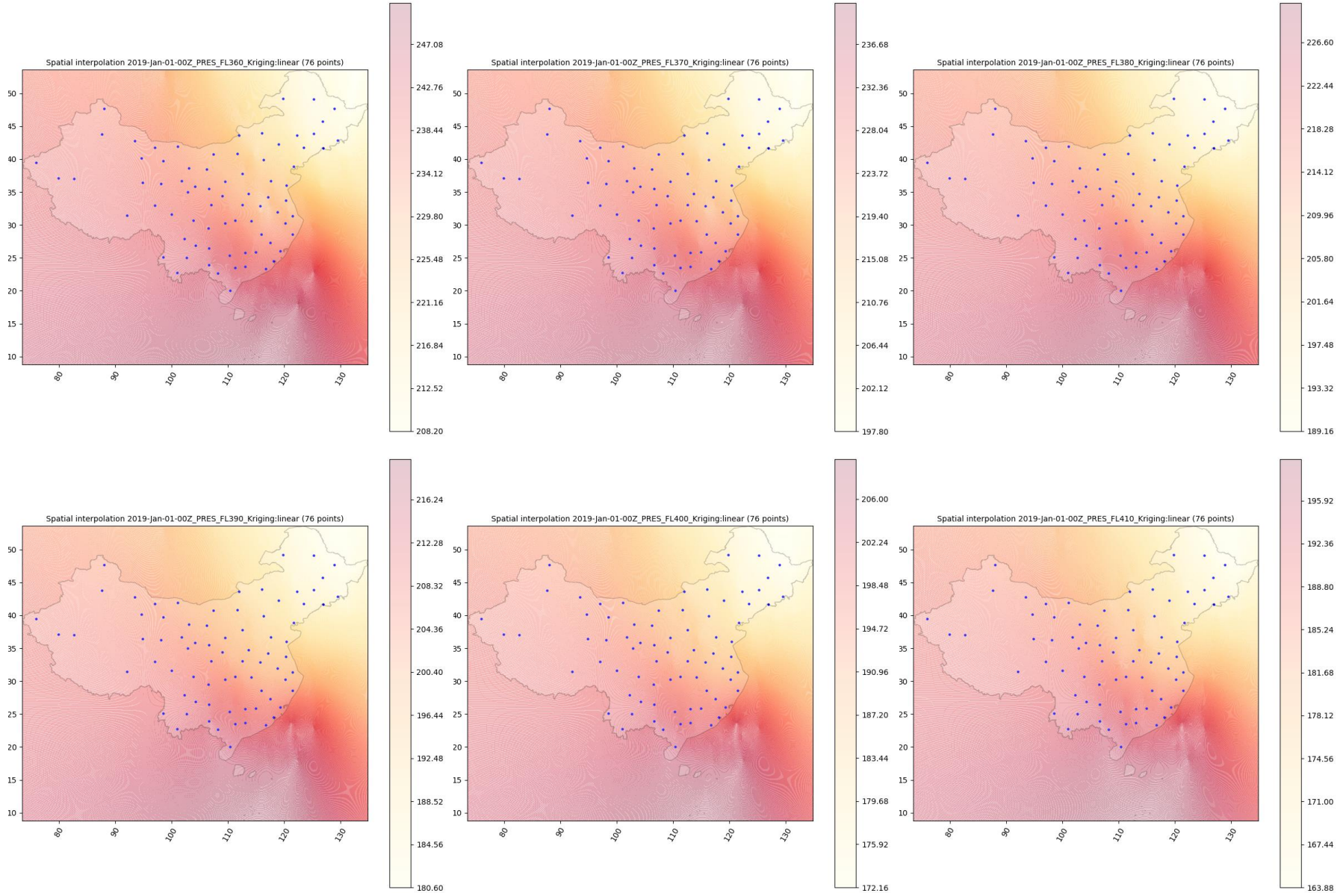

Figure 10. The spatial meteorological condition of air pressure at different flight levels (excluded FL430) on 1st Jan 2019

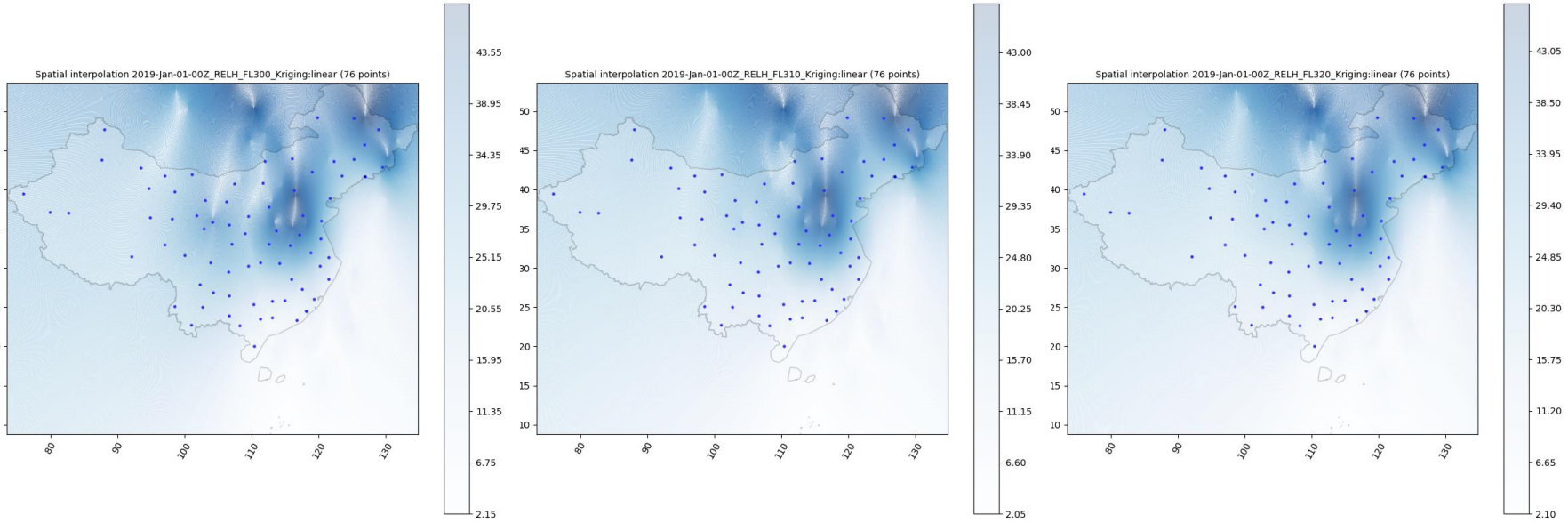
Spatial interpolation 2019-Jan-01-00Z_RELH_FL300_Kriging:linear (76 points)
Spatial interpolation 2019-Jan-01-00Z_RELH_FL310_Kriging:linear (76 points)
Spatial interpolation 2019-Jan-01-00Z_RELH_FL320_Kriging:linear (76 points)

1

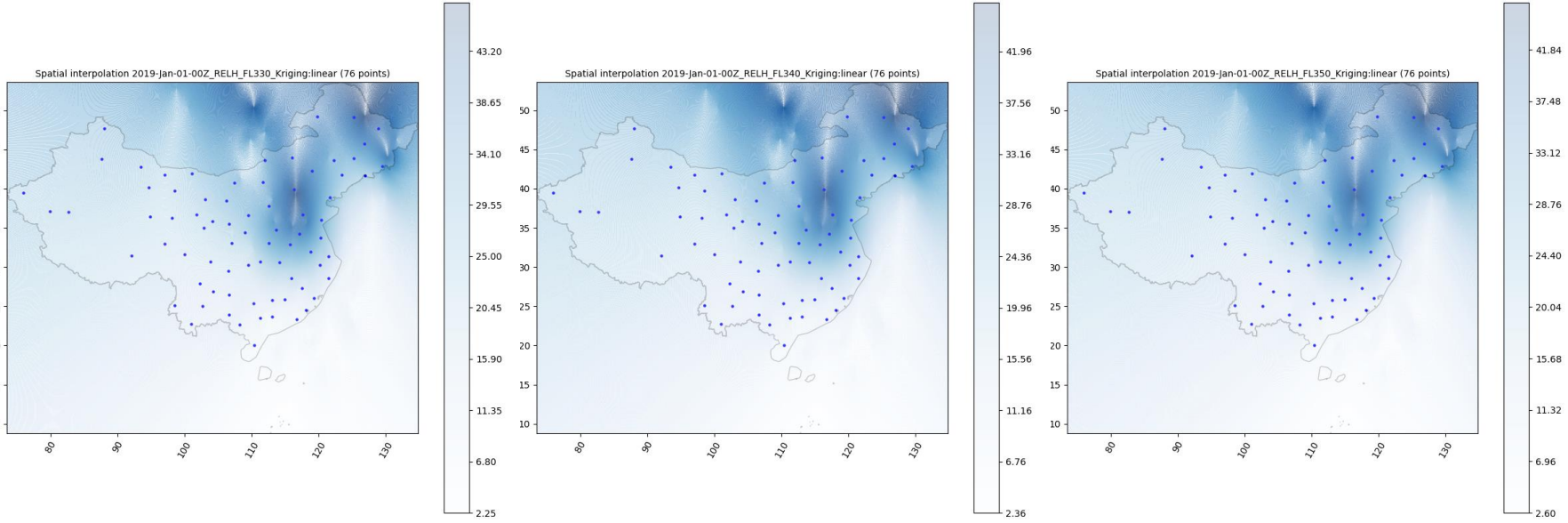
Spatial interpolation 2019-Jan-01-00Z_RELH_FL330_Kriging:linear (76 points)
Spatial interpolation 2019-Jan-01-00Z_RELH_FL340_Kriging:linear (76 points)
Spatial interpolation 2019-Jan-01-00Z_RELH_FL350_Kriging:linear (76 points)

2

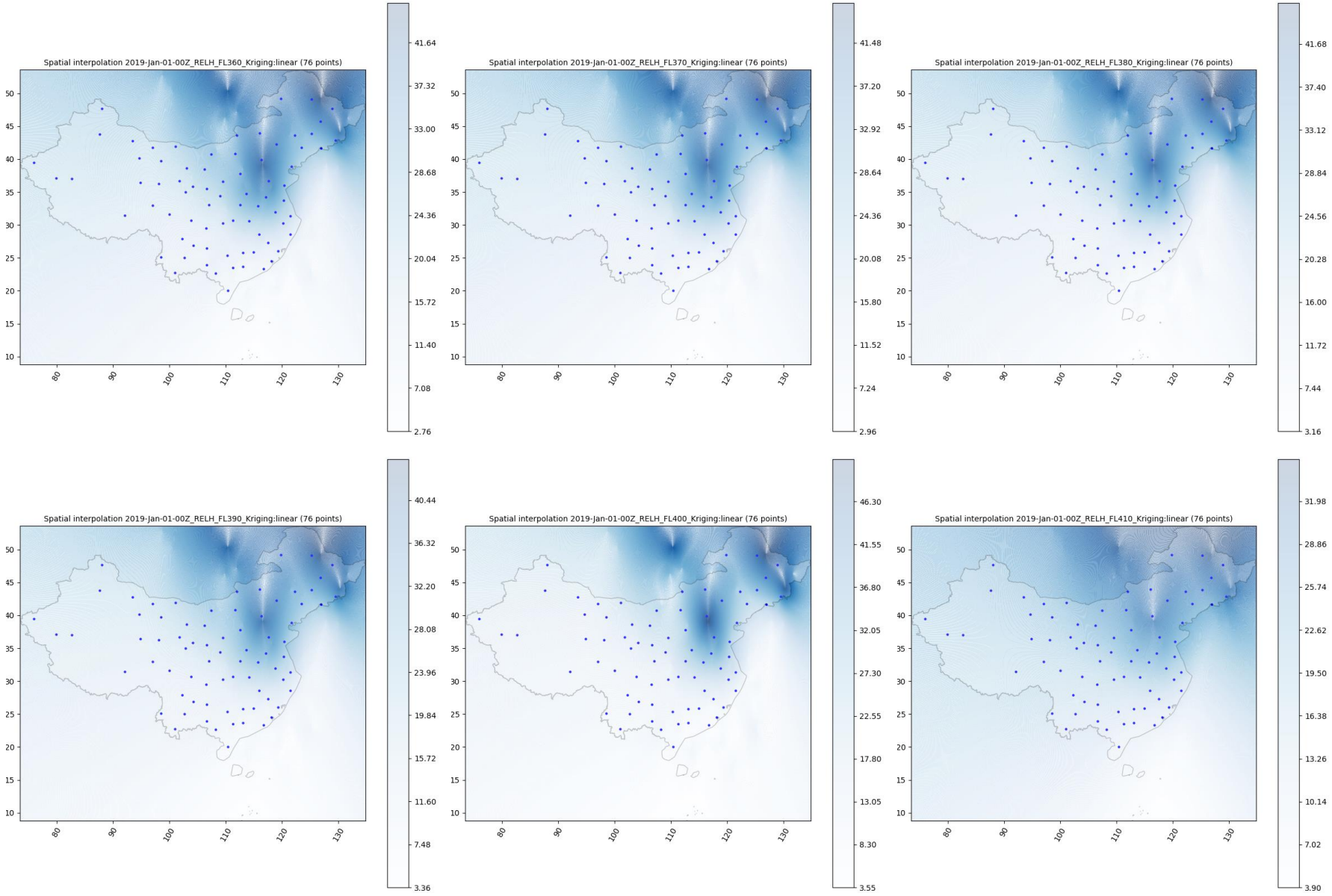

Figure 11. The spatial meteorological condition of relative humidity at different flight levels (excluded FL430) on 1st Jan 2019

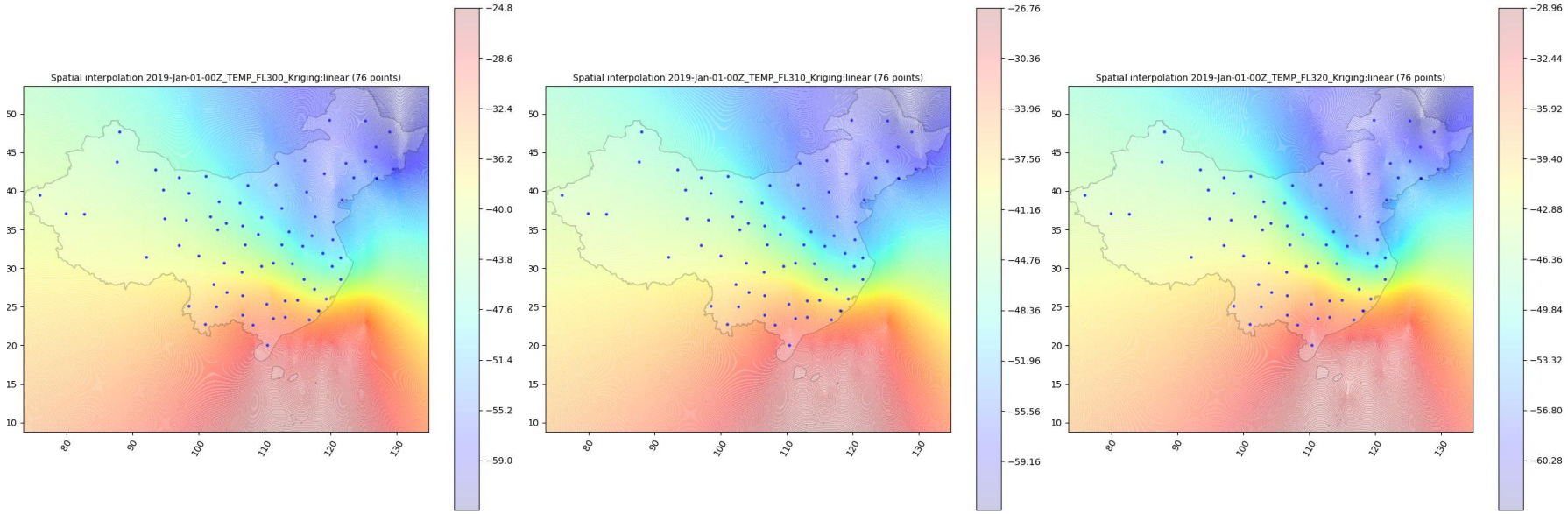
Spatial interpolation 2019-Jan-01-00Z_TEMP_FL300_Kriging:linear (76 points)
Spatial interpolation 2019-Jan-01-00Z_TEMP_FL310_Kriging:linear (76 points)
Spatial interpolation 2019-Jan-01-00Z_TEMP_FL320_Kriging:linear (76 points)

1

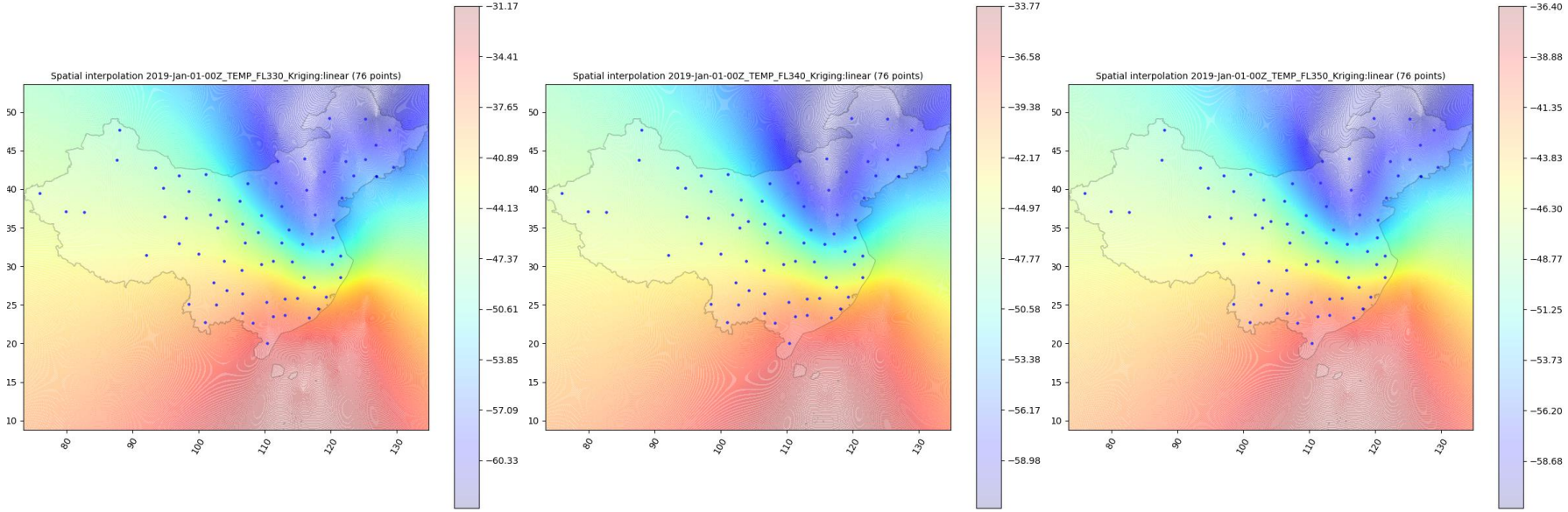
Spatial interpolation 2019-Jan-01-00Z_TEMP_FL330_Kriging:linear (76 points)
Spatial interpolation 2019-Jan-01-00Z_TEMP_FL340_Kriging:linear (76 points)
Spatial interpolation 2019-Jan-01-00Z_TEMP_FL350_Kriging:linear (76 points)

2

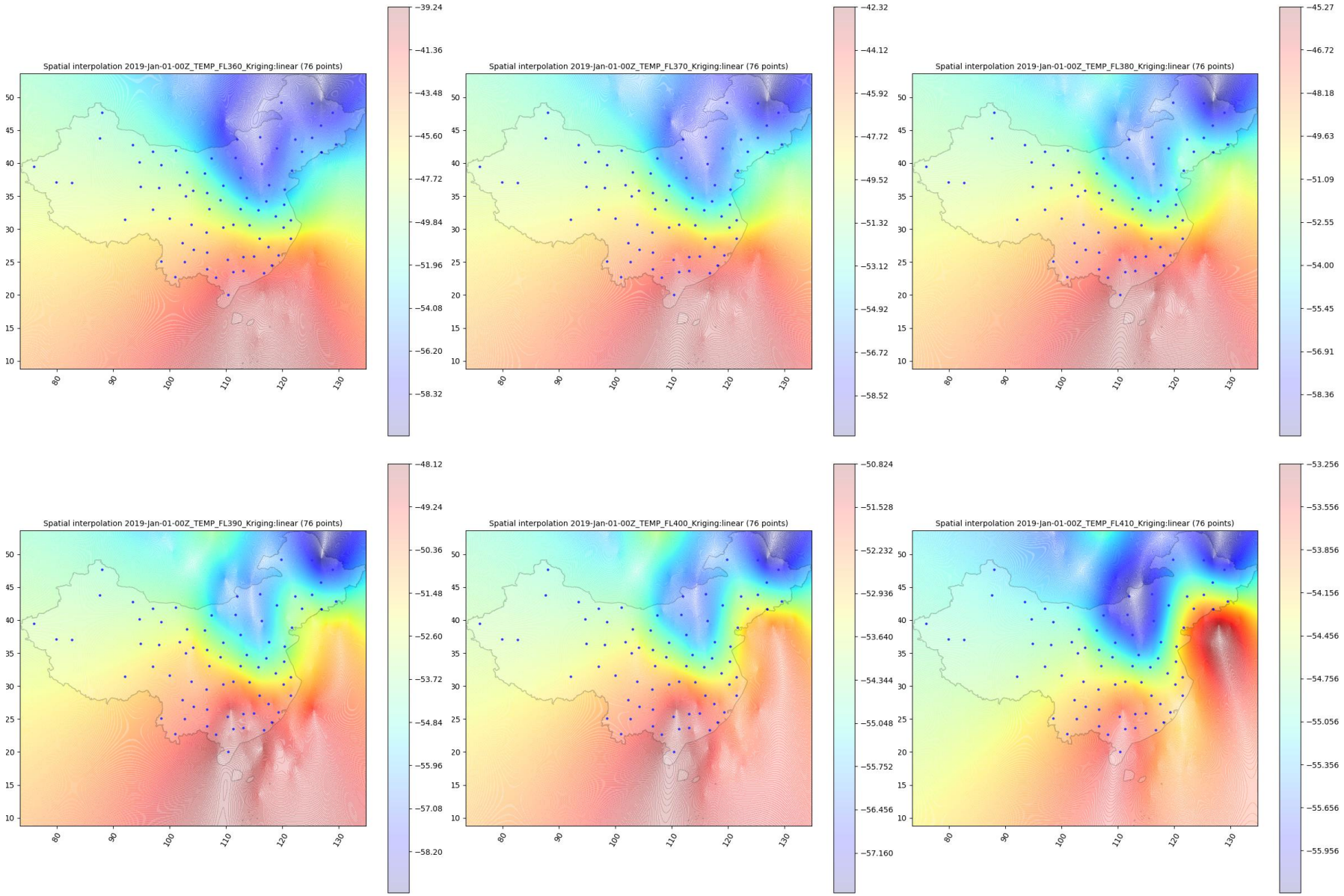

Figure 12. The spatial meteorological condition of temperature at different flight levels (excluded FL430) on 1st Jan 2019

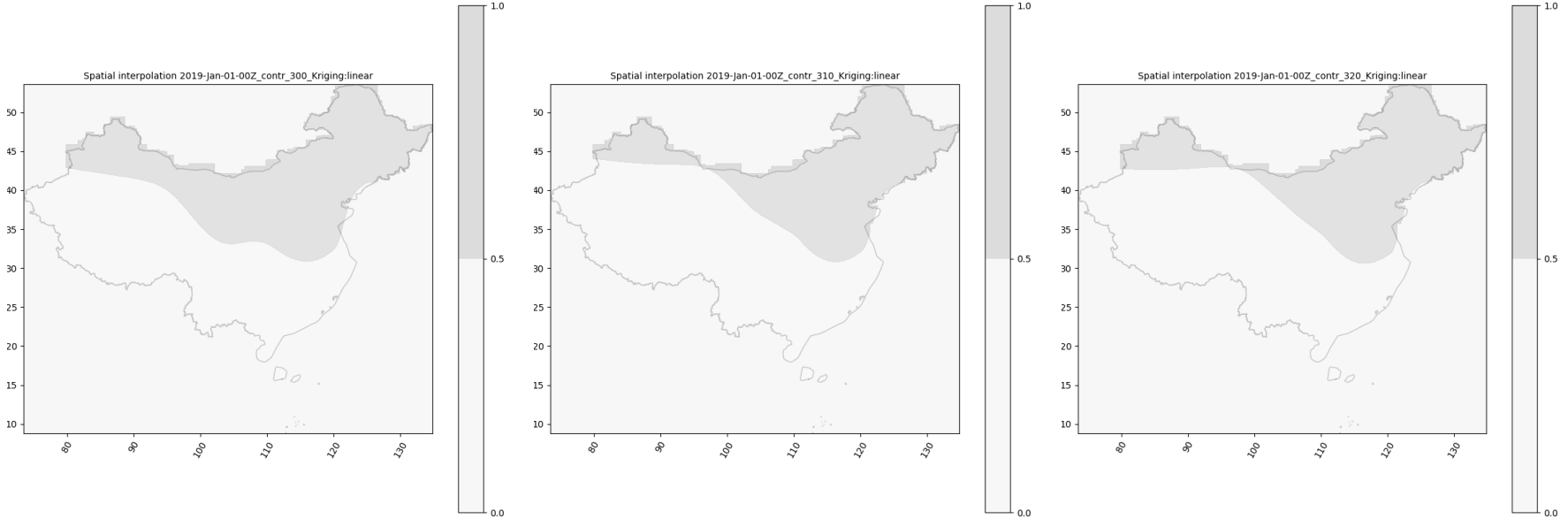
Spatial interpolation 2019-Jan-01-00Z_contr_300_Kriging:linear
Spatial interpolation 2019-Jan-01-00Z_contr_310_Kriging:linear
Spatial interpolation 2019-Jan-01-00Z_contr_320_Kriging:linear

1

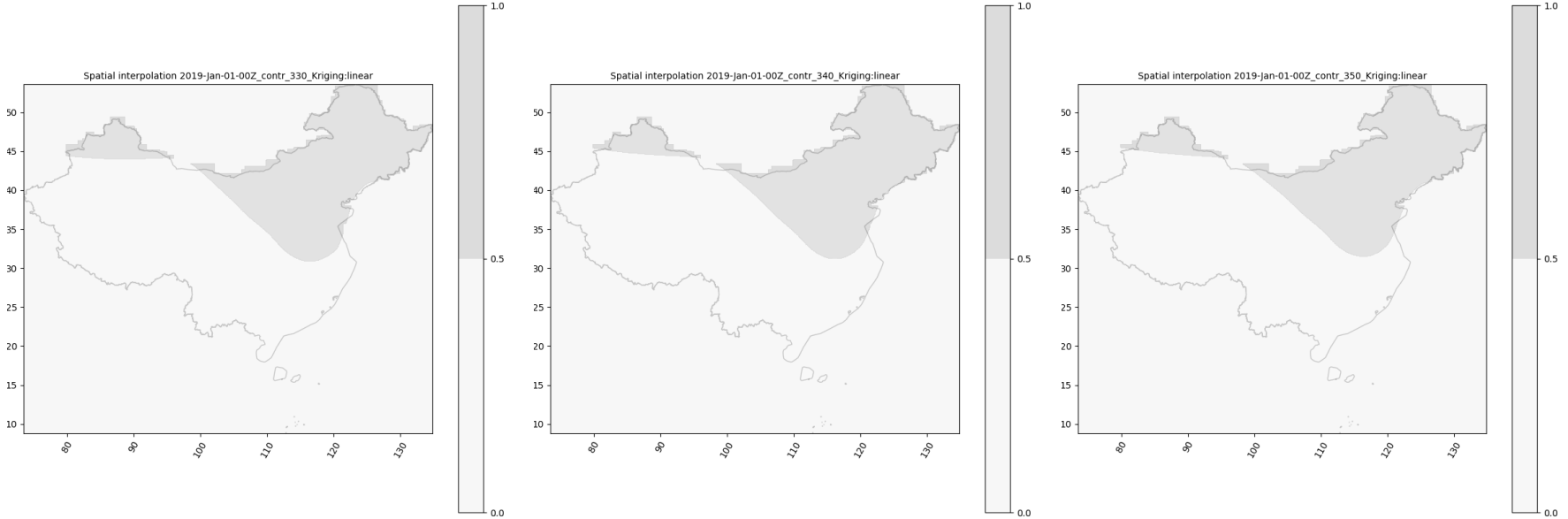
Spatial interpolation 2019-Jan-01-00Z_contr_330_Kriging:linear
Spatial interpolation 2019-Jan-01-00Z_contr_340_Kriging:linear
Spatial interpolation 2019-Jan-01-00Z_contr_350_Kriging:linear

2

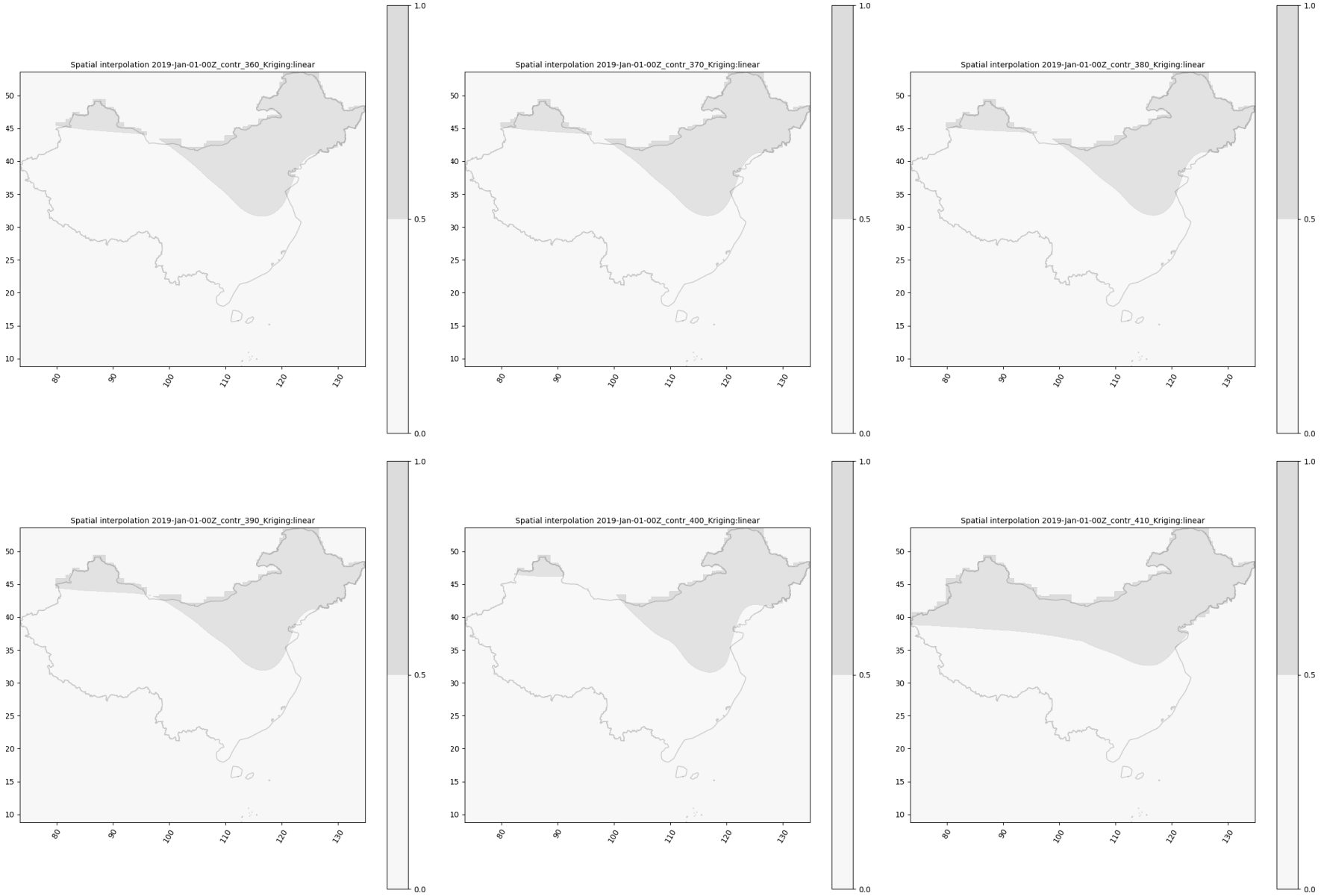

Figure 13. The high possibility of contrail formation region of flight operations at different flight levels (excluded FL430) on 1st Jan 2019

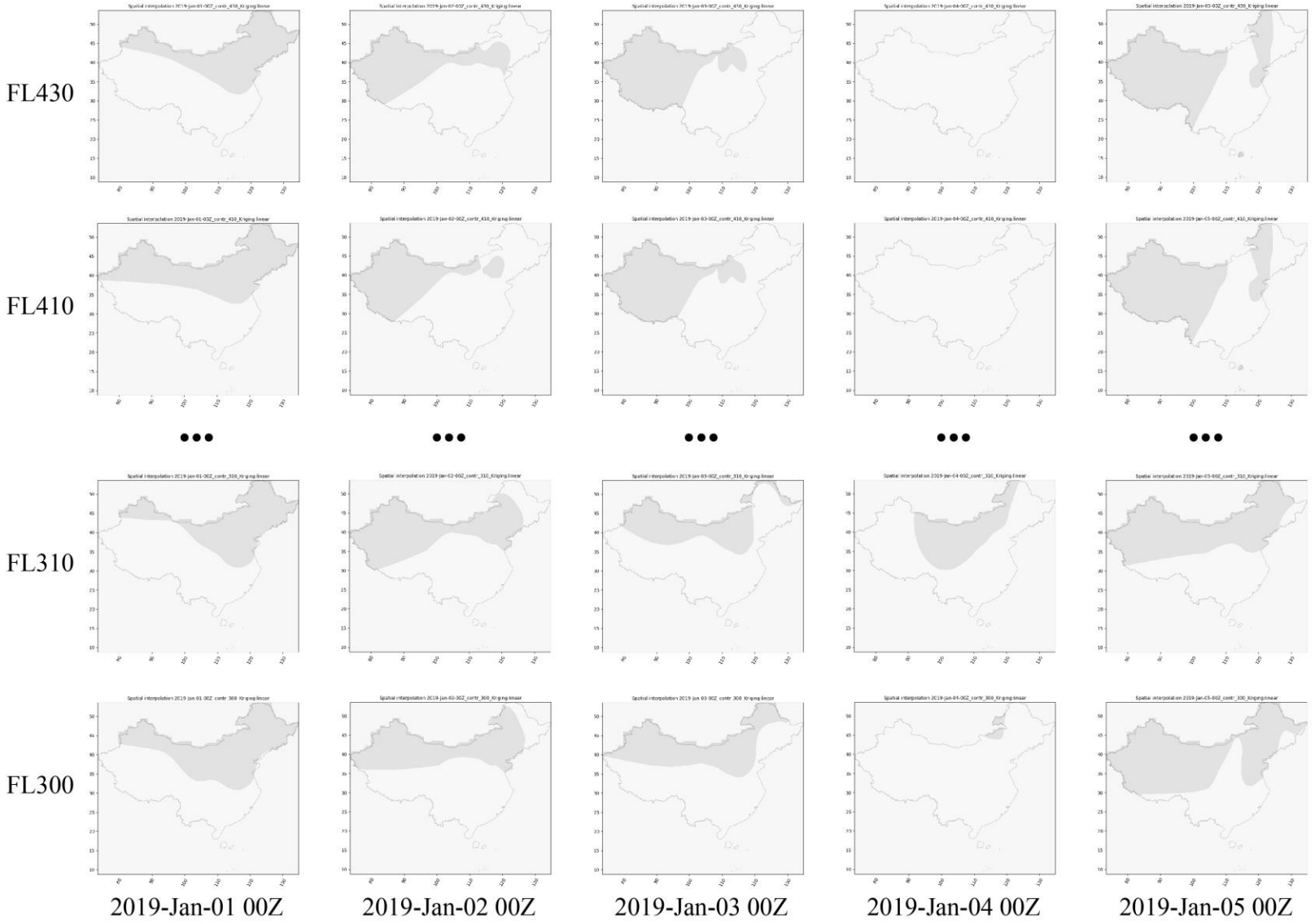

Figure 14. high possibility of contrail formation region of flight operations at different flight levels in a week

5.2. Results analysis

The spatial meteorological condition are generated using ordinary kriging method, and the resulting estimated air pressure, relative humidity, temperature and high possibility of contrail formation regions when flight operations are presented in **Figure 10**, **Figure 11**, **Figure 12** and **Figure 13** respectively. In this regard, we can map out possible contrail formation regions in a multi-layers 2D map as shown in **Figure 14** and estimate the contrail length of routes, so as to optimise the emission-ware adjustable robust flight path planning. **Figure 14** shows that flight can change to other flight levels and avoid the possible contrail formation regions during cruising operations.

In our analysis, BD and C&CG approaches yield global optimum for all instance sets of ZSSS-VHHH, as shown in **Table 2**, and ZUUU-VHHH, as shown in **Table 3**. It is intuitive that only two alternative paths for the ZSSS-VHHH and the ZUUU-VHHH flight routes. Given that identical solutions can be found in $\Delta = [0,2]$, this imply no changes to the flight levels occurred even with a maximum two times of flight levels adjustment allowed.

Table 2

Computational results for the instance set of ZSSS-VHHH $\Delta = [0,2]$

ZSSS-VHHH		$\Delta = [0,2]$^									
		BD approach					C&CG approach				
week	Γ	UB	LB	gap	$\overline{Z}$	CPU	UB	LB	gap	$\overline{Z}$	CPU
1st Jan – 5th Jan 2019 00Z	0	0	0	0.00%	1	0:00:02	0	0	0.00%	1	0:00:02
	0.2	0	0	0.00%	1	0:00:02	0	0	0.00%	1	0:00:02
	0.4	0	0	0.00%	1	0:00:02	0	0	0.00%	1	0:00:02
	0.5	0	0	0.00%	1	0:00:02	0	0	0.00%	1	0:00:02
	0.6	0	0	0.00%	1	0:00:02	0	0	0.00%	1	0:00:02
	0.8	0	0	0.00%	1	0:00:02	0	0	0.00%	1	0:00:02
	1	0	0	0.00%	1	0:00:02	0	0	0.00%	1	0:00:02
1st Jan – 5th Jan 2019 12Z	0	0	0	0.00%	1	0:00:02	0	0	0.00%	1	0:00:02
	0.2	0	0	0.00%	1	0:00:02	0	0	0.00%	1	0:00:02
	0.4	0	0	0.00%	1	0:00:02	0	0	0.00%	1	0:00:02
	0.5	0	0	0.00%	1	0:00:02	0	0	0.00%	1	0:00:02
	0.6	0	0	0.00%	1	0:00:02	0	0	0.00%	1	0:00:02
	0.8	0	0	0.00%	1	0:00:02	0	0	0.00%	1	0:00:02
	1	0	0	0.00%	1	0:00:02	0	0	0.00%	1	0:00:02
6th Jan – 12th Jan 2019 00Z	0	0	0	0.00%	1	0:00:02	0	0	0.00%	1	0:00:02
	0.2	1,151,329	1,151,329	0.00%	3	0:00:08	1,151,329	1,151,329	0.00%	2	0:00:05
	0.4	1,207,490	1,207,490	0.00%	3	0:00:08	1,207,490	1,207,490	0.00%	2	0:00:05
	0.5	1,207,490	1,207,490	0.00%	3	0:00:08	1,207,490	1,207,490	0.00%	2	0:00:05
	0.6	1,207,490	1,207,490	0.00%	3	0:00:08	1,207,490	1,207,490	0.00%	2	0:00:05
	0.8	1,207,490	1,207,490	0.00%	3	0:00:07	1,207,490	1,207,490	0.00%	2	0:00:05
	1	1,207,490	1,207,490	0.00%	3	0:00:08	1,207,490	1,207,490	0.00%	2	0:00:05
6th Jan – 12th Jan 2019 12Z	0	0	0	0.00%	1	0:00:02	0	0	0.00%	1	0:00:02
	0.2	0	0	0.00%	1	0:00:02	0	0	0.00%	1	0:00:02
	0.4	0	0	0.00%	1	0:00:02	0	0	0.00%	1	0:00:02
	0.5	0	0	0.00%	1	0:00:02	0	0	0.00%	1	0:00:02
	0.6	0	0	0.00%	1	0:00:02	0	0	0.00%	1	0:00:02
	0.8	0	0	0.00%	1	0:00:02	0	0	0.00%	1	0:00:02
	1	0	0	0.00%	1	0:00:02	0	0	0.00%	1	0:00:02
13th Jan – 19th Jan 2019 00Z	0	0	0	0.00%	1	0:00:02	0	0	0.00%	1	0:00:02
	0.2	1,375,977	1,375,977	0.00%	3	0:00:08	1,375,977	1,375,977	0.00%	3	0:00:08
	0.4	1,375,977	1,375,977	0.00%	3	0:00:08	1,375,977	1,375,977	0.00%	3	0:00:08
	0.5	1,375,977	1,375,977	0.00%	3	0:00:07	1,375,977	1,375,977	0.00%	3	0:00:08
	0.6	1,375,977	1,375,977	0.00%	3	0:00:08	1,375,977	1,375,977	0.00%	3	0:00:08
	0.8	1,375,977	1,375,977	0.00%	3	0:00:08	1,375,977	1,375,977	0.00%	3	0:00:08

	1	1,375,977	1,375,977	0.00%	3	0:00:08	1,375,977	1,375,977	0.00%	3	0:00:08
13th Jan – 19th Jan 2019 12Z	0	0	0	0.00%	1	0:00:02	0	0	0.00%	1	0:00:02
	0.2	0	0	0.00%	1	0:00:02	0	0	0.00%	1	0:00:02
	0.4	0	0	0.00%	1	0:00:02	0	0	0.00%	1	0:00:02
	0.5	0	0	0.00%	1	0:00:02	0	0	0.00%	1	0:00:02
	0.6	0	0	0.00%	1	0:00:02	0	0	0.00%	1	0:00:02
	0.8	0	0	0.00%	1	0:00:02	0	0	0.00%	1	0:00:02
	1	0	0	0.00%	1	0:00:02	0	0	0.00%	1	0:00:02
20th Jan – 26th Jan 2019 00Z	0	0	0	0.00%	1	0:00:02	0	0	0.00%	1	0:00:02
	0.2	0	0	0.00%	1	0:00:02	0	0	0.00%	1	0:00:02
	0.4	0	0	0.00%	1	0:00:02	0	0	0.00%	1	0:00:02
	0.5	0	0	0.00%	1	0:00:02	0	0	0.00%	1	0:00:02
	0.6	0	0	0.00%	1	0:00:02	0	0	0.00%	1	0:00:02
	0.8	0	0	0.00%	1	0:00:02	0	0	0.00%	1	0:00:02
	1	0	0	0.00%	1	0:00:02	0	0	0.00%	1	0:00:02
20th Jan – 26th Jan 2019 12Z	0	0	0	0.00%	1	0:00:02	0	0	0.00%	1	0:00:02
	0.2	0	0	0.00%	1	0:00:02	0	0	0.00%	1	0:00:02
	0.4	0	0	0.00%	1	0:00:02	0	0	0.00%	1	0:00:02
	0.5	0	0	0.00%	1	0:00:02	0	0	0.00%	1	0:00:02
	0.6	0	0	0.00%	1	0:00:02	0	0	0.00%	1	0:00:02
	0.8	0	0	0.00%	1	0:00:02	0	0	0.00%	1	0:00:02
	1	0	0	0.00%	1	0:00:02	0	0	0.00%	1	0:00:02
27th Jan – 31st Jan 2019 00Z	0	0	0	0.00%	1	0:00:02	0	0	0.00%	1	0:00:02
	0.2	0	0	0.00%	1	0:00:02	0	0	0.00%	1	0:00:02
	0.4	0	0	0.00%	1	0:00:02	0	0	0.00%	1	0:00:02
	0.5	0	0	0.00%	1	0:00:02	0	0	0.00%	1	0:00:02
	0.6	0	0	0.00%	1	0:00:02	0	0	0.00%	1	0:00:02
	0.8	0	0	0.00%	1	0:00:02	0	0	0.00%	1	0:00:02
	1	0	0	0.00%	1	0:00:02	0	0	0.00%	1	0:00:02
27th Jan – 31st Jan 2019 12Z	0	0	0	0.00%	1	0:00:02	0	0	0.00%	1	0:00:02
	0.2	0	0	0.00%	1	0:00:02	0	0	0.00%	1	0:00:02
	0.4	0	0	0.00%	1	0:00:02	0	0	0.00%	1	0:00:02
	0.5	0	0	0.00%	1	0:00:02	0	0	0.00%	1	0:00:02
	0.6	0	0	0.00%	1	0:00:02	0	0	0.00%	1	0:00:02
	0.8	0	0	0.00%	1	0:00:02	0	0	0.00%	1	0:00:02
	1	0	0	0.00%	1	0:00:02	0	0	0.00%	1	0:00:02

^: the optimal solutions with $\Delta = [0,2]$ are identical.

#: over 3600 seconds computational limit

Table 3

Computational results for the instance set of ZUUU-VHHH $\Delta = [0,2]$

ZUUU-VHHH		$\Delta = [0,2]$^									
		BD approach					C&CG approach				
week	Γ	UB	LB	gap	$\overline{Z}$	CPU	UB	LB	gap	$\overline{Z}$	CPU
1st Jan – 5th Jan 2019 00Z	0	0	0	0.00%	1	0:00:24	0	0	0.00%	1	0:00:25
	0.2	0	0	0.00%	1	0:00:25	0	0	0.00%	1	0:00:24
	0.4	0	0	0.00%	1	0:00:24	0	0	0.00%	1	0:00:25
	0.5	0	0	0.00%	1	0:00:24	0	0	0.00%	1	0:00:25
	0.6	0	0	0.00%	1	0:00:24	0	0	0.00%	1	0:00:24
	0.8	0	0	0.00%	1	0:00:25	0	0	0.00%	1	0:00:24
	1	0	0	0.00%	1	0:00:24	0	0	0.00%	1	0:00:24
1st Jan – 5th Jan 2019 12Z	0	0	0	0.00%	1	0:00:24	0	0	0.00%	1	0:00:24
	0.2	0	0	0.00%	1	0:00:24	0	0	0.00%	1	0:00:24
	0.4	0	0	0.00%	1	0:00:24	0	0	0.00%	1	0:00:24
	0.5	0	0	0.00%	1	0:00:24	0	0	0.00%	1	0:00:24
	0.6	0	0	0.00%	1	0:00:24	0	0	0.00%	1	0:00:23
	0.8	0	0	0.00%	1	0:00:24	0	0	0.00%	1	0:00:23

	1	0	0	0.00%	1	0:00:24	0	0	0.00%	1	0:00:24
6th Jan – 12th Jan 2019 00Z	0	0	0	0.00%	1	0:00:24	0	0	0.00%	1	0:00:24
	0.2	0	0	0.00%	1	0:00:24	0	0	0.00%	1	0:00:24
	0.4	0	0	0.00%	1	0:00:24	0	0	0.00%	1	0:00:24
	0.5	0	0	0.00%	1	0:00:24	0	0	0.00%	1	0:00:24
	0.6	0	0	0.00%	1	0:00:24	0	0	0.00%	1	0:00:24
	0.8	0	0	0.00%	1	0:00:23	0	0	0.00%	1	0:00:24
	1	0	0	0.00%	1	0:00:24	0	0	0.00%	1	0:00:24
6th Jan – 12th Jan 2019 12Z	0	0	0	0.00%	1	0:00:24	0	0	0.00%	1	0:00:24
	0.2	2,265,216	2,265,216	0.00%	17	0:09:11	2,265,216	2,265,216	0.00%	3	0:01:18
	0.4	2,503,906	2,503,906	0.00%	17	0:09:14	2,503,906	2,503,906	0.00%	4	0:01:47
	0.5	2,503,906	2,503,906	0.00%	17	0:09:05	2,503,906	2,503,906	0.00%	4	0:01:45
	0.6	2,503,906	2,503,906	0.00%	17	0:09:03	2,503,906	2,503,906	0.00%	4	0:01:48
	0.8	2,503,906	2,503,906	0.00%	17	0:09:03	2,503,906	2,503,906	0.00%	4	0:01:49
	1	2,503,906	2,503,906	0.00%	17	0:09:01	2,503,906	2,503,906	0.00%	4	0:01:48
13th Jan – 19th Jan 2019 00Z	0	0	0	0.00%	1	0:00:24	0	0	0.00%	1	0:00:24
	0.2	3,865,843	3,865,843	0.00%	17	0:08:59	3,865,843	3,865,843	0.00%	3	0:01:17
	0.4	3,865,843	3,865,843	0.00%	17	0:09:04	3,865,843	3,865,843	0.00%	3	0:01:17
	0.5	3,865,843	3,865,843	0.00%	17	0:09:04	3,865,843	3,865,843	0.00%	3	0:01:17
	0.6	3,865,843	3,865,843	0.00%	17	0:09:02	3,865,843	3,865,843	0.00%	3	0:01:16
	0.8	3,865,843	3,865,843	0.00%	17	0:09:03	3,865,843	3,865,843	0.00%	3	0:01:17
	1	3,865,843	3,865,843	0.00%	17	0:09:03	3,865,843	3,865,843	0.00%	3	0:01:17
13th Jan – 19th Jan 2019 12Z	0	0	0	0.00%	1	0:00:24	0	0	0.00%	1	0:00:23
	0.2	0	0	0.00%	1	0:00:23	0	0	0.00%	1	0:00:24
	0.4	0	0	0.00%	1	0:00:23	0	0	0.00%	1	0:00:24
	0.5	0	0	0.00%	1	0:00:24	0	0	0.00%	1	0:00:24
	0.6	0	0	0.00%	1	0:00:24	0	0	0.00%	1	0:00:23
	0.8	0	0	0.00%	1	0:00:23	0	0	0.00%	1	0:00:24
	1	0	0	0.00%	1	0:00:24	0	0	0.00%	1	0:00:23
20th Jan – 26th Jan 2019 00Z	0	0	0	0.00%	1	0:00:24	0	0	0.00%	1	0:00:23
	0.2	0	0	0.00%	1	0:00:24	0	0	0.00%	1	0:00:23
	0.4	0	0	0.00%	1	0:00:24	0	0	0.00%	1	0:00:23
	0.5	0	0	0.00%	1	0:00:24	0	0	0.00%	1	0:00:23
	0.6	0	0	0.00%	1	0:00:24	0	0	0.00%	1	0:00:23
	0.8	0	0	0.00%	1	0:00:24	0	0	0.00%	1	0:00:24
	1	0	0	0.00%	1	0:00:24	0	0	0.00%	1	0:00:24
20th Jan – 26th Jan 2019 12Z	0	0	0	0.00%	1	0:00:24	0	0	0.00%	1	0:00:23
	0.2	0	0	0.00%	1	0:00:24	0	0	0.00%	1	0:00:24
	0.4	0	0	0.00%	1	0:00:24	0	0	0.00%	1	0:00:23
	0.5	0	0	0.00%	1	0:00:24	0	0	0.00%	1	0:00:24
	0.6	0	0	0.00%	1	0:00:24	0	0	0.00%	1	0:00:24
	0.8	0	0	0.00%	1	0:00:24	0	0	0.00%	1	0:00:24
	1	0	0	0.00%	1	0:00:24	0	0	0.00%	1	0:00:24
27th Jan – 31st Jan 2019 00Z	0	0	0	0.00%	1	0:00:24	0	0	0.00%	1	0:00:23
	0.2	0	0	0.00%	1	0:00:23	0	0	0.00%	1	0:00:24
	0.4	0	0	0.00%	1	0:00:24	0	0	0.00%	1	0:00:24
	0.5	0	0	0.00%	1	0:00:24	0	0	0.00%	1	0:00:24
	0.6	0	0	0.00%	1	0:00:24	0	0	0.00%	1	0:00:24
	0.8	0	0	0.00%	1	0:00:23	0	0	0.00%	1	0:00:24
	1	0	0	0.00%	1	0:00:24	0	0	0.00%	1	0:00:24
27th Jan – 31st Jan 2019 12Z	0	0	0	0.00%	1	0:00:24	0	0	0.00%	1	0:00:24
	0.2	0	0	0.00%	1	0:00:25	0	0	0.00%	1	0:00:24
	0.4	0	0	0.00%	1	0:00:24	0	0	0.00%	1	0:00:25
	0.5	0	0	0.00%	1	0:00:24	0	0	0.00%	1	0:00:24
	0.6	0	0	0.00%	1	0:00:25	0	0	0.00%	1	0:00:25
	0.8	0	0	0.00%	1	0:00:24	0	0	0.00%	1	0:00:25
	1	0	0	0.00%	1	0:00:25	0	0	0.00%	1	0:00:24

1 ^: the optimal solutions with $\Delta = [0,2]$ are identical.

2 #: over 3600 seconds computational limit

The BD approach is almost unable to solve the instances of VHHH-ZBAA and ZUUU-ZBAA within the one-hour computational limit as the flight routes VHHH-ZBAA and ZUUU-ZBAA have five alternative paths, and the combinatory problems are much more complex to solve. The computational results of BD and C&CG approaches for VHHH-ZBAA with $\Delta = 0$ and $\Delta = 2$ are presented in **Table 4** and **Table 5** respectively, while the results for ZUUU-ZBAA are presented in **Table 6** and **Table 7**. We only present the distinctive solutions for $\Delta = 2$ in **Table 5** and **Table 7**. For those results not presented in the table, their optimal solutions and optimal values are identical to the one solved with the parameter of $\Delta = 0$.

Table 4

Computational results for the instance set of VHHH-ZBAA $\Delta = 0$

VHHH-ZBAA		$\Delta = 0$									
		BD approach					C&CG approach				
week	Γ	UB	LB	gap	$\overline{Z}$	CPU	UB	LB	gap	$\overline{Z}$	CPU
1st Jan – 5th Jan 2019 00Z	0	140,406	140,406	0.00%	1	0:01:12	140,406	140,406	0.00%	1	0:01:13
	0.2	11,138,868	140,406	98.74%	33	#	11,138,868	11,138,868	0.00%	3	0:03:52
	0.4	12,660,868	140,406	98.89%	33	#	12,660,868	12,660,868	0.00%	5	0:06:41
	0.5	12,842,459	140,406	98.91%	33	#	12,842,459	12,842,459	0.00%	5	0:06:31
	0.6	12,945,422	140,406	98.92%	33	#	12,945,422	12,945,422	0.00%	6	0:08:03
	0.8	12,945,422	140,406	98.92%	32	#	12,945,422	12,945,422	0.00%	6	0:08:03
	1	12,945,422	140,406	98.92%	33	#	12,945,422	12,945,422	0.00%	6	0:08:15
1st Jan – 5th Jan 2019 12Z	0	0	0	0.00%	1	0:01:14	0	0	0.00%	1	0:01:11
	0.2	10,979,741	0	100.00%	33	#	10,979,741	10,979,741	0.00%	3	0:03:41
	0.4	11,775,375	0	100.00%	34	#	11,775,375	11,775,375	0.00%	4	0:05:04
	0.5	11,775,375	0	100.00%	34	#	11,775,375	11,775,375	0.00%	4	0:05:02
	0.6	11,775,375	0	100.00%	34	#	11,775,375	11,775,375	0.00%	4	0:05:01
	0.8	11,775,375	0	100.00%	34	#	11,775,375	11,775,375	0.00%	4	0:05:05
	1	11,775,375	0	100.00%	33	#	11,775,375	11,775,375	0.00%	4	0:05:07
6th Jan – 12th Jan 2019 00Z	0	0	0	0.00%	1	0:01:10	0	0	0.00%	1	0:01:09
	0.2	11,700,490	0	100.00%	34	#	11,700,490	11,700,490	0.00%	3	0:03:42
	0.4	12,887,389	0	100.00%	34	#	12,887,389	12,887,389	0.00%	5	0:06:27
	0.5	13,020,306	0	100.00%	34	#	13,020,306	13,020,306	0.00%	6	0:07:55
	0.6	13,123,270	0	100.00%	34	#	13,123,270	13,123,270	0.00%	6	0:08:04
	0.8	13,123,270	0	100.00%	34	#	13,123,270	13,123,270	0.00%	6	0:07:58
	1	13,123,270	0	100.00%	34	#	13,123,270	13,123,270	0.00%	6	0:07:57
6th Jan – 12th Jan 2019 12Z	0	0	0	0.00%	1	0:01:11	0	0	0.00%	1	0:01:10
	0.2	11,382,237	0	100.00%	34	#	11,583,485	11,583,485	0.00%	3	0:03:45
	0.4	12,479,275	0	100.00%	34	#	12,479,275	12,479,275	0.00%	4	0:05:11
	0.5	12,594,408	0	100.00%	34	#	12,594,408	12,594,408	0.00%	4	0:05:18
	0.6	12,594,408	0	100.00%	34	#	12,594,408	12,594,408	0.00%	4	0:05:20
	0.8	12,594,408	0	100.00%	34	#	12,594,408	12,594,408	0.00%	4	0:05:19
	1	12,594,408	0	100.00%	34	#	12,594,408	12,594,408	0.00%	4	0:05:07
13th Jan – 19th Jan 2019 00Z	0	0	0	0.00%	1	0:01:09	0	0	0.00%	1	0:01:13
	0.2	11,382,237	0	100.00%	35	#	11,382,237	11,382,237	0.00%	3	0:03:53
	0.4	12,580,369	0	100.00%	34	#	12,580,369	12,580,369	0.00%	4	0:05:18
	0.5	12,683,332	0	100.00%	34	#	12,683,332	12,683,332	0.00%	4	0:05:21
	0.6	12,683,332	0	100.00%	34	#	12,683,332	12,683,332	0.00%	4	0:05:20
	0.8	12,683,332	0	100.00%	34	#	12,683,332	12,683,332	0.00%	4	0:05:20
	1	12,683,332	0	100.00%	34	#	12,683,332	12,683,332	0.00%	4	0:05:19
13th Jan – 19th Jan 2019 12Z	0	0	0	0.00%	1	0:01:11	0	0	0.00%	1	0:01:12
	0.2	11,382,237	0	100.00%	34	#	11,382,237	11,382,237	0.00%	3	0:03:48
	0.4	12,234,034	0	100.00%	34	#	12,234,034	12,234,034	0.00%	4	0:05:11
	0.5	12,234,034	0	100.00%	34	#	12,234,034	12,234,034	0.00%	4	0:05:05
	0.6	12,234,034	0	100.00%	34	#	12,234,034	12,234,034	0.00%	4	0:05:10
	0.8	12,234,034	0	100.00%	34	#	12,234,034	12,234,034	0.00%	4	0:05:13

	1	12,234,034	0	100.00%	34	#	12,234,034	12,234,034	0.00%	4	0:05:10
20th Jan – 26th Jan 2019 00Z	0	0	0	0.00%	1	0:01:10	0	0	0.00%	1	0:01:14
	0.2	11,583,485	0	100.00%	34	#	11,583,485	11,583,485	0.00%	3	0:03:58
	0.4	12,561,648	0	100.00%	34	#	12,561,648	12,561,648	0.00%	4	0:05:28
	0.5	12,608,450	0	100.00%	34	#	12,608,450	12,608,450	0.00%	4	0:05:25
	0.6	12,608,450	0	100.00%	34	#	12,608,450	12,608,450	0.00%	4	0:05:28
	0.8	12,608,450	0	100.00%	34	#	12,608,450	12,608,450	0.00%	4	0:05:26
	1	12,608,450	0	100.00%	34	#	12,608,450	12,608,450	0.00%	4	0:05:29
20th Jan – 26th Jan 2019 12Z	0	0	0	0.00%	1	0:01:11	0	0	0.00%	1	0:01:14
	0.2	11,916,717	0	100.00%	34	#	11,369,134	11,369,134	0.00%	4	0:05:20
	0.4	13,411,572	0	100.00%	34	#	13,411,572	13,411,572	0.00%	7	0:10:11
	0.5	13,595,971	0	100.00%	34	#	13,595,971	13,595,971	0.00%	7	0:10:27
	0.6	13,647,453	0	100.00%	34	#	13,647,453	13,647,453	0.00%	7	0:10:29
	0.8	13,647,453	0	100.00%	34	#	13,647,453	13,647,453	0.00%	7	0:10:20
	1	13,647,453	0	100.00%	34	#	13,647,453	13,647,453	0.00%	7	0:10:22
27th Jan – 31st Jan 2019 00Z	0	0	0	0.00%	1	0:01:09	0	0	0.00%	1	0:01:15
	0.2	11,180,989	0	100.00%	34	#	11,583,485	11,583,485	0.00%	3	0:03:52
	0.4	12,239,649	0	100.00%	34	#	12,280,836	12,280,836	0.00%	4	0:05:29
	0.5	12,280,836	0	100.00%	34	#	12,280,836	12,280,836	0.00%	4	0:05:31
	0.6	12,280,836	0	100.00%	34	#	12,280,836	12,280,836	0.00%	4	0:05:19
	0.8	12,280,836	0	100.00%	34	#	12,280,836	12,280,836	0.00%	4	0:05:27
	1	12,280,836	0	100.00%	34	#	12,280,836	12,280,836	0.00%	4	0:05:23
27th Jan – 31st Jan 2019 12Z	0	2,307,337	2,307,337	0.00%	1	0:01:11	2,307,337	2,307,337	0.00%	1	0:01:12
	0.2	11,774,438	2,307,337	80.40%	34	#	11,774,438	11,774,438	0.00%	4	0:05:10
	0.4	12,028,104	2,307,337	80.82%	34	#	12,028,104	12,028,104	0.00%	4	0:05:10
	0.5	12,028,104	2,307,337	80.82%	34	#	12,028,104	12,028,104	0.00%	4	0:05:12
	0.6	12,028,104	2,307,337	80.82%	34	#	12,028,104	12,028,104	0.00%	4	0:05:10
	0.8	12,028,104	2,307,337	80.82%	34	#	12,028,104	12,028,104	0.00%	4	0:05:07
	1	12,028,104	2,307,337	80.82%	34	#	12,028,104	12,028,104	0.00%	4	0:05:11

#: over 3600 seconds computational limit

Table 5

Computational results for the instance set of VHHH-ZBAA $\Delta = 2$

VHHH-ZBAA		$\Delta = 2$									
		BD approach					C&CG approach				
week	Γ	UB	LB	gap	$\overline{Z}$	CPU	UB	LB	gap	$\overline{Z}$	CPU
27th Jan – 31st Jan 2019 00Z	0	-	-	-	-	0:01:10	-	-	-	-	0:01:15
	0.2	-	-	-	-	#	11,382,237	11,382,237	0.00%	3	0:03:56
	0.4	-	-	-	-	#	-	-	-	-	0:05:31
	0.5	-	-	-	-	#	-	-	-	-	0:05:29
	0.6	-	-	-	-	#	-	-	-	-	0:05:25
	0.8	-	-	-	-	#	-	-	-	-	0:05:34
	1	-	-	-	-	#	-	-	-	-	0:05:28
Others		-									

-: the optimal solutions are identical to the solution with $\Delta = 0$ in **Table 4**.

#: over 3600 seconds computational limit

Table 6

Computational results for the instance set of ZUUU-ZBAA $\Delta = 0$

ZUUU-ZBAA		$\Delta = 0$									
		BD approach					C&CG approach				
week	Γ	UB	LB	gap	$\overline{Z}$	CPU	UB	LB	gap	$\overline{Z}$	CPU
1st Jan – Γth	0	1,216,850	1,216,850	0.00%	1	0:01:15	1,216,850	1,216,850	0.00%	1	0:01:15
	0.2	6,013,117	1,258,974	79.06%	35	#	6,013,117	6,013,117	0.00%	4	0:05:25
	0.4	8,267,100	1,258,974	84.77%	35	#	8,267,100	8,267,100	0.00%	6	0:08:25

	0.5	9,308,911	1,258,974	86.48%	35	#		9,308,911	9,308,911	0.00%	6	0:08:27
	0.6	10,023,108	1,258,974	87.44%	35	#		10,023,108	10,023,108	0.00%	7	0:10:02
	0.8	10,656,806	1,258,974	88.19%	35	#		10,656,806	10,043,702	5.75%	8	1:00:40
	1	10,731,691	1,258,974	88.27%	35	#		10,731,691	10,043,702	6.41%	8	1:00:40
1st Jan – 5th Jan 2019 12Z	0	0	0	0.00%	1	0:01:17		0	0	0.00%	1	0:01:13
	0.2	6,428,719	70,203	98.91%	35	#		6,428,719	6,428,719	0.00%	6	0:08:14
	0.4	9,512,968	0	100.00%	32	#		9,512,968	9,512,968	0.00%	7	0:09:47
	0.5	10,808,913	0	100.00%	30	#		10,808,913	10,808,913	0.00%	7	0:09:44
	0.6	11,958,838	0	100.00%	30	#		11,958,838	11,958,838	0.00%	9	0:13:29
	0.8	13,460,244	70,203	99.48%	35	#		13,460,244	13,460,244	0.00%	11	0:17:13
	1	13,460,244	0	100.00%	30	#		13,460,244	13,460,244	0.00%	11	0:16:16
6th Jan – 12th Jan 2019 00Z	0	0	0	0.00%	1	0:01:13		0	0	0.00%	1	0:01:16
	0.2	6,428,719	0	100.00%	35	#		6,428,719	6,428,719	0.00%	6	0:08:38
	0.4	9,512,968	0	100.00%	35	#		9,512,968	9,512,968	0.00%	7	0:10:13
	0.5	10,808,913	0	100.00%	35	#		10,808,913	10,808,913	0.00%	7	0:10:18
	0.6	11,958,838	0	100.00%	35	#		11,958,838	11,958,838	0.00%	9	0:13:47
	0.8	13,460,244	0	100.00%	35	#		13,460,244	13,460,244	0.00%	10	0:15:35
	1	13,460,244	0	100.00%	38	#		13,460,244	13,460,244	0.00%	10	0:15:29
6th Jan – 12th Jan 2019 12Z	0	0	0	0.00%	1	0:01:14		0	0	0.00%	1	0:01:14
	0.2	6,428,719	0	100.00%	35	#		6,428,719	6,428,719	0.00%	3	0:04:06
	0.4	9,512,968	0	100.00%	35	#		9,512,968	9,512,968	0.00%	4	0:05:34
	0.5	10,808,913	0	100.00%	35	#		10,808,913	10,808,913	0.00%	5	0:06:56
	0.6	11,958,838	0	100.00%	35	#		11,958,838	11,958,838	0.00%	8	0:11:56
	0.8	13,460,244	0	100.00%	35	#		13,460,244	13,460,244	0.00%	10	0:15:19
	1	13,460,244	0	100.00%	35	#		13,460,244	13,460,244	0.00%	10	0:15:28
13th Jan – 19th Jan 2019 00Z	0	0	0	0.00%	1	0:01:13		0	0	0.00%	1	0:01:15
	0.2	6,428,719	0	100.00%	35	#		6,428,719	6,428,719	0.00%	5	0:06:45
	0.4	9,448,380	0	100.00%	35	#		9,448,380	9,448,380	0.00%	7	0:09:59
	0.5	10,729,350	0	100.00%	35	#		10,729,350	10,729,350	0.00%	8	0:11:37
	0.6	11,879,274	0	100.00%	35	#		11,879,274	11,879,274	0.00%	9	0:13:23
	0.8	13,380,681	0	100.00%	35	#		13,380,681	13,380,681	0.00%	9	0:13:23
	1	13,380,681	0	100.00%	35	#		13,380,681	13,380,681	0.00%	9	0:13:24
13th Jan – 19th Jan 2019 12Z	0	0	0	0.00%	1	0:01:11		0	0	0.00%	1	0:01:15
	0.2	6,428,719	0	100.00%	35	#		7,267,409	7,267,409	0.00%	5	0:06:58
	0.4	9,512,968	0	100.00%	35	#		9,512,968	9,512,968	0.00%	7	0:10:05
	0.5	10,808,913	0	100.00%	35	#		10,808,913	10,808,913	0.00%	7	0:10:03
	0.6	11,958,838	0	100.00%	35	#		11,958,838	11,958,838	0.00%	9	0:13:20
	0.8	13,460,244	0	100.00%	35	#		13,460,244	13,460,244	0.00%	11	0:16:55
	1	13,460,244	0	100.00%	35	#		13,460,244	13,460,244	0.00%	11	0:16:54
20th Jan – 26th Jan 2019 00Z	0	0	0	0.00%	1	0:01:12		0	0	0.00%	1	0:01:12
	0.2	6,428,719	0	100.00%	35	#		6,428,719	6,428,719	0.00%	6	0:08:27
	0.4	9,512,968	0	100.00%	35	#		9,512,968	9,512,968	0.00%	7	0:09:57
	0.5	10,808,913	0	100.00%	35	#		10,808,913	10,808,913	0.00%	7	0:10:01
	0.6	11,958,838	0	100.00%	35	#		11,958,838	11,958,838	0.00%	9	0:13:18
	0.8	13,460,244	0	100.00%	35	#		13,460,244	13,460,244	0.00%	10	0:15:01
	1	13,460,244	0	100.00%	35	#		13,460,244	13,460,244	0.00%	10	0:14:57
20th Jan – 26th Jan 2019 12Z	0	0	0	0.00%	1	0:01:13		0	0	0.00%	1	0:01:12
	0.2	6,428,719	0	100.00%	35	#		6,428,719	6,428,719	0.00%	6	0:08:14
	0.4	9,380,987	0	100.00%	35	#		9,380,987	9,380,987	0.00%	7	0:09:42
	0.5	10,588,944	0	100.00%	35	#		10,588,944	10,588,944	0.00%	7	0:09:42
	0.6	11,738,869	0	100.00%	35	#		11,738,869	11,738,869	0.00%	9	0:12:52
	0.8	13,460,244	0	100.00%	35	#		13,460,244	13,460,244	0.00%	11	0:16:18
	1	13,460,244	0	100.00%	35	#		13,460,244	13,460,244	0.00%	11	0:16:20
27th Jan – 31st Jan 2019 00Z	0	0	0	0.00%	1	0:01:14		0	0	0.00%	1	0:01:14
	0.2	16,736,384	0	100.00%	35	#		7,574,430	7,574,430	0.00%	6	0:08:10
	0.4	23,677,113	0	100.00%	35	#		9,512,968	9,512,968	0.00%	7	0:09:48
	0.5	25,600,675	0	100.00%	35	#		10,808,913	10,808,913	0.00%	7	0:09:46
	0.6	27,292,096	0	100.00%	35	#		11,958,838	11,958,838	0.00%	10	0:14:39
	0.8	29,316,749	0	100.00%	35	#		13,460,244	13,460,244	0.00%	11	0:16:16
	1	30,074,941	0	100.00%	35	#		13,460,244	13,460,244	0.00%	11	0:16:19

27th Jan – 31st Jan 2019 12Z	0	898,597	898,597	0.00%	1	0:01:14	898,597	898,597	0.00%	1	0:01:14
	0.2	17,713,607	898,597	94.93%	35	#	8,096,740	8,096,740	0.00%	5	0:06:51
	0.4	24,664,636	898,597	96.36%	35	#	10,843,078	10,843,078	0.00%	7	0:09:50
	0.5	26,588,196	898,597	96.62%	35	#	11,993,003	11,993,003	0.00%	9	0:13:07
	0.6	28,279,620	898,597	96.82%	35	#	13,051,194	13,051,194	0.00%	11	0:16:24
	0.8	32,330,796	898,597	97.22%	34	#	13,460,244	13,460,244	0.00%	11	0:16:25
	1	32,405,680	898,597	97.23%	34	#	13,460,244	13,460,244	0.00%	11	0:16:33

#: over 3600 seconds computational limit

Table 7

Computational results for the instance set of ZUUU-ZBAA $\Delta = 1$

ZUUU-ZBAA		$\Delta = 2$									
		BD approach					C&CG approach				
week	Γ	UB	LB	gap	$\overline{Z}$	CPU	UB	LB	gap	$\overline{Z}$	CPU
27th Jan – 31st Jan 2019 00Z	0	-	-	-	-	0:01:14	-	-	-	-	0:01:16
	0.2	-	-	-	-	#	7,214,055	7,214,055	0.00%	5	0:06:40
	0.4	-	-	-	-	#	-	-	-	-	0:09:41
	0.5	-	-	-	-	#	-	-	-	-	0:09:40
	0.6	-	-	-	-	#	-	-	-	-	0:11:12
	0.8	-	-	-	-	#	-	-	-	-	0:14:38
	1	-	-	-	-	#	-	-	-	-	0:14:30
Other		-									

-: the optimal solutions are identical to the solution with $\Delta = 0$ in **Table 6**.

#: over 3600 seconds computational limit

The two results were extracted for further analysis in **Table 8** and **Table 9**. The estimated fuel cost of instance VHHH-ZBAA, using the weather dataset from 27th Jan – 31st Jan 2019 at 00Z with $\Delta = 0$, is $39,148.17; however, the solution chose another route with a 0.1% fuel cost increase. The flight climbed up one flight level from FL310 to FL330 at (114.525, 32.3300) until it reached (114.532, 32.4100) and maintained cruising level. The flight then descended from FL330 to FL310 starting from (114.715,0, 34.3017) to (114.717, 34. 3251). The reduced estimated contrail cost from the common route is 1.77%. The alternative paths are presented in **Figure 15** and the proposed flight route (only with the change in flight level presented in yellow) is shown in **Figure 16**.

Similar approach can also be found for the instance ZUUU-ZBAA, using the weather dataset from 27th Jan – 31st Jan 2019 at 00Z. The flight ascended one flight level from FL310 to FL330 from (108.31200, 33.31830) to (108.345, 33.3725) and maintained cruising from (108.345, 33.3725) to (108.85300, 34.22170). The flight descended to FL310 from (108.915, 34.5983) to (108.9198 to 34.6116) and remained at that cruising level until it reached (108.91500, 34.59830). The reduction of the cost is 5.00%. The alternative paths are presented in **Figure 17** and the proposed flight route (only with the change in flight level presented in yellow) is shown in **Figure 18**.

Table 10 illustrated that the C&CG approach could yield global optimum, while BD approach can only solve very limited number of instances for the global optimal. The average optimal gap and average CPU time are presented.

Table 8

The optimal estimated fuel cost in numerical analysis

Instances	**Optimal solutions**	**The estimated**	**Percentage change in estimated**

			fuel cost	fuel cost from common route
ZSSS-VHHH	Common route		$67,358.99	Nil
ZUUU-VHHH	Common route		$25,797.06	Nil
VHHH-ZBAA	27th Jan – 31st Jan 2019 00Z, $\Gamma = 0.2$	Common route	$39,148.17	Nil
		$\Delta = 0$	$39,148.17	Nil
		$\Delta = 2$	$39,185.89	+0.1%
ZUUU-ZBAA	27th Jan – 31st Jan 2019 00Z, $\Gamma = 0.2$	Common route	$18,178.63	Nil
		$\Delta = 0$	$18,178.63	Nil
		$\Delta = 2$	$18,706.64	+2.82%

Table 9

The optimal robust solutions of estimated contrail cost in numerical analysis

Instances	Optimal robust solutions		The estimated contrail cost	Percentage change in estimated contrail cost from common route
VHHH-ZBAA	27th Jan – 31st Jan 2019 00Z, $\Gamma = 0.2$	$\Delta = 0$	$11,583,486	Nil
		$\Delta = 2$	$11,382,238	-1.77%
ZUUU-ZBAA	27th Jan – 31st Jan 2019 00Z, $\Gamma = 0.2$	$\Delta = 0$	$7,754,430	Nil
		$\Delta = 2$	$7,214,055	-5.00%

Table 10

Summary of computational performance

Instances	Average optimal gap		Average CPU time (hh:mm:ss)	
Algorithms	BD approach	C&CG approach	BD approach	C&CG approach
ZSSS-VHHH	0.00%	0.00%	0:00:03	0:00:03
ZUUU-VHHH	0.00%	0.00%	0:01:53	0:01:14
VHHH-ZBAA	83.97%	0.00%	0:51:36	0:05:17
ZUUU-ZBAA	83.97%	0.00%	0:51:36	0:10:41

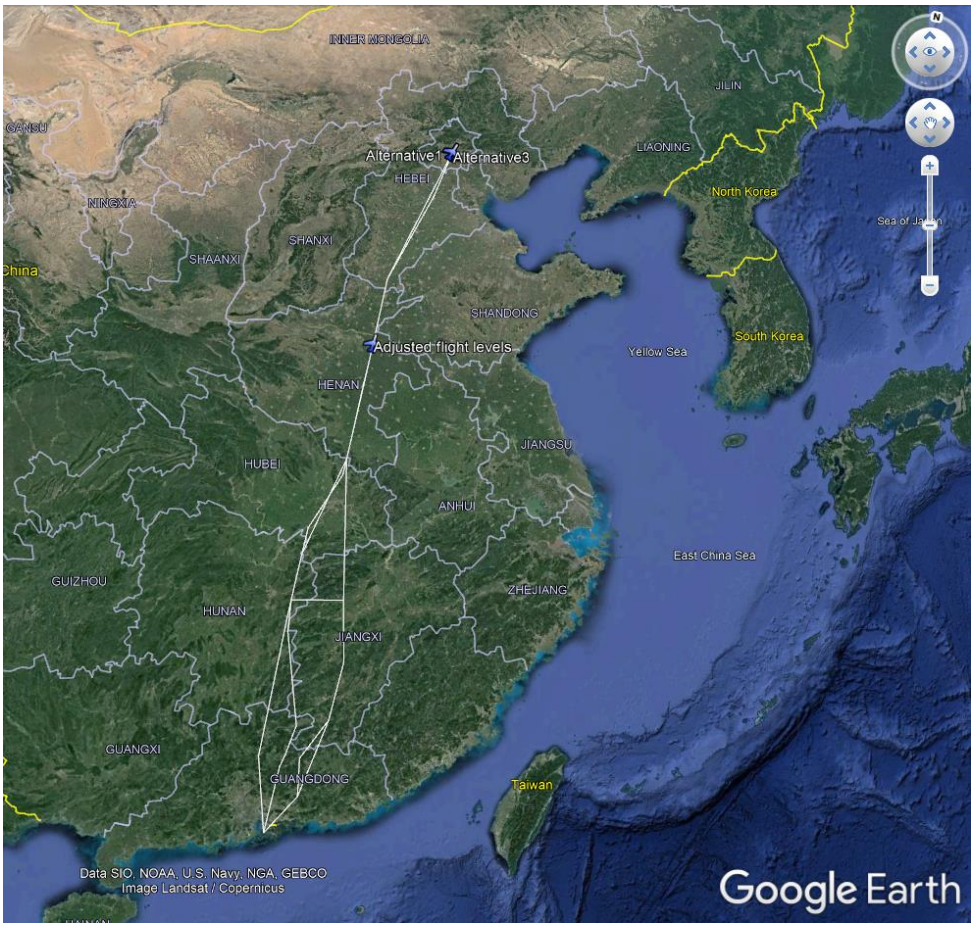

Figure 15. The VHHH-ZBAA alternative paths

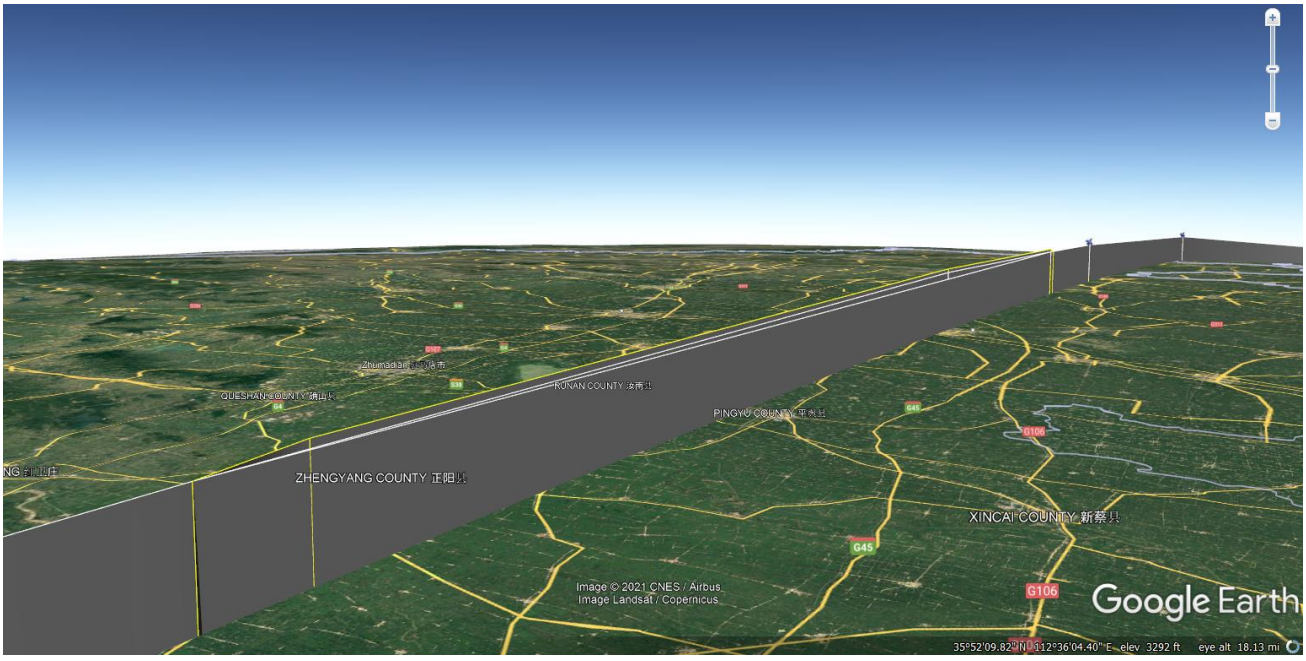

Figure 16. Change of flight levels for one of the VHHH -ZBAA alternative paths with 1.77% contrail cost reduction and 0.1% fuel consumption cost increase

Figure 17. The ZUUU-VBAA alternative paths

Figure 18. Change of flight levels for one of the VHHH -ZBAA alternative paths with 5.00% contrail cost reduction and 2.82% fuel consumption cost increase

5.3. Managerial insights

The proposed emission-aware adjustable robust flight path planning model can provide many competitive advantages to further enhance the operational efficiency, as well as the reduction on aviation emission. In the coming future, technological advancements in aircraft engine design, fuel choices and availability of renewable energy may result in a lower fuel price in flight operations. The cost reduction will create fundamental changes to the competition between airlines. Air ticket pricing may no longer be the major factor affecting the passengers' choices of airlines. They may shift their concerns to the airline's service quality (Lee et al. 2018) and the demonstration of corporate social responsibility initiatives by the airline. Corporate reputation, passenger satisfaction and trust between the consumers and the company can further boost the airline's profit margin in the long run (Zhang, Cao, et al. 2020). Meanwhile, airlines are pressured to comply with different internationally recognised climate and emission trade policies, as well as the global initiative to reduce the impacts of aviation emission has on climate change. Adoption of eco-friendly practices in flight path planning are welcomed by the public. As a matter of fact, "going green" provides many financial, societal and environmental benefits to the brand value, while the additional costs incurred due to changes in operational costs and flight time are insignificant. Moreover, the proposed data-driven emission-aware adjustable robust flight path planning offers a better integration with spatial meteorological informatics regarding the flight route problem. The weather data-driven approach in flight path planning can secure an accurate prediction of the most eco-friendly and operationally efficient flight path solution and achieve better business and societal goals.

6. Conclusion

This paper presents an emission-aware adjustable robust flight path planning model. A Two-stage optimisation framework with Benders cuts and column-and-constraints generation approaches is adopted to evaluate the flight path alternatives in terms of fuel consumption and contrail cost. The data-driven framework generates spatial meteorological conditions within the concerned regions and estimate the contrail map at different flights levels. Given the spatial meteorological information, airlines can determine a reduced-contrail-generating flight path for operational use. As flight route requests are usually provided by airlines ahead of a season, the actual weather conditions at time of operation cannot be accounted for during flight route planning, and we will have to rely on historical weather data for temperature, air pressure and relative humidity to water predictions, causing the predicted spatial meteorological information to deviate from the actual weather information. Thus, the introduction of uncertain contrail length to each alternative route can provide certain degree of protection from worse-case scenarios. The adjustability of budgeted uncertainty, pre-determined constrained flight levels set, and maximum number of flight levels change can provide airlines with the flexibility of developing a flight path planning solution in accordance with the degree of robustness, operational efficiency and other airline desired outcomes.

We consider a set of budget uncertainty and the maximum time for flight levels change as model parameters, with the objective function considering the total cost of fuel consumption and contrail cost. The fuel consumption cost is associated with the business objective, while the contrail cost is linked with the societal objective. In our study, the total cost of fuel consumption and contrail cost are reduced. At the same time, the reduction of total contrail cost can be enhanced further with a slightly increase in total fuel consumption cost compared to baseline scenario. The trade-off between additional fuel consumption and aviation emission is sensitive to the cost index of fuel consumption and contrail cost. The sustainability of flight route planning relies on the airline's policy on corporate responsibility and contrail cost taxation. We can see the potential of adopting the emission-aware flight route planning in future business model. The proposed approach can help sustain an adequate level of service, while reducing aviation emissions within the atmosphere.

Several interesting aspects of the emission-aware adjustable robust flight path planning model can be considered as future research directions. First, data analytics can be included in the classification of spatial meteorological condition. In this paper, we assumed that the recorded weather data will have the same pattern when compared to the actual condition during operations. However, one could utilise a data mining approach to classify the weather information into different groups as input parameters and yield a reliable data-driven solution. Second, the proposed model only considered the generation of flight path planning in pre-tactical decision-making level. Large-scale air traffic flow modelling can be adopted in future research by considering the constrained regional emission levels, cross waypoint conflict resolution and efficient flight trajectory optimisation. However, such large-scale optimisation problem will require a more advanced optimisation algorithm. Third, matheuristics, meta-heuristics and hyper-heuristics can be incorporated to solve the large-scale optimisation problem and yield a promising solution to meet the industry's needs. Alternatively, the decomposition of multi-flight path optimisation problem into different sub-regions can increase computational efficiency for each scenario.

Appendix A. estimation of spatial meteorological data

The saturation vapour pressure over water is measured by a function $e^{liq}(\cdot)$ at a given temperature. We can then estimate the threshold of the first condition of contrail formation based on the temperature $\hat{\phi}(T_z)$ at geographic coordinate z. The estimated of threshold, presented in equation (43), is calculated with respect to the value of temperature threshold at liquid saturation t_z^{contr}, temperature $\hat{\phi}(k_z^{TEMP})$, while the value of temperature threshold at liquid saturation t_z^{contr}, presented in equation (44) is associated with G_z. G_z is the value associated with the emission index of water vapor El_{H_2O}, isobaric heat capacity of air C_p, the estimated air pressure $\hat{\phi}(k_z^{AP})$ as presented in Equation (45). Detailed explanations of the saturation vapour pressure over water and estimation of the 1st condition threshold of contrail formation can be found in Soler, Zou, and Hansen (2014)'s work.

The estimation of 1st condition threshold $\hat{\phi}(r_z^{contr})$

$$\hat{\phi}(r_z^{contr}) = \frac{G_z\left(\hat{\phi}(T_z) - t_z^{contr}\right) + e^{liq}(t_z^{contr})}{e^{liq}(T_z)}, \forall z \in Z \tag{43}$$

$$t_z^{contr} = -46.46 + 9.43\, log(G_z - 0.053) + 0.72\, log^2(G_z - 0.053), \forall z \in Z \tag{44}$$

$$G_z = \frac{El_{H_2O} C_p \hat{\phi}(k_z^{AP})}{\varepsilon Q(1-\eta)}, \forall z \in Z$$
$$, where\ El_{H_2O} = 1.25$$
$$C_p = 1004\ [j\ per\ kg]$$
$$\varepsilon = 0.6222$$
$$Q = 4.3 \times 10^6 [j\ per\ kg]$$
$$\eta = 0.15 \tag{45}$$

The estimation of relative humanity to ice $\hat{\phi}\left(k_z^{RH\_ice}\right)$ is subject to the relative humidity to water $\hat{\phi}\left(k_z^{RH\_water}\right)$ and temperature $\hat{\phi}(k_z^{TEMP})$ at geographic coordinate z for each flight level $f \in FL$, as illustrated in equation (46).

The estimation of relative humidity to ice

$$\hat{\phi}\left(k_z^{RH\_ice}\right) = \hat{\phi}\left(k_z^{RH\_water}\right) \frac{6.0612 \exp \frac{18.102\hat{\phi}(k_z^{TEMP})}{249.52 + \hat{\phi}(k_z^{TEMP})}}{6.1162 \exp \frac{22.577\hat{\phi}(k_z^{TEMP})}{237.78 + \hat{\phi}(k_z^{TEMP})}}, \forall z \in Z \tag{46}$$

Appendix B. The OpenAP model

The OpenAP model is defined by the four-degrees-of-freedom point-mass model as illustrated in Equations set (47) and **Figure 19Error! Reference source not found.**. For the detail of the analysis of aircraft surveillance data and performance model, readers can refer to a Ph.D. thesis (Sun 2019).

$$\begin{aligned}
\frac{dx}{dt} &= V \sin\psi \cos\gamma \\
\frac{dy}{dt} &= V \cos\psi \cos\gamma \\
\frac{dh}{dt} &= V \sin\gamma \\
\frac{d\psi}{dt} &= \frac{g \tan\chi}{V \cos\gamma} \\
\frac{dV}{dt} &= \frac{T - D}{m} - g \sin\gamma
\end{aligned} \tag{47}$$

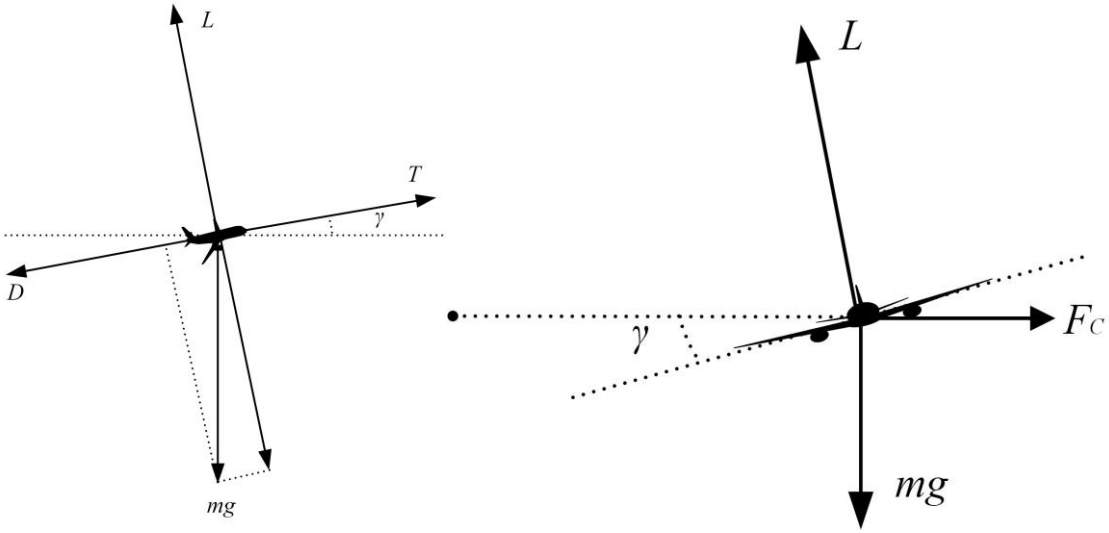

Figure 19. The point-mass dynamic performance model (Sun, Hoekstra, and Ellerbroek 2020).

In our proposed model, we only measure the contrail length at the cruising stage. The presence of contrail at flight level f_i is considered as a piece-wise decision. If flight remain at the same flight level from waypoints i to j, we will calculate the accumulated contrail length from waypoints i to j, as shown in **Figure 20Error! Reference source not found.**. If flight is ascending or descending to target flight level $f_j, f_i \neq f_j$, we will only calculate the accumulated contrail length after change of flight levels, as shown in **Figure 21Error! Reference source not found.** and **Figure 22Error! Reference source not found.**. The estimated time and distance for flight level changes are calculated by using the OpenAP model. Thus, we can estimate the true effect of contrail length and its cost in a flight path planning model.

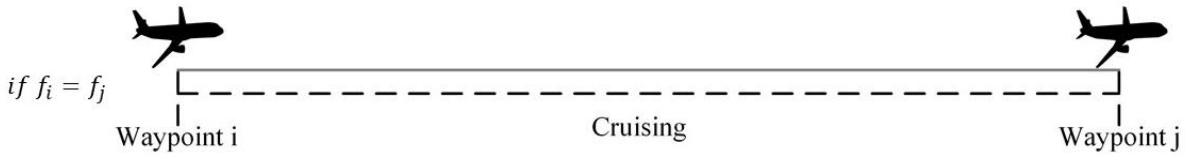

Figure 20. Illustration of cruising stage with no flight level changes

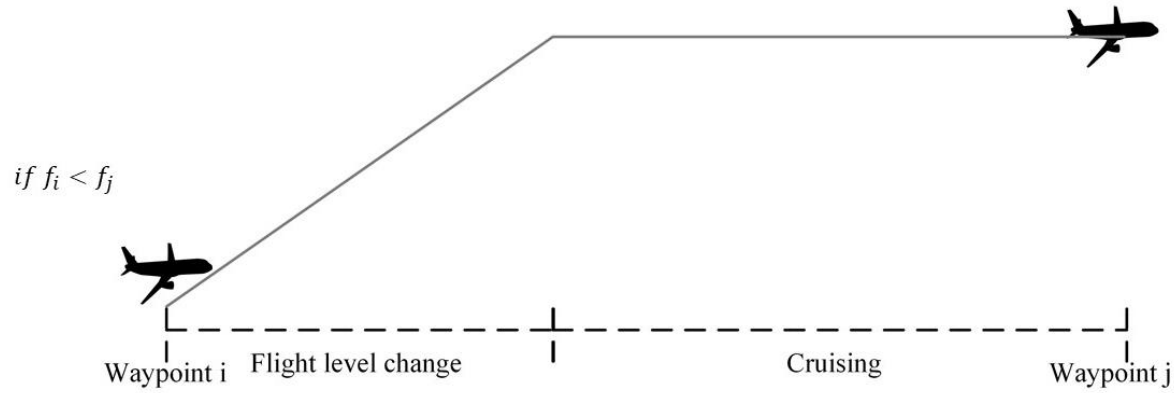

Figure 21. Illustration of cruising stage by increasing the flight levels

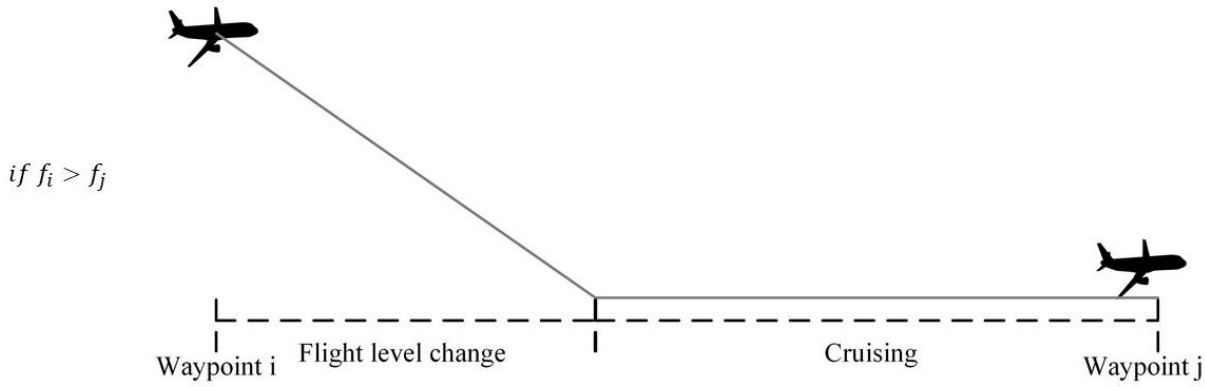

Figure 22. Illustration of cruising stage by reducing the flight levels

Appendix C. The locations and ID of weather stations provided the Wyoming weather web, University of Wyoming, Laramie, USA

ID	Weather stations	Latitude	Longitude	ID	Weather stations	Latitude	Longitude
51463	Urumqi	87.62	43.78	54161	YCC Changchun	125.21	43.9
52418	Dunuang	94.68	40.15	54218	Chifeng	118.96	42.26
52866	Xining	101.75	36.71	54292	Yanji	129.46	42.88
52983	Yuzhong	104.15	35.87	54342	YYY Shenyang	123.43	41.76
53915	Pingliang	106.66	35.55	54374	Linjiang	126.91	41.71
57131	Jinghe	108.97	34.43	54511	BAA Beijing	116.28	39.93
58203	Fuyang	115.73	32.86	54662	YTL Dalian	121.63	38.9
58238	Nanjing	118.8	32	55299	Nagqu	92.06	31.48
58362	Shanghai	121.46	31.4	56029	Yushu	97.01	33.01
58150	Sheyang	120.25	33.76	56080	Hezuo	102.9	35
54857	Qingdao	120.33	36.06	56146	Garze	100	31.61
54727	Zhangqiu	117.55	36.7	56187	Wenjiang	103.83	30.7
53772	Taiyuan	112.55	37.78	56571	Xichang	102.26	27.9
57083	Zhengzhou	113.65	34.71	56691	Weining	104.28	26.86
58027	Xuzhou	117.15	34.28	56739	Tengchong	98.48	25.11
57178	Nanyang	112.58	33.03	56778	PPP Kunming	102.68	25.01
53845	Yan An	109.5	36.6	56964	Simao	100.98	22.76
53463	Hohhot	111.68	40.81	57127	Hanzhong	107.03	33.06
53513	Linhe	107.4	40.76	57447	Enshi	109.46	30.28
53614	Yinchuan	106.21	38.48	57461	Yichang	111.3	30.7
52533	Jiuquan	98.48	39.76	57494	HHH Wuhan	114.13	30.61
52267	Ejin Qi	101.06	41.95	57516	UCK Chongqing	106.48	29.51
52323	Mazong Shan	97.03	41.8	57679	GCS Changsha	113.08	28.2
52681	Minqin	103.08	38.63	57816	UGY Guiyang	106.65	26.48
52203	Hami	93.51	42.81	57957	GKL Guilin	110.3	25.33
45504	Kings Park	114.17	22.31	57972	Chenzhou	113.03	25.8
50527	Hailar	119.75	49.21	57993	SGZ Ganzhou	114.95	25.85
50557	Nenjiang	125.23	49.16	58457	SHC Hangzhou	120.16	30.23
50774	Yichun	128.9	47.71	58606	SCN Nanchang	115.91	28.6
50953	Harbin	126.76	45.75	58665	Hongjia	121.41	28.61
51076	Altay	88.08	47.73	58725	Shaowu	117.46	27.33
51709	WSH Kashi	75.98	39.46	58847	SFZ Fuzhou	119.28	26.08
51828	WTN Hotan	79.93	37.13	59134	SAM Xiamen	118.08	24.48
51839	Minfeng	82.71	37.06	59211	Baise	106.6	23.9
52818	Golmud	94.9	36.41	59265	Wuzhou	111.3	23.48
52836	Dulan	98.1	36.3	59280	Qing Yuan	113.05	23.66
53068	Erenhot	112	43.65	59316	GOW Shantou	116.66	23.35
54102	Xilin Hot	116.06	43.95	59431	GNN Nanning	108.21	22.63
54135	Tongliao	122.26	43.6	59758	GHK Haikou	110.35	20.03

Appendix D. The alternative paths of the case instances

Instances	AltPath	Flight plan
VHHH-ZBAA	5	{VHHH, UBDOB, XEBUL, EGEDA, PANBO, ANISA, ESDOS, OBLIK, IDULA, AKOMA, WXI, AVNIX, ZBAA} {VHHH, UBDOB, MABAG, EGEDA, PANBO, ANISA, ESDOS, OBLIK, IDULA, AKOMA, WXI, AVNIX, ZBAA} {VHHH, UBDOB, MABAG, EGEDA, PANBO, ANISA, PAVTU, AKUBA, DAPRO, ESDOS, OBLIK, IDULA, AKOMA, WXI, AVNIX, ZBAA} {VHHH, SANIP, WYN, NNX, BEMAG, NIVEM, PAVTU, AKUBA, DAPRO, ESDOS, OBLIK, IDULA, AKOMA, WXI, AVNIX, ZBAA} {VHHH, YIN, BUBDA, LIG, PAVTU, LUMKO, AKUBA, DAPRO, LKO, HOK, ESDOS, OBLIK, ZHO, IDULA, AKOMA, WXI, ZBAA}
ZSSS-VHHH	2	{ZSSS, TOL, ELNEX, SHR, XUVGI, SAGON, PLT, VHHH} {ZSSS, TOL, ELNEX, SHR, XUVGI, SAGON, PLT, MABAG, BILAT, VHHH}
ZUUU-VHHH	2	{ZUUU, XYO, UKEGO, IDSEG, QNX, KWE, KAGRA, ESNIB, ELKAL, MUBEL, VHHH} {ZUUU, XYO, IDSEG, QNX, KWE, ESNIB, ELKAL, MAMSI, MUBEL, GYA, VHHH}
ZUUU-ZBAA	5	{ZUUU, ARAPA, SUBUL, NSH, DOVOP, LOVRA, OKVUM, TYN, EXUMI, ZBAA} {ZUUU, DOREX, ARAPA, SUBUL, ONEBA, NSH, MIZ, WJC, OKVUM, TYN, EXUMI, NONIT, LARAD, BOBAK, ZBAA} {ZUUU, OGOMO, TOREG, SUBUL, ONEBA, NSH, MIZ, WJC, OKVUM, TYN, UBLAT, ISGOD, UBTAB, SAKOD, ENGIL, ZBAA} {ZUUU, SUBUL, NSH, OKVUM, EXUMI, NONIT, LARAD, ZBAA} {ZUUU, ARAPA, SUBUL, NSH, DOVOP, LOVRA, OKVUM, TYN, EXUMI, ZBAA}

AltPath: The number of alternative paths

Do not use the flight plan in actual operations. Only for simulation purpose.

References

Abdelghany, Khaled, Ahmed Abdelghany, and Tim Niznik. 2007. "Managing severe airspace flow programs: The Airlines' side of the problem." *Journal of Air Transport Management* 13 (6):329-37. doi: https://doi.org/10.1016/j.jairtraman.2007.05.004.

Abeyratne, Ruwantissa. 2019. "Aviation and the Carbon Debate: Aircraft Engine Emissions–Carbon Offsetting or Carbon Tax?" *Environmental Policy and Law* 49:4-5.

Alam, Sameer, Kamran Shafi, Hussein A. Abbass, and Michael Barlow. 2009. "An ensemble approach for conflict detection in Free Flight by data mining." *Transportation Research Part C: Emerging Technologies* 17 (3):298-317. doi: https://doi.org/10.1016/j.trc.2008.12.002.

Amirfakhrian, Majid, and Faramarz Samavati. 2021. "Weather daily data approximation using point adaptive ellipsoidal neighborhood in scattered data interpolation methods." *Applied Mathematics and Computation* 392:125717. doi: https://doi.org/10.1016/j.amc.2020.125717.

An, Y., and B. Zeng. 2015. "Exploring the Modeling Capacity of Two-Stage Robust Optimization: Variants of Robust Unit Commitment Model." *IEEE Transactions on Power Systems* 30 (1):109-22. doi: 10.1109/TPWRS.2014.2320880.

Balakrishnan, Hamsa, and Bala G. Chandran. 2010. "Algorithms for Scheduling Runway Operations Under Constrained Position Shifting." *Operations Research* 58 (6):1650-65. doi: 10.1287/opre.1100.0869.

Barrett, Steven RH, Rex E Britter, and Ian A Waitz. 2010. "Global mortality attributable to aircraft cruise emissions." *Environmental science & technology* 44 (19):7736-42.

Beck, Amir, and Aharon Ben-Tal. 2009. "Duality in robust optimization: primal worst equals dual best." *Operations Research Letters* 37 (1):1-6.

Bertsimas, Dimitris, Guglielmo Lulli, and Amedeo Odoni. 2011. "An integer optimization approach to large-scale air traffic flow management." *Operations research* 59 (1):211-27.

Bier, Andreas, and Ulrike Burkhardt. 2019. "Variability in contrail ice nucleation and its dependence on soot number emissions." *Journal of Geophysical Research: Atmospheres* 124 (6):3384-400.

Blasi, Luciano, Simeone Barbato, and Massimiliano Mattei. 2013. "A particle swarm approach for flight path optimization in a constrained environment." *Aerospace Science and Technology* 26 (1):128-37. doi: https://doi.org/10.1016/j.ast.2012.02.021.

BnnoBRs, J. 1962. "Partitioning procedures for solving mixed-variables programming problems '." *Numerische mathematik* 4 (1):238-52.

Bodur, Merve, and James R Luedtke. 2017. "Mixed-integer rounding enhanced benders decomposition for multiclass service-system staffing and scheduling with arrival rate uncertainty." *Management Science* 63 (7):2073-91.

Borbely, Daniel. 2019. "A case study on Germany's aviation tax using the synthetic control approach." *Transportation Research Part A: Policy and Practice* 126:377-95. doi: https://doi.org/10.1016/j.tra.2019.06.017.

Brueckner, Jan K., and Anming Zhang. 2010. "Airline emission charges: Effects on airfares, service quality, and aircraft design." *Transportation Research Part B: Methodological* 44 (8):960-71. doi: https://doi.org/10.1016/j.trb.2010.02.006.

Bruni, M. E., L. Di Puglia Pugliese, P. Beraldi, and F. Guerriero. 2017. "An adjustable robust optimization model for the resource-constrained project scheduling problem with uncertain activity durations." *Omega* 71:66-84. doi: https://doi.org/10.1016/j.omega.2016.09.009.

———. 2018. "A computational study of exact approaches for the adjustable robust resource-constrained project scheduling problem." *Computers & Operations Research* 99:178-90. doi: https://doi.org/10.1016/j.cor.2018.06.016.

Casellas, Enric, Joan Bech, Roger Veciana, Josep Ramon Miró, Abdel Sairouni, and Nicolau Pineda. 2020. "A meteorological analysis interpolation scheme for high spatial-temporal resolution in complex terrain." *Atmospheric Research* 246:105103. doi: https://doi.org/10.1016/j.atmosres.2020.105103.

Chai, Runqi, Al Savvaris, Antonios Tsourdos, Senchun Chai, and Yuanqing Xia. 2019. "A review of optimization techniques in spacecraft flight trajectory design." *Progress in Aerospace Sciences* 109:100543. doi: https://doi.org/10.1016/j.paerosci.2019.05.003.

Chaimatanan, S., D. Delahaye, and M. Mongeau. 2014. "A Hybrid Metaheuristic Optimization Algorithm for Strategic Planning of 4D Aircraft Trajectories at the Continental Scale." *IEEE Computational Intelligence Magazine* 9 (4):46-61. doi: 10.1109/MCI.2014.2350951.

Chassein, André, Trivikram Dokka, and Marc Goerigk. 2019. "Algorithms and uncertainty sets for data-driven robust shortest path problems." *European Journal of Operational Research* 274 (2):671-86. doi: https://doi.org/10.1016/j.ejor.2018.10.006.

Cheng, Chun, Mingyao Qi, Ying Zhang, and Louis-Martin Rousseau. 2018. "A two-stage robust approach for the reliable logistics network design problem." *Transportation Research Part B: Methodological* 111:185-202. doi: https://doi.org/10.1016/j.trb.2018.03.015.

Choi, Jong Hae. 2021. "Changes in airport operating procedures and implications for airport strategies post-COVID-19." *Journal of Air Transport Management* 94:102065. doi: https://doi.org/10.1016/j.jairtraman.2021.102065.

de Sá, Elisangela Martins, Reinaldo Morabito, and Ricardo Saraiva de Camargo. 2018. "Benders decomposition applied to

a robust multiple allocation incomplete hub location problem." *Computers Operations Research* 89:31-50.
de Werra, D. 1981. "On some characterisations of totally unimodular matrices." *Mathematical Programming* 20 (1):14-21. doi: 10.1007/BF01589329.
Detwiler, Andrew G, and Arthur Jackson. 2002. "Contrail formation and propulsion efficiency." *Journal of aircraft* 39 (4):638-44.
Dougui, Nourelhouda, Daniel Delahaye, Stéphane Puechmorel, and Marcel Mongeau. 2013. "A light-propagation model for aircraft trajectory planning." *Journal of Global Optimization* 56 (3):873-95. doi: 10.1007/s10898-012-9896-1.
Edwards, Holly A., Darron Dixon-Hardy, and Zia Wadud. 2016. "Aircraft cost index and the future of carbon emissions from air travel." *Applied Energy* 164:553-62. doi: https://doi.org/10.1016/j.apenergy.2015.11.058.
Environmental Protection Agnecy. 2000. "Aircraft Contrails Factsheet." In, 1-6. United States.
EUROCONTROL. 2022. "Reducing the impact of non-CO_2 climate impact: EUROCONTROL MUAC and DLR partnering on contrail prevention." Accessed 18th Jan. https://www.eurocontrol.int/article/reducing-impact-non-co2-climate-impact-eurocontrol-muac-and-dlr-partnering-contrail.
Federal Aviation Administration. 2022. "2021 Aviation Climate Action Plan." Accessed 18th Jan. https://www.faa.gov/sites/faa.gov/files/2021-11/Aviation_Climate_Action_Plan.pdf.
———. 2022. "Contrails 101." Accessed 18th Jan. https://www.faa.gov/about/office_org/headquarters_offices/apl/noise_emissions/contrails.
Ford, Lester Randolph, and Delbert Ray Fulkerson. 2015. *Flows in networks*: Princeton university press.
Franco, Antonio, Damián Rivas, and Alfonso Valenzuela. 2018. "Probabilistic aircraft trajectory prediction in cruise flight considering ensemble wind forecasts." *Aerospace Science and Technology* 82-83:350-62. doi: https://doi.org/10.1016/j.ast.2018.09.020.
Friedl, Randall R. 1997. "Atmospheric effects of subsonic aircraft: Interim assessment report of the advanced subsonic technology program."
García-Heredia, David, Antonio Alonso-Ayuso, and Elisenda Molina. 2019. "A Combinatorial model to optimize air traffic flow management problems." *Computers & Operations Research* 112:104768. doi: https://doi.org/10.1016/j.cor.2019.104768.
Geoffrion, Arthur M. 1972. "Generalized benders decomposition." *Journal of optimization theory and applications* 10 (4):237-60.
Ghouila-Houri, Alain. 1962. "Caractérisation des matrices totalement unimodulaires." *Comptes Redus Hebdomadaires des Séances de l'Académie des Sciences (Paris)* 254:1192-4.
Girardet, Daniel, and Stefan Spinler. 2013. "Does the aviation Emission Trading System influence the financial evaluation of new airplanes? An assessment of present values and purchase options." *Transportation Research Part D: Transport and Environment* 20:30-9. doi: https://doi.org/10.1016/j.trd.2013.01.002.
Goding, Louise, Mikael Andersson-Franko, and Carl Johan Lagerkvist. 2018. "Preferences for bio jet fuel in Sweden: The case of business travel from a city airport." *Sustainable Energy Technologies and Assessments* 29:60-9. doi: https://doi.org/10.1016/j.seta.2018.06.015.
Guan, Xiangmin, Xuejun Zhang, Dong Han, Yanbo Zhu, Ji Lv, and Jing Su. 2014. "A strategic flight conflict avoidance approach based on a memetic algorithm." *Chinese Journal of Aeronautics* 27 (1):93-101. doi: https://doi.org/10.1016/j.cja.2013.12.002.
Hamaguchi, Yoshihiro. 2021. "Does the trade of aviation emission permits lead to tourism-led growth and sustainable tourism?" *Transport Policy* 105:181-92. doi: https://doi.org/10.1016/j.tranpol.2021.03.012.
Harkness, Duane, Mark S Taylor, Gary S Jackson, and Robert W Stephens. 2006. An architecture for system-wide information management. Paper presented at the 2006 ieee/aiaa 25TH Digital Avionics Systems Conference.
Hu, X. B., W. H. Chen, and E. Di Paolo. 2007. "Multiairport Capacity Management: Genetic Algorithm With Receding Horizon." *IEEE Transactions on Intelligent Transportation Systems* 8 (2):254-63. doi: 10.1109/TITS.2006.890067.
IATA. 2020. "Number of flights performed by the global airline industry from 2004 to 2021 (in millions)." In.: Statista.
International Civil Aviation Organisation. 2022. "Climage change." https://www.icao.int/environmental-protection/pages/climate-change.aspx.
Jacquillat, Alexandre, Amedeo R Odoni, and Mort D Webster. 2016. "Dynamic control of runway configurations and of arrival and departure service rates at JFK airport under stochastic queue conditions." *Transportation Science* 51 (1):155-76.
Jacquillat, Alexandre, and Amedeo R. Odoni. 2015a. "Endogenous control of service rates in stochastic and dynamic queuing models of airport congestion." *Transportation Research Part E: Logistics and Transportation Review* 73:133-51. doi: http://dx.doi.org/10.1016/j.tre.2014.10.014.
———. 2015b. "An Integrated Scheduling and Operations Approach to Airport Congestion Mitigation." *Operations Research* 63 (6):1390-410. doi: https://doi.org/10.1287/opre.2015.1428.
Jacquillat, Alexandre, Amedeo R. Odoni, and Mort D. Webster. 2017. "Dynamic Control of Runway Configurations and of Arrival and Departure Service Rates at JFK Airport Under Stochastic Queue Conditions." *Transportation*

Science 51 (1):155-76. doi: https://doi.org/10.1287/trsc.2015.0644.
Kafle, Nabin, and Bo Zou. 2016. "Modeling flight delay propagation: A new analytical-econometric approach." *Transportation Research Part B: Methodological* 93:520-42. doi: http://dx.doi.org/10.1016/j.trb.2016.08.012.
Kärcher, Bernd. 2018. "Formation and radiative forcing of contrail cirrus." *Nature communications* 9 (1):1-17.
Ketkov, Sergey S., Oleg A. Prokopyev, and Evgenii P. Burashnikov. 2021. "An approach to the distributionally robust shortest path problem." *Computers & Operations Research* 130:105212. doi: https://doi.org/10.1016/j.cor.2021.105212.
Koop, Thomas, Beiping Luo, Athanasios Tsias, and Thomas Peter. 2000. "Water activity as the determinant for homogeneous ice nucleation in aqueous solutions." *Nature* 406 (6796):611-4.
Kuhn, Peter M. 1970. "Airborne observations of contrail effects on the thermal radiation budget." *Journal of the Atmospheric Sciences* 27 (6):937-42.
Kyriakidis, Phaedon C. 2004. "A geostatistical framework for area-to-point spatial interpolation." *Geographical Analysis* 36 (3):259-89.
Lee, C. K. M., K. K. H. Ng, Hing Kai Chan, K. L. Choy, W. C. Tai, and L. S. Choi. 2018. "A multi-group analysis of social media engagement and loyalty constructs between full-service and low-cost carriers in Hong Kong." *Journal of Air Transport Management* 73:46-57. doi: https://doi.org/10.1016/j.jairtraman.2018.08.009.
Lee, David S, David W Fahey, Piers M Forster, Peter J Newton, Ron CN Wit, Ling L Lim, Bethan Owen, and Robert Sausen. 2009. "Aviation and global climate change in the 21st century." *Atmospheric Environment* 43 (22-23):3520-37.
Li, Qinbiao, Kam K. H. Ng, Zhijun Fan, Xin Yuan, Heshan Liu, and Lingguo Bu. 2021. "A human-centred approach based on functional near-infrared spectroscopy for adaptive decision-making in the air traffic control environment: A case study." *Advanced Engineering Informatics* 49:101325. doi: https://doi.org/10.1016/j.aei.2021.101325.
Liao, Weijun, Ying Fan, Chunan Wang, and Zixun Wang. 2021. "Emissions from intercity aviation: An international comparison." *Transportation Research Part D: Transport and Environment* 95:102818. doi: https://doi.org/10.1016/j.trd.2021.102818.
Liu, Shuli, Yulai Wan, Hun-Koo Ha, Yuichiro Yoshida, and Anming Zhang. 2019. "Impact of high-speed rail network development on airport traffic and traffic distribution: Evidence from China and Japan." *Transportation Research Part A: Policy and Practice* 127:115-35. doi: https://doi.org/10.1016/j.tra.2019.07.015.
Malaek, S. M., A. Alaeddini, and D. S. Gerren. 2011. "Optimal Maneuvers for Aircraft Conflict Resolution Based on Efficient Genetic Webs." *IEEE Transactions on Aerospace and Electronic Systems* 47 (4):2457-72. doi: 10.1109/TAES.2011.6034644.
Meserole, Jere S, and John W Moore. 2006. What is system wide information management (SWIM)? Paper presented at the 2006 ieee/aiaa 25TH Digital Avionics Systems Conference.
Minnis, Patrick, J Kirk Ayers, Rabindra Palikonda, and Dung Phan. 2004. "Contrails, cirrus trends, and climate." *Journal of Climate* 17 (8):1671-85.
Montemanni, Roberto, and Luca Maria Gambardella. 2005. "The robust shortest path problem with interval data via Benders decomposition." *4OR* 3 (4):315-28. doi: 10.1007/s10288-005-0066-x.
Nas, Bilgehan, and Ali Berktay. 2010. "Groundwater quality mapping in urban groundwater using GIS." *Environmental Monitoring and Assessment* 160 (1):215-27. doi: 10.1007/s10661-008-0689-4.
Neumayr, Bernd, Eduard Gringinger, Christoph G Schuetz, Michael Schrefl, Scott Wilson, and Audun Vennesland. 2017. Semantic data containers for realizing the full potential of system wide information management. Paper presented at the 2017 IEEE/AIAA 36th Digital Avionics Systems Conference (DASC).
Ng, K. K. H., K. L. Keung, C. K. M. Lee, and Y. T. Chow. 2020. A Large Neighbourhood Search Approach to Airline Schedule Disruption Recovery Problem. Paper presented at the 2020 IEEE International Conference on Industrial Engineering and Engineering Management (IEEM), 14-17 Dec. 2020.
Ng, K. K. H., and C. K. M. Lee. 2016a. Makespan minimization in aircraft landing problem under congested traffic situation using modified artificial bee colony algorithm. Paper presented at the 2016 IEEE International Conference on Industrial Engineering and Engineering Management (IEEM), Bali, Indonesia, 4-7 Dec. 2016.
———. 2016b. A modified Variable Neighborhood Search for aircraft Landing Problem. Paper presented at the 2016 IEEE International Conference on Management of Innovation and Technology (ICMIT), Bangkok, Thailand, 19-22 Sept. 2016.
Ng, K. K. H., C. K. M. Lee, and F. T. S. Chan. 2017. A robust optimisation approach to the aircraft sequencing and scheduling problem with runway configuration planning. Paper presented at the 2017 IEEE International Conference on Industrial Engineering and Engineering Management (IEEM), Singapore, Singapore.
Ng, K. K. H., C. K. M. Lee, F. T. S. Chan, and S. Z. Zhang. 2018. Dynamic semi-mixed mode runway configuration planning and runway scheduling. Paper presented at the Proceedings of International Conference on Computers and Industrial Engineering, CIE.
Ng, K. K. H., C. K. M. Lee, Felix T. S. Chan, Chun-Hsien Chen, and Yichen Qin. 2020. "A two-stage robust optimisation for terminal traffic flow problem." *Applied Soft Computing* 89:106048. doi: https://doi.org/10.1016/j.asoc.2019.106048.

Ng, K. K. H., C. K. M. Lee, Felix T. S. Chan, and Yaqiong Lv. 2018. "Review on meta-heuristics approaches for airside operation research." *Applied Soft Computing* 66:104-33. doi: https://doi.org/10.1016/j.asoc.2018.02.013.
Ng, K. K. H., C. K. M. Lee, Felix T. S. Chan, and Yichen Qin. 2017. "Robust aircraft sequencing and scheduling problem with arrival/departure delay using the min-max regret approach." *Transportation Research Part E: Logistics and Transportation Review* 106:115-36. doi: https://doi.org/10.1016/j.tre.2017.08.006.
Ng, Kam K. H., Chun-Hsien Chen, and C. K. M. Lee. 2021. "Mathematical programming formulations for robust airside terminal traffic flow optimisation problem." *Computers & Industrial Engineering* 154:107119. doi: https://doi.org/10.1016/j.cie.2021.107119.
Ng, Kam K. H., Chun-Hsien Chen, C. K. M. Lee, Jianxin Jiao, and Zhi-Xin Yang. 2021. "A systematic literature review on intelligent automation: Aligning concepts from theory, practice, and future perspectives." *Advanced Engineering Informatics* 47:101246. doi: https://doi.org/10.1016/j.aei.2021.101246.
Ng, Kam K. H., C. K. M. Lee, S. Z. Zhang, and K. L. Keung. 2020. "The impact of heterogeneous arrival and departure rates of flights on runway configuration optimization." *Transportation Letters*:1-12. doi: https://doi.org/10.1080/19427867.2020.1852496.
Owen, Bethan, David S Lee, and Ling Lim. 2010. "Flying into the future: aviation emissions scenarios to 2050." In.: ACS Publications.
Poles, Damir. 2009. "Base of aircraft data (BADA) aircraft performance modelling report." *EEC Technical/Scientific Report* 9.
Poll, D. I. A. 2017. "21st-Century civil aviation: Is it on course or is it over-confident and complacent? – thoughts on the conundrum of aviation and the environment." *The Aeronautical Journal* 121 (1236):115-40. doi: 10.1017/aer.2016.140.
Prakash, Rakesh, Rajesh Piplani, and Jitamitra Desai. 2018. "An optimal data-splitting algorithm for aircraft scheduling on a single runway to maximize throughput." *Transportation Research Part C: Emerging Technologies* 95:570-81. doi: https://doi.org/10.1016/j.trc.2018.07.031.
Rostami, Ali Asghar, Vahid Karimi, Rahman Khatibi, and Biswajeet Pradhan. 2020. "An investigation into seasonal variations of groundwater nitrate by spatial modelling strategies at two levels by kriging and co-kriging models." *Journal of Environmental Management* 270:110843. doi: https://doi.org/10.1016/j.jenvman.2020.110843.
Samà, Marcella, Andrea D'Ariano, Francesco Corman, and Dario Pacciarelli. 2017. "Metaheuristics for efficient aircraft scheduling and re-routing at busy terminal control areas." *Transportation Research Part C: Emerging Technologies* 80:485-511. doi: https://doi.org/10.1016/j.trc.2016.08.012.
Samà, Marcella, Andrea D'Ariano, Paolo D'Ariano, and Dario Pacciarelli. 2017. "Scheduling models for optimal aircraft traffic control at busy airports: Tardiness, priorities, equity and violations considerations." *Omega* 67:81-98. doi: https://doi.org/10.1016/j.omega.2016.04.003.
Samà, Marcella, Andrea D'Ariano, and Dario Pacciarelli. 2013. "Rolling horizon approach for aircraft scheduling in the terminal control area of busy airports." *Transportation Research Part E: Logistics and Transportation Review* 60:140-55. doi: https://doi.org/10.1016/j.tre.2013.05.006.
Santos, Kristiana, and Laurence Delina. 2021. "Soaring sustainably: Promoting the uptake of sustainable aviation fuels during and post-pandemic." *Energy Research & Social Science* 77:102074. doi: https://doi.org/10.1016/j.erss.2021.102074.
Schumann, U. 1997. "The impact of nitrogen oxides emissions from aircraft upon the atmosphere at flight altitudes—Results from the AERONOX project." *Atmospheric Environment* 31 (12):1723-33.
Sheth, Kapil S, Mike Madson, Stephanie J Harrison, and Doug Helton. 2018. "Air Traffic Management Technology Demonstration–3 (ATD-3) Operational Concept for the Integration of ATD-3 Capabilities."
Sluiter, R. 2012. *Interpolation methods for the climate atlas*: KNMI.
Soler, Manuel, Bo Zou, and Mark Hansen. 2014. "Flight trajectory design in the presence of contrails: Application of a multiphase mixed-integer optimal control approach." *Transportation Research Part C: Emerging Technologies* 48:172-94. doi: https://doi.org/10.1016/j.trc.2014.08.009.
Sun, Junzi. 2019. "Open aircraft performance modeling: based on an analysis of aircraft surveillance data."
Sun, Junzi, Joost Ellerbroek, and Jacco M. Hoekstra. 2019. "WRAP: An open-source kinematic aircraft performance model." *Transportation Research Part C: Emerging Technologies* 98:118-38. doi: https://doi.org/10.1016/j.trc.2018.11.009.
Sun, Junzi, Jacco M Hoekstra, and Joost Ellerbroek. 2020. "OpenAP: An open-source aircraft performance model for air transportation studies and simulations." *Aerospace* 7 (8):104.
Sun, Xiaoqian, Sebastian Wandelt, and Anming Zhang. 2021. "Comparative accessibility of Chinese airports and high-speed railway stations: A high-resolution, yet scalable framework based on open data." *Journal of Air Transport Management* 92:102014. doi: https://doi.org/10.1016/j.jairtraman.2020.102014.
Takeichi, Noboru. 2018. "Adaptive prediction of flight time uncertainty for ground-based 4D trajectory management." *Transportation Research Part C: Emerging Technologies* 95:335-45. doi: https://doi.org/10.1016/j.trc.2018.07.028.
Teoh, Roger, Ulrich Schumann, Arnab Majumdar, and Marc EJ Stettler. 2020. "Mitigating the climate forcing of aircraft

contrails by small-scale diversions and technology adoption." *Environmental science & technology* 54 (5):2941-50.
Tian, Yong, Lili Wan, Bojia Ye, and Dawei Xing. 2019. "Cruise Flight Performance Optimization for Minimizing Green Direct Operating Cost." *Sustainability* 11 (14). doi: 10.3390/su11143899.
van Manen, J., and V. Grewe. 2019. "Algorithmic climate change functions for the use in eco-efficient flight planning." *Transportation Research Part D: Transport and Environment* 67:388-405. doi: https://doi.org/10.1016/j.trd.2018.12.016.
Wang, Zhuolin, Keyou You, Shiji Song, and Yuli Zhang. 2020. "Wasserstein distributionally robust shortest path problem." *European Journal of Operational Research* 284 (1):31-43. doi: https://doi.org/10.1016/j.ejor.2020.01.009.
Williams, Victoria, Robert B. Noland, and Ralf Toumi. 2002. "Reducing the climate change impacts of aviation by restricting cruise altitudes." *Transportation Research Part D: Transport and Environment* 7 (6):451-64. doi: https://doi.org/10.1016/S1361-9209(02)00013-5.
Xu, Yan, Ramon Dalmau, Marc Melgosa, Adeline Montlaur, and Xavier Prats. 2020. "A framework for collaborative air traffic flow management minimizing costs for airspace users: Enabling trajectory options and flexible pre-tactical delay management." *Transportation Research Part B: Methodological* 134:229-55. doi: https://doi.org/10.1016/j.trb.2020.02.012.
Xue, Dabin, Zhizhao Liu, Bing Wang, and Jian Yang. 2021. "Impacts of COVID-19 on aircraft usage and fuel consumption: A case study on four Chinese international airports." *Journal of Air Transport Management* 95:102106. doi: https://doi.org/10.1016/j.jairtraman.2021.102106.
Yang, Yuanchao, Zichen Gao, and Chao He. 2020. "Stochastic terminal flight arrival and departure scheduling problem under performance-based navigation environment." *Transportation Research Part C: Emerging Technologies* 119:102735. doi: https://doi.org/10.1016/j.trc.2020.102735.
Yin, Feijia, Volker Grewe, Christine Frömming, and Hiroshi Yamashita. 2018. "Impact on flight trajectory characteristics when avoiding the formation of persistent contrails for transatlantic flights." *Transportation Research Part D: Transport and Environment* 65:466-84. doi: https://doi.org/10.1016/j.trd.2018.09.017.
Zeng, Bo, and Long Zhao. 2013. "Solving two-stage robust optimization problems using a column-and-constraint generation method." *Operations Research Letters* 41 (5):457-61. doi: https://doi.org/10.1016/j.orl.2013.05.003.
Zhang, Anming, Yulai Wan, and Hangjun Yang. 2019. "Impacts of high-speed rail on airlines, airports and regional economies: A survey of recent research." *Transport Policy* 81:A1-A19. doi: https://doi.org/10.1016/j.tranpol.2019.06.010.
Zhang, Anming, Yahua Zhang, and Zhibin Huang. 2021. "Airline Economics." In *International Encyclopedia of Transportation*, edited by Roger Vickerman, 392-6. Oxford: Elsevier.
Zhang, Huili, Yunming Fang, Meng Wang, Lise Appels, and Yimin Deng. 2020. "Prospects and perspectives foster enhanced research on bio-aviation fuels." *Journal of Environmental Management* 274:111214. doi: https://doi.org/10.1016/j.jenvman.2020.111214.
Zhang, Qingyu, Mei Cao, Fangfang Zhang, Jing Liu, and Xin Li. 2020. "Effects of corporate social responsibility on customer satisfaction and organizational attractiveness: A signaling perspective." *Business Ethics: A European Review* 29 (1):20-34.